

Atmospheric Variability in Sulawesi, Indonesia -  
Regional Atmospheric Model Results and Observations

Dissertation  
zur Erlangung des akademischen Grades Doctor of Philosophy (PhD)  
der Fakultät für Forstwissenschaften und Waldökologie  
der Georg-August-Universität Göttingen

vorgelegt von

Dodo Gunawan

geboren in Subang, Indonesien

Göttingen, 2006

1. Gutachter: Prof. Dr. A. Ibrom

2. Gutachter: Prof. Dr. D. Hölscher

Tag der mündlichen Prüfung: 01.12.2006

## CONTENTS

TABLE OF CONTENTS .....	iii
LIST OF FIGURES.....	vi
LIST OF TABLES.....	x
SUMMARY .....	xi
ZUSAMMENFASSUNG.....	xiii
1. INTRODUCTION.....	1
1.1. Background and motivation.....	1
1.2. Climate variability in Indonesia.....	3
1.3. Description of IMPENSO research area .....	6
1.4. Objectives of study as the atmospheric part of IMPENSO.....	7
2. ANALYSIS OF ANNUAL RAINFALL PATTERNS IN CENTRAL SULAWESI ..	9
2.1. Introduction .....	10
2.2. Data and Methods .....	11
2.3. Results .....	14
2.4. Discussion .....	21
2.5. Conclusion.....	23
3. SIMULATION OF RAINFALL VARIABILITY USING THE REGIONAL ATMOSPHERIC MODEL REMO.....	25
3.1. Introduction .....	26
3.2. Material and Methods.....	27
3.2.1. Data .....	27
3.2.2. Description of the model.....	28
3.2.3. Model setup.....	31
3.3. Results and discussion.....	31
3.3.1. REMO model climatology.....	33
3.3.2. The rainfall simulated by REMO related to the ENSO phenomenon.....	35
3.4. Concluding remarks .....	51

---

4. COMPARISON OF LONG-TERM SIMULATED, GROUND-BASED AND SATELLITE-BASED RAINFALL ESTIMATES FOR INDONESIA AND SULAWESI.....	53
4.1. Introduction.....	54
4.2. Material and methods.....	55
4.2.1. Data sources.....	55
4.2.2. The regional atmospheric model (REMO).....	57
4.2.3. Statistical methods.....	57
4.3. Results.....	57
4.4. Discussion.....	68
4.5. Conclusion.....	69
5. SPECTRAL ANALYSIS OF RAINFALL VARIABILITY IN SULAWESI.....	71
5.1. Introduction.....	72
5.2. Data and methods.....	74
5.2.1. Data.....	74
5.2.2. Methods.....	74
5.3. Results.....	76
5.3.1. Maximum Entropy Method.....	76
5.3.2. Multi Taper Method.....	77
5.3.3. Wavelet Method.....	78
5.3.4. Coherency Analysis.....	84
5.4. Discussion.....	89
5.5. Conclusion.....	90
6. THE LOCAL ATMOSPHERIC CIRCULATION IN CENTRAL SULAWESI.....	93
6.1. Introduction.....	94
6.2. Material and Methods.....	96
6.2.1. Model Description.....	96
6.2.2. Representation of the study area in the simulations.....	98
6.2.3. Data.....	100



---

6.3. Results.....	100
6.3.1. Rainfall simulation on complex terrain.....	100
6.3.2. Land-Sea breeze circulation.....	103
6.4. Discussion.....	110
6.5. Conclusion.....	113
7. MAIN CONCLUSIONS AND FUTURE RESEARCH.....	114
7.1. Main conclusions.....	114
7.2. Implications for future research.....	115
ACKNOWLEDGEMENTS .....	116
APPENDIX.....	118
REFERENCES.....	119
CURRICULUM VITAE.....	132

## LIST OF FIGURES

Figure 1.1:	Down scaling of atmospheric models from REMO 1/2° covers Indonesia region with a cell (grid) size of 55 km to REMO 1/6° covering Sulawesi Island domain with a grid size of 18 km and to MM5 covering Palu watershed and Lore Lindu National Park with a grid size of 5 km. Legends show the topographic altitude above sea level in meters.....	5
Figure 2.1:	Distribution of 33 rain gauge stations in Central Sulawesi. The numbers are related to the station's name in Table 2.1.....	12
Figure 2.2:	Dendrogram of rainfall in Central Sulawesi as a result of cluster analysis..	14
Figure 2.3:	The annual rainfall pattern distribution in Central Sulawesi. The numbers refer to the graphs in Figure 2.4 and Figure 2.5. See text for an explanation of each rainfall pattern. The stations with the same colour represent the same annual rainfall pattern.....	18
Figure 2.4:	Annual courses of average rainfall at 33 stations classified into 10 rainfall patterns. The ordinate label in each graph indicates the month from January to December and the abscissa label indicates the monthly rainfall amount (mm month <sup>-1</sup> ).....	19
Figure 2.5:	The average rainfall pattern for each cluster from 33 rainfall stations in Central Sulawesi. The graph attributes are the same as in Figure 2.4.....	20
Figure 3.1:	The REMO model domain including the down scaling scheme from REMO 1/2° (Indonesia region, the outer box) to REMO 1/6° cover Sulawesi Island (the inner box). The shaded areas are the South Sulawesi and Central Sulawesi sub domains which are used for comparison with ground-based rainfall measurements.....	32
Figure 3.2:	Topography of the REMO 1/6° model domain. The two framed boxes indicate the model sub domains in South Sulawesi province and in Central Sulawesi province.....	34
Figure 3.3:	Monthly rainfall (mm/month) in South Sulawesi sub domain as simulated by REMO and as observed by rain gauges, in line graph (a) and scatter diagrams (b). The dashed line in the scatter diagram (b) is a 1:1 line and the solid line is a linier trend line.....	36
Figure 3.4:	Same as in Fig.3.3 but for the Central Sulawesi sub domain .....	37
Figure 3.5:	The correlation coefficient of monthly rainfall between the REMO model and data observation for the sub domain area rainfall amounts in the South Sulawesi sub domain (solid line) and the Central Sulawesi sub domain (dashed line). The value of running window is put in the first month of the window of period. The reason for this approximation is to show the ENSO events.....	38
Figure 3.6:	REMO 1/6° modelled monthly mean rainfall rate derived from accumulated 6-hour rainfall rates. The time period for monthly mean rainfall is 1979 to 1999.....	39
Figure 3.7:	As in Fig.3.6, but for GPCP monthly mean (1980 -1999) rainfall.....	40

Figure 3.8:	Monthly relative rainfall rates in South Sulawesi (1979 to 1993) during El Niño-, La Niña- and Non-ENSO years in % of Non-ENSO year rates. a). REMO model, b) measured.....	41
Figure 3.9:	Same as Figure 3.8 but for Central Sulawesi.....	44
Figure 3.10:	Monthly deviation (percentage) of all year average rainfall of REMO model during a strong El Niño event. The figure only displays data from April to December 1987.....	47
Figure 3.11:	Same as Fig. 3.10, but for a strong La Niña event in the year 1999.....	48
Figure 3.12:	Annual rainfall rates ( $\text{mm year}^{-1}$ ) simulated by the REMO model (dark grey) and measurement derived rainfall amounts (GPCC, light grey) for the period 1986 to 1999 over the land area of the REMO model domain (entire Sulawesi).....	49
Figure 3.13:	Annual rainfall rates in millimetres per year over the land area of the REMO model domain during different types of ENSO events and on average. Left bars are in El Niño years, centre bars are averaged over simulation period and right bars are in La Niña years. The dark grey bars represent the REMO model results and the light grey bars represent the GPCC rainfall values...	50
Figure 4.1:	Figure 4.1: Spatial comparison of rainfall rates for August 1992 between model REMO $0.5^\circ$ results (upper), satellite derived values (middle) and values derived from ground-based measurement by GPCC (bottom) for Indonesia Maritime Continent. Unit is in mm/month. Pixels size is $0.5^\circ$ by $0.5^\circ$ .....	59
Figure 4.2:	Correlation coefficient between the REMO $1/6^\circ$ model rainfall and the satellite-based estimate for Sulawesi Island. The years 1986 to 1999 were used for the correlation analysis.....	60
Figure 4.3:	Correlation coefficients between the REMO $1/6^\circ$ model rainfall and the GPCC ground-based rainfall over Sulawesi Island. The comparison period extends over the years 1986 to 1999.....	62
Figure 4.4:	Time series of area averaged monthly rainfall over entire Sulawesi area derived from ground-based measurements (GPCC), model simulations (REMO $1/6^\circ$ ) and satellite-derived (GPCP) data.....	63
Figure 4.5:	Scatter plots between REMO $1/6^\circ$ model rainfall results and ground-based observed rainfall rates, GPCC (upper), the REMO results and satellite-based estimates (middle) and the observed GPCC rainfall rates and satellite-based estimates (bottom) for monthly average rates in the time period 1986 to 1999 for the entire Sulawesi Island area.....	65
Figure 4.6:	Time-longitude diagram (averaged over $6^\circ\text{S}$ - $2^\circ\text{N}$ latitude) of monthly rainfall as simulated by REMO $1/6^\circ$ (left panels) and GPCC gridded observed rainfall (right panels). The upper panel shows the results of the REMO simulation (1986 – 1999, left) and from GPCC (1986 – 1999, right). The middle panel depicts the same but only for the El Niño year 1987/1988 and the bottom panel displays the data for the normal years 1989/1990.....	66

Figure 4.7:	Time-latitude diagram of monthly rainfall average over Sulawesi (117°E – 129°E) as simulated by the REMO 1/6° (upper) and GPCC gridded rainfall (lower) for the period of 1986 to 1999.....	67
Figure 5.1:	Monthly averaged (1979 to 1993) rainfall as modelled by REMO 1/6° and observed for the South Sulawesi (a) and the Central Sulawesi (b) sub domain.....	79
Figure 5.2:	Maximum entropy method (MEM) power spectrum of rainfall time series as modelled by REMO 1/6° and observed in the South Sulawesi sub domain ( <b>above</b> ) and the Central Sulawesi sub domain ( <b>bottom</b> ).....	80
Figure 5.3:	Multi Taper Method (MTM) power spectrum of rainfall time series as modelled by REMO 1/6° (upper) and observed (bottom) in South Sulawesi sub domain. The first three lines from the top are significant levels 99%, 95% and 90% respectively; fourth line is the median of the power.....	81
Figure 5.4:	As Figure 5.3, but for Central Sulawesi sub domain.....	82
Figure 5.5:	Data REMO South Sulawesi (a) and the wavelet power spectrum (b). The contour levels are chosen so that 75%, 50%, 25% and 5% of the wavelet power is above each level, respectively. The black contour is the 10% significance level, using a red-noise (autoregressive lag 1) background spectrum.....	84
Figure 5.6:	As Figure 5.5, but for the observed rainfall.....	85
Figure 5.7:	As Figure 5.5, but for Central Sulawesi sub domain.....	86
Figure 5.8:	As Figure 5.6, but for Central Sulawesi sub domain.....	86
Figure 5.9:	Coherency calculated between REMO modelled rainfall and SOI (a), observed rainfall and SOI (b), modelled rainfall and NIÑO3 (c) and observed rainfall and NIÑO3 (d) for South Sulawesi sub domain.....	87
Figure 5.10:	As Figure 5.9, but for Central Sulawesi sub domain.....	88
Figure 6.1:	Schematic illustrations of different mechanisms of orographic rainfall. (a) stable upslope ascent, (b) partial blocking of the impinging air mass, (c) down valley flow induced by evaporative cooling, (d) lee-side convergence, (e) convection triggered by solar heating, (f) convection owing to the mechanical lifting above level of free convection, and (g) seeder-feeder mechanism (Roe, 2005).....	95
Figure 6.2:	Flowchart of MM5 Modeling system (Dudhia et al.,1995).....	98
Figure 6.3:	Three dimensional view of topography over Central Sulawesi. The elevation data are obtained from the Shuttle Radar Topography Mission - SRTM of the United State Geological Survey (USGS) at 90 m resolution.....	99
Figure 6.4:	Spatial distribution of modelled monthly rainfall (shaded) and wind direction at the 800 hPa level (streamlines) for December 2003 (a) and June 2003 (b). ....	102
Figure 6.5:	Zonally average modelled rainfall and altitude along the 1.0° S latitude. Orographic rainfall is shown for two months, December 2003 (open squares) and June 2003 (solid squares). The shaded bar graph shows the elevation in 10 meter units.....	104

Figure 6.6: Wind analysis (wind rose) of the Automatic Weather Stations (AWS) Mutiara Palu (a) and Gimpu (b) in September 2004, showing the dominant wind directions (see stars in Figure 6.7 for the position of both locations).....	105
Figure 6.7: Horizontal distribution of the wind vector (m/sec) showing the sea-breeze circulation during the day (upper panels) and land-breeze circulation during the night (lower panels). The two stars on the middle lower panel mark the position of the automatic weather stations at Palu and at Gimpu (see Figure 6.6). Shading of the lower right panel depicts the topography in m a.s.l, as is shown in the legend .....	106
Figure 6.8: The Total Totals Index (TTI) values show the atmospheric stability at day time (upper panel) and night time (lower panel).....	107
Figure 6.9: Distribution of latent heat fluxes (Watt m <sup>-2</sup> ) on land and on sea during day and night.....	108
Figure 6.10: Same as Fig.6.9 but for sensible heat fluxes (Watt m <sup>-2</sup> ).....	109
Figure 6.11: Daily average of air temperature (°C) at 2 m above the surface for September 2004.....	110
Figure 6.12: Mean air temperatures (°C) at day (a) and night time (b); the temperature difference between day time air temperatures and night time air temperatures (c).....	111
Figure 6.13: Daily cycle of wind speed and direction at several pressure levels at Palu (a) and Gimpu (b). The contour lines represent location of wind speed (1.0 m/sec interval).....	112

---

Table 2.1:	List of rain gauge stations in Central Sulawesi. The numbers correspond to the stations distribution as in Figure 2.1.....	13
Table 2.2:	Monthly average and annual rainfall (mm) in each rainfall pattern .....	17
Table 2.3:	Wet and dry season periods in 6 seasonal rainfall patterns in Central Sulawesi.....	21
Table 3.1:	The difference of annual rainfall (mm) between the GPCC and the REMO model rainfall.....	46

## SUMMARY

This dissertation discusses the modelling of atmosphere parameters on Sulawesi Island, Indonesia using different atmospheric models from a hydrostatic model with horizontal resolution of 18 km to a non-hydrostatic approach with a horizontal resolution of 5 km. The main geographical research area in Central Sulawesi is the forest margin area around the Palu Valley with the Palu River and the Lore Lindu National Park, adjacent to one another, an agricultural area (valley) and the protected area of the National Park of Lore Lindu (mountains).

In order to better understand the climate conditions in this study area, one of the main climate parameters in the tropics, namely the monthly rainfall amount was analysed. In Chapter 2 the implemented method of cluster analysis method allowed obtains 10 rainfall patterns. The main character of climate in Central Sulawesi is a rather dry region showed by lower monthly rainfall during a year in most rainfall patterns.

In Chapter 3 the atmospheric model REMO was applied to study climate variability as the result of the ENSO events. The patterns of long-term annual rainfall simulated by REMO and measured at meteorological stations clearly indicate such influence. During the El Niño years (e.g.1987, 1992, 1997) the annual rainfall amount is lower than the long-term mean and during the La Niña years (e.g.1988, 1996, 1999) the annual rainfall amount is correspondently higher than the long- term annual mean).

The Chapter 4 analyzes the rainfall estimate using satellite technology. Data from satellite enables us to investigate the remote areas which are almost inaccessible and where the rainfall observation using conventional rain gauges are rare. The three rainfall data sets (observed, modelled and satellite estimate) showed the best agreement for the period of July to September, whereas in the period of November to February the differences between satellite and REMO were 200 mm month<sup>-1</sup>.

In Chapter 5 the results of time series analysis are presented. Several methods of spectral analysis were applied and the results showed that the rainfall variability in South and in Central Sulawesi is governed by different factors. In South Sulawesi the main cause of variability is the annual cycle of Asia-Australia Monsoon and the second factor is the ENSO in Central Sulawesi the ENSO is the main factor. Since the rainfall pattern around the equatorial belt including the Palu region, does not show a distinct correspondence to monsoon, then the main variability is produced by ENSO.

Chapter 6 discusses the local atmospheric circulation which can not be neglected as a rainfall-forming factor. The study clearly showed that the wind direction in the Palu Valley is dominated by the sea-land from the north in the morning to late afternoon. The wind penetrates far inland along the valley up to 75 km as is observed by automatic weather station in Gimpu. In the late afternoon and in the evening, the land breeze dominates the wind direction on the coastal line where it blows to the sea. The orographic rainfalls are well reconstructed by the MM5 model: 1) when the air coming from the ocean enters the mountain chain area of Central Sulawesi, it is orographically lifted, and the rainfall increase with the elevation at the upwind side (the maximum rainfall falls just on the top of the mountain); 2) at the leeward side the air becomes drier and on its descent the amount of rainfall decreases.

The dissertation concludes that three factors govern the climate and its variability in Sulawesi and especially in Central Sulawesi, Indonesia. They are the large-scaled atmosphere-ocean interaction phenomenon ENSO (El Nino Southern Oscillation), the regional circulation of Asian-Australian Monsoon and the locally specific regional factors. The regional atmospheric model REMO and the meso scale atmospheric model MM5 have been used to investigate the rainfall variability caused by the interaction of these factors.

The atmospheric model MM5 can be used as numerical weather prediction tools for the daily weather-forecast of the National Meteorological and Geophysical Agency, BMG.



## ZUSAMMENFASSUNG

Die vorliegende Arbeit behandelt die Charakterisierung der atmosphärischen Parameter Sulawesi, Indonesien, auf Grundlage eines hydrostatischen Modelansatzes mit einer horizontalen Auflösung von 18 km sowie einer nichtstatischen Methode mit einer feineren horizontalen Auflösung von 5 km. Das Hauptuntersuchungsgebiet liegt in Zentral-Sulawesi und umfasst das Palu-Flusseinzugsgebiet (2725 km<sup>2</sup>), das durch landwirtschaftlich intensiv genutzten Täler und das Bergregenwaldökosystem des geschützten Lore Lindu Nationalparks geprägt ist.

Zur genaueren Analyse der Klimafaktoren des Untersuchungsgebietes wurde die monatliche Niederschlagssumme, eine der Hauptklimacharakteristika der Tropen, an Hand einer Clusteranalyse in Gruppen unterschiedlicher Niederschlagsmuster differenziert. Durch die Clusteranalyse der untersuchten monatlichen Niederschlagszeitreihen wurden zehn verschiedene Gruppen von Niederschlagsmustern beschrieben (Kapitel 2).

Zur Analyse der durch ENSO - Ereignisse bedingten Klimavariabilität wurde das regionale Klimamodell REMO verwendet. Die Validierung mit gemessenen Stationsniederschlagsdaten zeigte, dass das regionale Klimamodell REMO im relativ ebenen Modellgebiet Süd-Sulawesi die Niederschlagszeitreihe mit einer sehr hohen Güte simulierte. Entgegen diesen zufrieden stellenden Simulationsergebnissen für Süd-Sulawesi wurden für Zentral-Sulawesi, das durch eine starke Topographie mit steilen Hanglagen geprägt ist, nur unzureichende Modellgüten berechnet. In El Niño – Jahren (z.B. 1987, 1992 und 1997) ist die jährliche Niederschlagssumme deutlich geringer als das langjährige Mittel. La Niña Jahre (1988, 1996 und 1999) sind dagegen durch eine wesentlich höhere Niederschlagssumme gegenüber dem langjährigen Mittel gekennzeichnet (Kapitel 3).

Satellitengestützte Niederschlagsmessungen ermöglichen es, die Niederschlagscharakteristika einer abgelegenen Region zu untersuchen, die von Stationsmessungen nur unzureichend abgedeckt ist. Die Bilanzen zeigen, dass alle drei Niederschlagszeitreihen in den Monaten Juli bis September gute Übereinstimmungen aufweisen, jedoch in den Monaten November bis Dezember bis zu 200 mm/Monat große Differenzen, insbesondere zwischen satellitengestützten Niederschlagsmessungen und REMO Simulationen auftreten (Kapitel 4).

Zeitreihenanalysen (Kapitel 5) ermöglichen im Zusammenhang mit variabilitätsbestimmenden physikalischen Faktoren die Ermittlung von Periodizitäten der Niederschlagsereignisse. Die Hauptfaktoren der Niederschlagsvariabilität Süd-Sulawesis unterscheiden sich deutlich von den Faktoren Zentral-Sulawesis. Eine der treibenden Faktoren der Niederschlagsvariabilität in Süd-Sulawesi ist der Asiatisch-Australische Monsun. ENSO-Ereignisse, die als Faktor der Niederschlagsvariabilität in Süd-Sulawesi zweitrangig sind, sind dahingegen in Zentral-Sulawesi der Hauptfaktor der Niederschlagsvariabilität. Das Untersuchungsgebiet in der Palu-Region liegt in unmittelbarer Äquatornähe, daher weist es kein eindeutiges monsunbedingtes Niederschlagsmuster auf, somit ist die Niederschlagsperiodizität dort hauptsächlich durch ENSO - Ereignisse bedingt.

Der letzte Teil der vorliegenden Arbeit (Kapitel 6) diskutiert die lokale atmosphärische Zirkulation, eines der Hauptmerkmale zur Beschreibung des lokalen Klimas einer Region. Das Palu-Tal im Hauptuntersuchungsgebiet liegt im Regenschatten von zwei parallel nordsüdlicher Gebirgszügen. Die Ergebnisse stellen deutlich heraus, dass die Windrichtung des Palu-Tals überwiegend von morgens bis in den späten Nachmittag durch die Land-Seewind-Zirkulation aus nördlicher Richtung bestimmt wird. Dieser lokale Effekt der Land-Seewind-Zirkulation wird noch in der 75 km in südlicher Richtung des Tales entfernten automatischen Wetterstation Gimpu registriert. Ebenfalls wird der orographische Niederschlag durch die MM5 Modell-Simulation wiedergegeben. Sobald die vom Ozean kommenden Luftmassen auf die Bergkette Zentral-Sulawesis

treffen, werden diese orographisch angehoben. Die höchsten Niederschlagssummen werden für die Bergkämme des Untersuchungsgebietes simuliert. Wenn die Luftmassen das Palu–Tal passieren, nimmt ihre Feuchte an der Leeseite des Tals ab, was wiederum zu einer Verringerung der Niederschlagssummen führt.

Zusammenfassend zeigt die Dissertation auf, daß drei Faktoren das Klima und seine Variabilität in Zentralsulawesi, Indonesien, bestimmen. Dies sind:

1. das großräumig wirkende Atmosphäre-Ozean Interaktion Phänomen ENSO (El Nino, südliche Oszillation)
2. die regionale Zirkulation des Asiatisch-Australischen Monsuns
3. lokal spezifische Faktoren.

Das regionale Klimamodell REMO und das Atmosphärenmodell MM5 im mittleren Maßstab wurden verwendet, um die Niederschlagsvariabilität, die durch die Interaktionen dieser Faktoren hervorgerufen wurde, zu untersuchen.

Das atmosphärische Modell MM5 kann als numerisches Wettervorhersagemodell für die tägliche Wettervorhersage des nationalen indonesischen meteorologischen Dienstes (Meteorological and Geophysical Agency, BMG) genutzt werden.



# CHAPTER 1

## INTRODUCTION

### 1.1. Background and motivation

Indonesia is one of the most interesting parts in the world to study climate. It is located between two continents (Asia and Australia) and between two oceans (Indian and Pacific Ocean). This situation results in an air mass character of a maritime continent, such that the Indonesian Archipelago is named also the Maritime Continent (Ramage, 1968). As it is, the air is mostly humid, and the enhanced cloudiness indicates massive exchanges of energy that are fundamentally important in the general circulation of the global atmosphere (Tapper, 2002). Of this region, none is more important in global climate dynamics than the Maritime Continent region, because of its role in providing energy for the operation of the north-south tropical Hadley cell and the east-west Walker circulation, both important components of the global circulation (Sturman and Tapper, 1996). McBride (1999) and recently Slingo et al. (2003) have shown that the Maritime Continent heat source is a major driver of the global circulation.

Among the meteorological/climatologically parameters rainfall plays the most important role for inhabitants of Indonesia. It varies considerably with respect to space and time. According to the geographical position and factors driving the climate, the rainfall patterns over the Indonesian Maritime Continent are grouped into three types: the monsoonal, the anti-monsoonal and the two peaks type. Monsoon is a wind system that influences large climatic regions and reverses direction seasonally. The Indonesian Meteorological and Geophysical Agency (BMG, 2002) has documented this rainfall type according to the monthly rainfall analyses of the last normal period of 1961 – 1990. Regional seasonality of rainfall for Indonesia was investigated by Kirono and Tapper (1999). Recent research conducted by Aldrian (2003) with Double Correlation Methods characterizes three climate regions over the Indonesian region. The monsoonal type covers most parts of the Indonesia region especially south of the equator. According to its

name, the rainfall pattern in this region is affected by monsoon circulation. It is characterised by the contrast between a dry season which coincides with the Australian monsoon episode and a wet season which coincides with the Asian monsoon. The Australian monsoon season takes place between April and September and the Asian monsoon season between October and March. The anti-monsoonal rainfall pattern is located on Maluku Island, on the northern part of Papua Island and on the eastern part of Sulawesi Island. The anti-monsoonal rainfall pattern refers to the monthly rainfall distribution in this region which is similar to the monsoon type, except the time of dry and wet season occurrence is the opposite of this pattern. The driving factor comes mainly from the sea air interaction (Bony et al., 1997; Qian et al., 2002; Aldrian, 2003; Aldrian and Susanto, 2003). The Two Peaks Region is associated with the southward and northward movement of the Inter Tropical Convergence Zone (ITCZ). Therefore the locations of this rainfall pattern are found along the equator line especially in the western part of Indonesia.

According to the seasonality of the rainfall pattern, the Indonesian Meteorological and Geophysics Agency (BMG) uses 102 rainfall regions all over the country as the Seasonal Prediction Areas for its routine operational of the preparation of the seasonal prediction bulletin. In all of these areas the rainfall regime has the monsoonal type of rainfall. In the bulletin, which is published twice a year, BMG predicts the onset and rainfall characteristic of dry/wet season (related to the Australian/Asian monsoon). Beyond these 102 Seasonal Prediction Areas, the rainfall predictions are made on a monthly basis. One of the motivations of this study is to analyze and regionalize the rainfall pattern in Central Sulawesi. This area has a rainfall pattern which is a mixture between a monsoonal and anti-monsoonal type due to the heterogeneity of the topography within a short distance. The rainfall variability connected to the ENSO is studied in this dissertation for selected regions in Sulawesi Island.

To study some factors governing the climate and the climate processes in Sulawesi, several atmospheric models have been applied. Using simulation data from atmospheric

models, one can select the study area even in the remote areas which are not usually covered by a dense meteorological observation network. This is the advantages of using models. They, of course, should have been tested to simulate any meteorological parameter under question. For this purpose, the model output should be validated with observational data. Therefore data observations are just as important as the sophisticated atmospheric model. The observations nowadays could be differentiated into two kinds i.e. the conventional/automated ground-based observation or modern ground-based radar measurements and the sophisticated remote measurements by satellites. Several satellites are present to derive meteorological parameters especially rainfall (Wilheit et al., 1991; Ferraro et al., 1996; Nakajima et al., 1999; Kummerow et al., 2000). The satellite derived rainfall data will be used to compare them with the output values of atmospheric models. The atmospheric models used to carry out this study are the Regional Model (REMO), developed at the Max Planck Institute for Meteorology (MPI-M), Hamburg and the fifth generation mesoscale atmospheric model MM5 developed by Pennsylvania State University/National Centre for Atmospheric Research (PSU/NCAR). REMO is a hydrostatic model which is used in this study with a 18 km horizontal resolution covering the entire Sulawesi Island (REMO  $1/6^\circ$ ). The boundary and initial conditions come from the same model with a horizontal resolution of 55 km (REMO  $1/2^\circ$ ) covering the entire Indonesian region implemented by Aldrian (2003). The MM5 is a non-hydrostatic model, applied here with double nesting from a coarse grid spacing of 15 km by 15 km horizontal resolution as the first domain which covers the Sulawesi Island, to the second domain with 5 km by 5 km horizontal resolution covering a part of Central Sulawesi to resolve local phenomenon such as land-sea breeze or valley-mountain circulation. The structure of atmospheric models applied in this study is displayed in Figure 1.1.

## 1.2. Climate variability in Indonesia

The causes of the climate variability and extremes in Indonesia are divided into three main factors according to the space and time scale. The first factor is the El Niño Southern Oscillation (ENSO) which is a rather hemispheric or global factor, occurring

periodically every 2 to 7 years (Torrence and Compo, 1998; IPCC, 2001; EL-Askary et al., 2004) and causing severe droughts during the El Niño events or flooding during the La Niña events in Indonesia.

It is considered that the global phenomenon of the El Niño Southern Oscillation (ENSO) has a significant impact in Indonesia on the inter-annual climate variability and furthermore on the social-economy of the Indonesian population. The prolonged dry seasons causing droughts are the impact of the El Niño events, whereas the extreme wet season as the impact of La Niña events. Roppelwesi and Halpert (1987) have related the rainfall variability in Indonesia to ENSO events. The parameters used to identifying ENSO events are the Sea Surface Temperature SST anomalies in the Pacific and the Southern Oscillation Index for the pressure gradient between Tahiti and Darwin.

A second factor for the variability of atmospheric phenomena having a more regional scale is the monsoon, which influences the wet and dry seasons altering roughly every six months. The wet season coincides in most part of Indonesia with the Asian monsoon from October to March and the dry season coincides with the Australian monsoon from April to September. Further discussion on the monsoon phenomenon can be found in Ramage (1971). Several studies to investigate Asian Australian Monsoon-related rainfall variability have been conducted by several researchers (e.g. Nicholls, 1981; Haylock and McBride, 2001; Tangang, 2001; Hendon, 2003; Aldrian and Susanto, 2003; Chang et al., 2003; Tangang and Juneng, 2004). One of these results is that the time pattern of rainfall is somehow regionally similar and coherent. Within the monsoon circulation, there is an intra seasonal oscillation with a 40 to 50 day period, which is called the Madden-Julian Oscillation (MJO) (Madden and Julian, 1972; 1994; Knutson and Weickmann 1987; Annamalai and Slingo 2001). The MJO affects the monsoon circulation by a break of the general monsoon features.



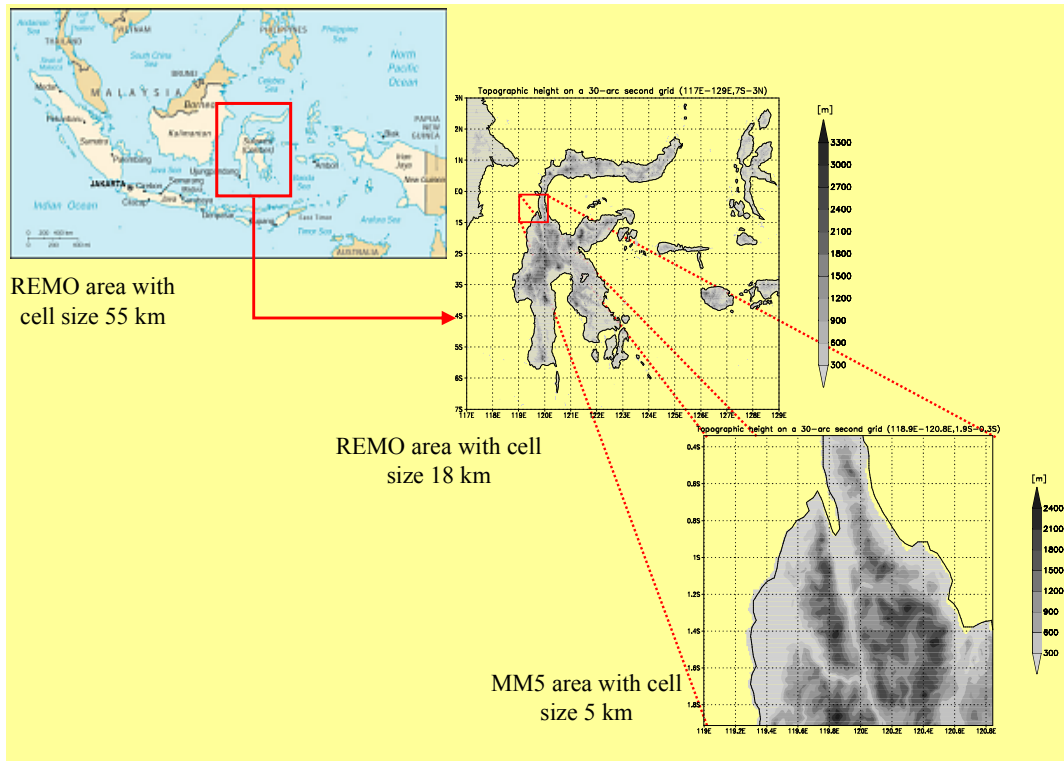


Figure 1.1: Down scaling of atmospheric models from REMO  $1/2^\circ$  covers Indonesia region with a cell (grid) size of 55 km to REMO  $1/6^\circ$  covering Sulawesi Island domain with a grid size of 18 km and to MM5 covering Palu watershed and Lore Lindu National Park with a grid size of 5 km. Legends show the topographic altitude above sea level in meters.

The third factor driving the climate variability in Indonesia region is more local and specific for each region. The rainfall regime, for example, in a flat region differs from the one within mountainous regions. A region at the windward side of mountains and affected by land-sea breeze circulation like in Bogor, West Java, receives high amounts of rainfall throughout the year. On the contrary, in the Palu region, which is a leeward region for the main wind directions and is located in a valley, the air flow is dominated by subsiding air. Consequently this region receives a low monthly rainfall amount throughout the year (Braak, 1929; BMG Palu, 2001). The local factors mainly affect the

rainfall characteristics which differentiate among the regions with respect to the onset and length of rainfall season and the monthly rainfall amount.

### 1.3. Description of IMPENSO research area

Most of Sulawesi lies above 500 m and about 20 percent of the total land area, mostly the central region, is above 1,000 m (Whitten et al., 1988). Based on the Köppen climate zone system, this island falls in the tropical wet climate zone (Kottek et al., 2006).

The IMPENSO research area around the Palu Valley in Central Sulawesi of Sulawesi Island, in which the fate of the water and its influence on household activities is investigated are the settlements, along the Palu River. Adjacent to this ecologically man-made agricultural area is a protected area of rain forest, the National Park of Lore Lindu. Recent human activities within this area have degraded the stability of rain forest margins within the national park. Like in other parts of the Indonesian archipelago, this area is also affected by the atmosphere-ocean interaction phenomenon which is called El Niño Southern Oscillation (ENSO) events. A prolonged and intensified dry season during the El Niño events and high rainfall during the La Niña events are the impacts of ENSO in most parts of the Indonesian region. In order to better understand the ENSO impact on human activities in this region, a research project concerning the impact of ENSO (IMPENSO) on the water balance and on agricultural activities has been established, which investigates the impact of ENSO events on climate variability, availability of water resources as well as on the socio-economy and policy implications on catchments scales (Keil et al., 2005). The IMPENSO is an interdisciplinary project on the role of water on the livelihood of a rural population. It consists of three components i.e. climatology, hydrology and socio-economy. The objective of this project are: (1) to quantify the local and regional manifestation of global climate variability, (2) to analyze their implication for water resources and agriculture land use, (3) to assess the socio-economic impact of ENSO on rural communities living in an agro-ecologically sensitive region and (4) to develop participatory approach strategies and policy recommendations that help improve

the capacity of this developing region to cope with ENSO events. The IMPENSO research project is a part of German Climate Research Program (DEKLIM), funded by the Federal Ministry of Research and Education (BMBF), Germany.

#### 1.4. Objectives of study as the atmospheric part of IMPENSO

The objectives of this research study is to investigate the climate processes and its variability on Sulawesi Island using ground-based and satellite observation data, the hydrostatic regional atmospheric model REMO and the non-hydrostatic atmospheric model MM5. The dissertation is divided into several chapters according to the model approach and to the scale of analysis and thus the phenomena to be investigated. The dissertation is organised as follows:

In Chapter 2 the regionalization of rainfall in Central Sulawesi using observed data is described. In this chapter it is intended to recognize the climate characteristics represented by the annual rainfall pattern at different sites in the research area. The Cluster analysis method is used to regionalize this rainfall pattern.

In Chapter 3 the annual rainfall pattern at different sites is analyzed and a rainfall variability study using regional atmospheric model REMO is carried out and is described. The climate variability in relation to global phenomena, ENSO, is investigated in this chapter.

In Chapter 4 the rainfall amount for entire Sulawesi derived from ground-based observation, satellite-based estimates and model simulation are compared.

In Chapter 5 it is determined which component of climate influencing factors are most affecting or dominant at any sub domain of the REMO model. For this purposes, an analysis at the frequency domain have been conducted using several methods of spectral analysis.

---

In Chapter 6 the local phenomena contribute to influence the climate of any region. In order to understand the process involved such as the land-sea breeze circulation or orographic rainfall formation, the mesoscale atmospheric model MM5 is applied to analyze the local climate's generating factors in Central Sulawesi.

In Chapter 7 main conclusions and the implications for future research is given.

## CHAPTER 2

# ANALYSIS OF ANNUAL RAINFALL PATTERNS IN CENTRAL SULAWESI

### *Abstract*

*A hierarchical cluster analysis of 33 rain gauge stations in Central Sulawesi has been performed using monthly averaged data from the period of 1983 to 1999 in order to group the annual pattern and to derive reasons for this grouping. The results are 10 characteristics annual rainfall pattern ensemble having different types in terms of monthly rainfall rate courses.*

*The variability of monthly averaged during a year in most of cases is quite smooth and does not show a strong monsoon contrast as usually found in other areas of Indonesia. The monsoon rainfall pattern with pronounce wet and dry season, which is the generally pattern found in Indonesia, is in Central Sulawesi only representative at two rainfall ensembles.*

*The annual pattern with a contrasting rainfall amount between dry and wet season and representing a pattern with the half year shift in the wet and dry season (anti-monsoon pattern) is found in Singkoyo (rainfall pattern 5), Mayoa, Pandayora (rainfall pattern 6) and Waru (rainfall pattern 7).*

## 2.1. Introduction

It is helpful if the rainfall regime of different sites can be grouped into two pattern due to high variability of rainfall in time and space. Grouping of the stations with similar rainfall pattern is useful for scientific purposes i.e. to describe the physical reason for different rainfall pattern in time and space and for practical purposes i.e. to determine the growing season and planting date for certain crops as well as for climate impact monitoring and seasonal predictions.

A big challenge of studying the rainfall variability in time and space this area is the sparse network of ground-based rain gauges. The scarce rain gauges do not represent the topographical distribution of the very heterogeneous terrain. Human activities such as irrigated agriculture are concentrated mostly in low land areas where the rain gauges are set up. Therefore the rain gauge distribution is rather unbalanced between the low land and highland regions.

A technique frequently used in climatology for grouping cases in classes (synoptic types or climate regimes, for example) or for grouping stations or grid points to define regions is cluster analysis (Mimmack et al., 2000). Unal et al. (2003) used data from 113 climate stations to redefine the climate of Turkey using the cluster analysis. Stooksbury and Michaels (1991) performed a two-step cluster analysis of 449 climate stations in the southeast of the United States, in order to objectively determine general climate clusters (groups of climate stations) for eight states. Fovell and Fovell (1993) and DeGaetano (2001) defined the climate zones of the entire the United States by cluster analysis also.

In this chapter the Group Average Method (Average Linkage Method) of the Hierarchical Cluster Analysis (Struss and Plieske, 1998) is used to classify climatically homogenous rainfall pattern, based on the data available for Central Sulawesi.

## 2.2. Data and methods

Data used to perform the cluster analysis is the total amount of monthly rainfall from 33 rain gauge stations spread over Central Sulawesi (Figure 2.1) averaged within the period of 1980 to 1999. Data was measured at rainfall and climate stations that were operated by several different institutions (Department of Agriculture, Irrigation Section of the Department of Public Works and BMG). Most of the stations are located in irrigation networks such as at the main inflow dam, as in the region of secondary channels and as in the area of the distribution channels of the agricultural fields. A list of the stations is shown in Table 2.1.

The Hierarchical Cluster Analysis (HCA) (Wilks, 1995; Gillian et al., 2001; Alhamed et al., 2002; Treffeisen et al., 2004), used in the grouping of rainfall patterns in Central Sulawesi, is a statistical method for finding relative homogeneous clusters of cases based on measured characteristics. The most common HCA techniques are single linkage, complete linkage, centroid, Ward's method and average linkage (Stooksbury and Michaels, 1991). The techniques differ in how the distance between entries is defined. The HCA techniques all follow a basic four-step routine:

Step 1: The Euclidean distance between all entries (rain gauge stations) is calculated.

Step 2: The two closest entries are merged to form a new cluster

Step 3: The distance between all entries is recalculated.

Step 4: Steps two and three are repeated until all entries are merged into one cluster.

Data used to implement the HCA cluster analysis is the raw data of monthly average rainfall over the period as mentioned above. The array thus had 12 elements containing the average rainfall for 33 stations. The technique of clustering is Group Average Method (Average Linkage Method) also referred to as the unweighed pair-group method using arithmetic averages (UPGMA) (Struss and Plieske, 1998). It was mentioned in literature that the average linkage method give the most realistic results in climatological research (Kalkstein et al., 1987).

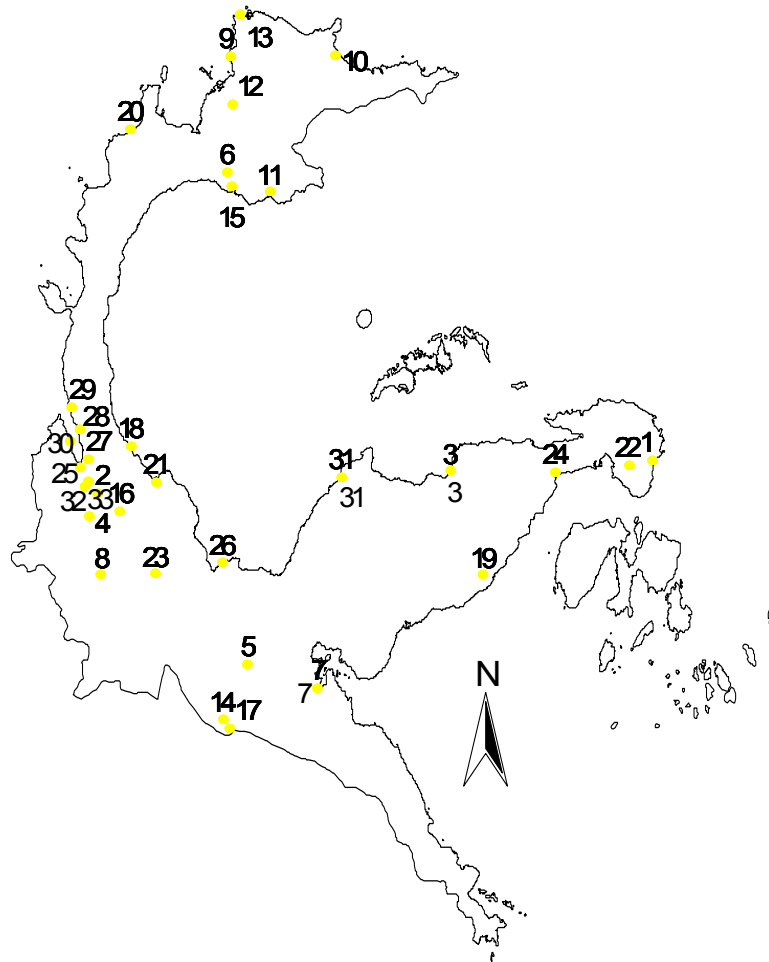


Figure 2.1: Distribution of 33 rain gauge stations in Central Sulawesi. The numbers are related to the station's name in Table 2.1.

The advantage of the average linkage technique, unlike the single linkage and centroid methods, has a reduced tendency to form chains (Stooksbury and Michaels, 1991). Unlike Wards's technique, which minimize within a cluster sum of square distance, average linkage minimizes within group variance and maximizes between group variance (Kalkstein et al., 1987). The clustering procedure was implemented by the KyPlot statistical package. It needed 32 iterations for searching the smallest distances, followed by a calculation of new distances until all entries are merged into one cluster.



Table 2.1: List of rain gauge stations in Central Sulawesi. The numbers correspond to the stations distribution as in Figure 2.1.

No.	Stations	Latitude	Longitude	Elevation (m)
1	BALANTAK	1°52'30"S	123°22'39"E	110.0
2	BORA	1°01'39"S	119°55'53"E	327.0
3	HEK-BUNTA	0°57'51"S	122°08'16"E	27.0
4	KALAWARA	1°10'00"S	119°55'31"E	126.0
5	KAMBA	1°52'55"S	120°53'14"E	382.0
6	AGUNG	0°33'18"N	120°44'31"E	33.0
7	KOLONDALE	2°00'49"S	121°18'08"E	150.0
8	KULAWI	1°28'11"S	119°84'43"E	612.0
9	LALOS	1°07'34"N	120°49'41"E	85.0
10	LAMADONG	1°07'04"N	121°25'03"E	16.0
11	LAMBUNU	0°44'51"N	120°10'07"E	200.0
12	LAMPASIO	0°53'58"N	120°47'47"E	635.0
13	LIBOK	1°21'47"N	120°50'41"E	6.0
14	MAYOA	2°09'17"S	120°44'45"E	550.0
15	ONGKO P	0°34'26"S	120°45'56"E	10.0
16	PALOLO	1°04'07"S	120°04'44"E	327.0
17	PANDAYORA	2°08'16"S	120°44'06"E	680.0
18	PARIGI	0°47'31"S	120°10'00"E	21.0
19	SINGKOYO	1°26'51"S	122°20'09"E	41.0
20	TAMPIALA	0°45'12"N	120°08'15"E	1.0
21	TOLAE	0°59'11"S	120°19'35"E	9.0
22	WARU	1°50'44"S	120°04'44"E	28.0
23	WUASA	1°25'30"S	120°19'22"E	1178.0
24	LUWUK	0°57'43"S	122°47'26"E	70.0
25	BALAROA	0°54'27"S	119°51'08"E	9.0
26	POSO	1° 23' 54S	120°45' 0"E	64.0
27	PALU	0°51'59"S	119°53'59"E	84.0
28	TAWAELI	0°43'16"S	119°50'49"E	18.0
29	TOAYA	0°36'24"S	119°48'24"E	29.0
30	MANTIKOLE	0°46'44"S	119°47'35"E	98.0
31	MAROWO	0°57'13"S	121°27'46"E	295.0
32	DOLO	1°00'23"S	119°52'52"E	29.0
33	BIROMARU	0°58'39"S	119°54'20"E	63.0

### 2.3. Results

Figure 2.2 shows, the dendrogram for HCA classification of rainfall patterns in Central Sulawesi. According to this figure, the 33 rain gauges are grouped into 11 rainfall patterns. Consider the predefined of thresholds value of monthly rainfall ( $150 \text{ mm month}^{-1}$ ), the physical geography of locations and the similar distance as is observed in Figure 2.2, the cluster of Kalawara, Wuasa, Dolo is combined to the cluster of Bora-Biromaru. Therefore the final cluster is 10 as is shown in Figure 2.4 and Figure 2.5. Each pattern contains one to nine locations of rain gauges which have a similar monthly variation. Figure 2.3 shows the rainfall pattern distribution.

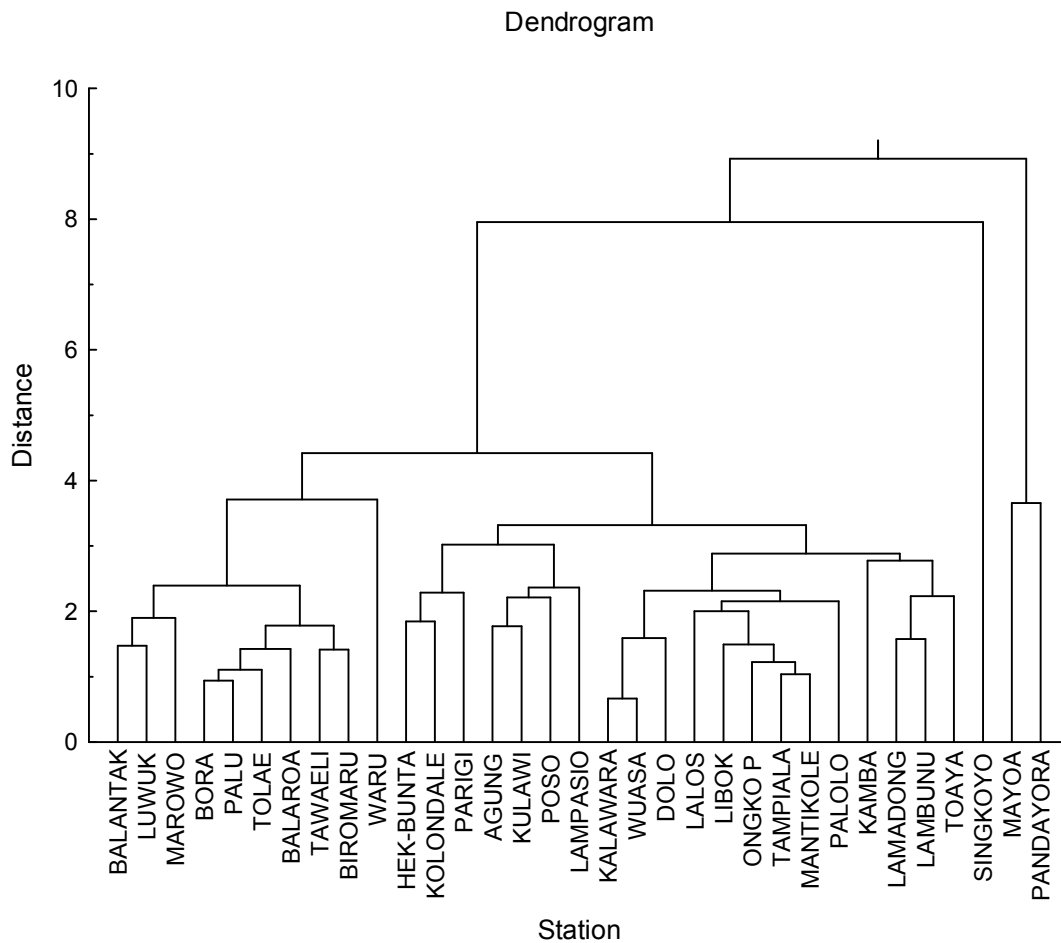


Figure 2.2: Dendrogram of rainfall in Central Sulawesi as a result of cluster analysis.

To distinguish between a wet and a dry season a rainfall threshold value of 150 mm month<sup>-1</sup> is used. This rainfall rate is set equal to an average daily evaporation rate in the area, which is assumed to be 5 mm day<sup>-1</sup>. To define a wet and dry season there must be at least two consecutive months with rainfall amounts above or below this threshold value (BMG, 2002). The definition is based on the BMG's seasonal prediction scheme. In that scheme one of the parameter predicted by statistical means is the change of one season to the next season. Most of the rainfall patterns show a more or less constant rainfall rate that is lower than 200 mm month<sup>-1</sup>. The rainfall pattern for individual stations is shown in Figure 2.4. Figure 2.5 depicts the averaged annual courses of the clustered rainfall patterns.

Rainfall pattern 1 around the Palu Valley is characterized by the observation that all monthly rainfall rates are less than 150 mm. This pattern with an average annual rainfall of 973 mm is the driest region compared to all other patterns. It covers Bora, Tolae, Palu, Tawaeli, Biromaru, Kalawara, Balaroo, Dolo and Wuasa. Geographically most of these stations are located in the lowland region of the Palu Valley except Wuasa which is located in the highland of the Besoa valley. This is the cluster that has a lot of members to construct this pattern.

Rainfall pattern 2 is represented by the stations Ongko P, Tampiala and Mantikole. This pattern has only two months of rainfall amount above 150 mm (163 mm and 161 mm) in May and June respectively. The average of annual rainfall is 1575 mm. The rainfall amount varies slightly below the threshold value of 150 mm and there are two months having an amount of less than 100 mm (August and September). In view of the monthly rainfall amount this pattern is moderately dry compared to the rainfall pattern 1.

The rainfall pattern 3 consists of stations Kamba, Lamadong, Lambunu and Toaya. This pattern is adequate the monsoon pattern with the dry period in June and July (slightly dry, monthly rainfall amount both are 148 mm month<sup>-1</sup>) and the really dry period in August to October. The average annual rainfall is 1804 mm.

Rainfall pattern 4 and 7 represent the anti-monsoon pattern. The dry period is in May to August and in April to August and the peak of wet season both are in June with a rainfall amount of 233 mm and 241 mm for pattern 4 and pattern 7 respectively. The dry period in pattern 7 is less dry compared to pattern 4. Therefore, the average of annual rainfall is less in pattern 7 compared to pattern 4. They are 1361 mm and 1761 mm for pattern 7 and pattern 4 respectively. Pattern 4 is represented by Hek Bunta, Kolonodale and Parigi, whereas pattern 7 is only represented by Waru.

Rainfall pattern 5 is very different from the patterns concerning the rainfall amount. It is perfectly bell shaped like a normal distribution curve. Rainfall exceeds 150 mm month<sup>-1</sup> in May; then it has the maximum in July (505 mm) and decreases to the value of less than 150 mm month<sup>-1</sup> in September. The average annual rainfall is 2279 mm which is the second highest annual amount from the ten patterns. This pattern represents the anti-monsoon pattern and has a contrast difference in the dry and wet season. This pattern is only found in Singkoyo.

Rainfall pattern 6 represents the monsoon pattern with slightly dry period in terms of duration and monthly rainfall amount. The dry period only occurs in August and September with the rainfall amount of 138 mm and 139 mm respectively. The monthly rainfall amount in the wet period varies from 196 mm in October to the peak in March with 462 mm. The average of annual rainfall is 3387 mm which is the highest annual amount among the ten patterns. Regarding the monthly rainfall this is also the wettest pattern among the ten patterns. This pattern is represented by Mayo and Pandayora.

Rainfall patterns 8 and 9 do not represent the three main patterns commonly found in Indonesia. These patterns are slightly wet (dry) because the monthly rainfall amount varies slightly above (below) 150 mm and only interrupted by two slightly dry (wet) months. In pattern 8 (pattern 9) the interrupters are the slightly dry (wet) months in February and September (January and July). Pattern 9 is just interrupted by a wet month after every 5 months of a slightly dry period. The average annual rainfall is 2113 mm and

1838 mm in pattern 8 and 9 respectively. Pattern 8 is represented by Kulawi, Agung, Poso and Parigi, while pattern 9 is represented by Lalos, Libok and Palolo.

Rainfall pattern 10 is the second driest after pattern 1. The average annual rainfall is 1179 mm. Like the rainfall pattern 1, the monthly rainfall is less than 150 mm over the year. The different with pattern 1 is the existence of the slightly dry in the period of April to June, whereas pattern 1 has a monthly rainfall is of far below 150 mm in every month of the year.

The average monthly and annual rainfall of the ten patterns is resumed in Table 2.2. Hence, the patterns 1, 8, 9 and 10 are not the seasonal rainfall patterns. Patterns 1 and 10, for instance, have not an onset to alter the dry to the wet season whereas patterns 8 and 9 have only one month to alter/break the season. Table 2.3 resumes the seasonality of 6 patterns are adequate in the seasonal rainfall pattern and will be described in the next paragraph.

Table 2.2: Monthly average and annual rainfall (mm) for each rainfall pattern

No	JAN	FEB	MAR	APR	MAY	JUN	JUL	AUG	SEP	OCT	NOV	DEC	ANNUAL
1	74	78	82	85	111	84	99	61	57	73	92	76	973
2	144	122	143	119	163	161	132	93	88	127	139	144	1575
3	214	173	196	178	160	148	148	96	62	117	158	154	1804
4	92	89	145	167	195	233	216	162	115	112	134	101	1762
5	63	54	72	135	276	441	505	360	138	57	79	99	2279
6	297	242	463	450	387	316	213	138	139	196	254	293	3387
7	47	50	98	106	182	241	229	204	66	38	52	48	1361
8	168	138	194	201	230	197	187	160	138	164	169	166	2113
9	165	130	124	94	141	145	162	125	124	142	150	138	1638
10	106	85	129	134	144	145	139	73	29	42	55	98	1179

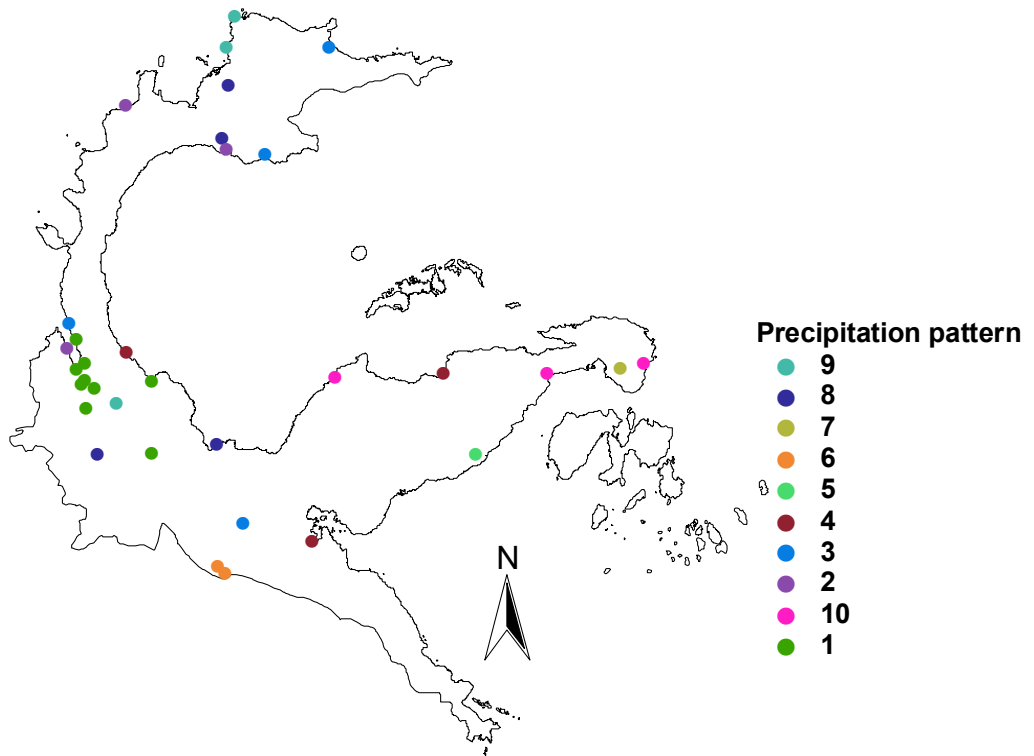


Figure 2.3: The annual rainfall pattern distribution in Central Sulawesi. The numbers refer to the graphs in Figure 2.4 and Figure 2.5. See text for an explanation of each rainfall pattern. The stations with the same colour represent the same annual rainfall pattern.

The onset of the wet season varies from May to November, whereas the onset of the dry season varies from June to September. There are three of the rainfall patterns have the onset of the wet season in May, one rainfall pattern in April, one rainfall pattern in November and one rainfall patterns in October. There is one rainfall pattern has the onset of the dry season in June, one rainfall pattern in July, one rainfall pattern in August and three rainfall patterns have the onset of dry season in September.

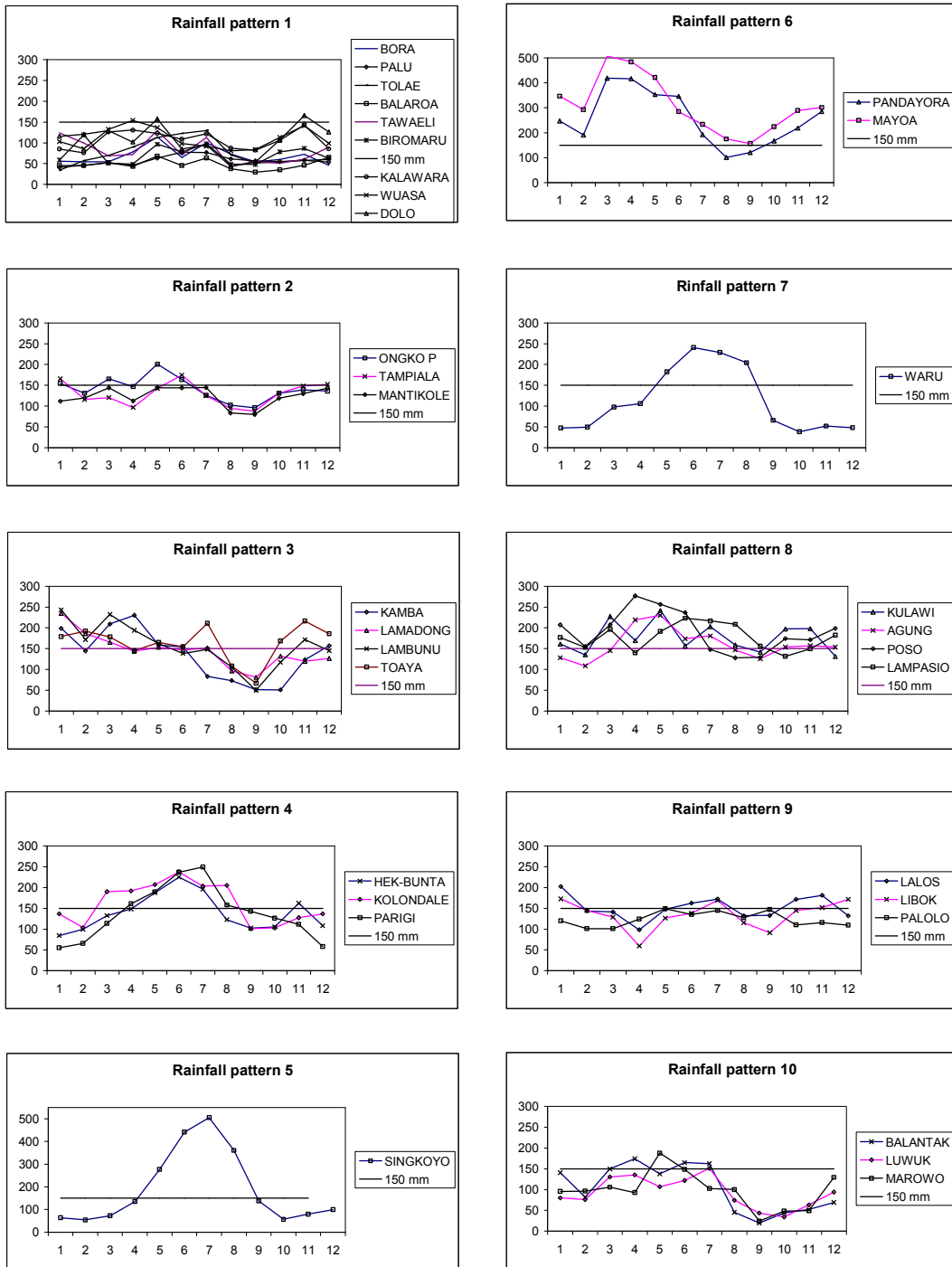


Figure 2.4: Annual courses of average rainfall at 33 stations classified into 10 rainfall patterns. The ordinate label in each graph indicates the month from January to December and the abscissa label indicates the monthly rainfall amount ( $\text{mm month}^{-1}$ ).

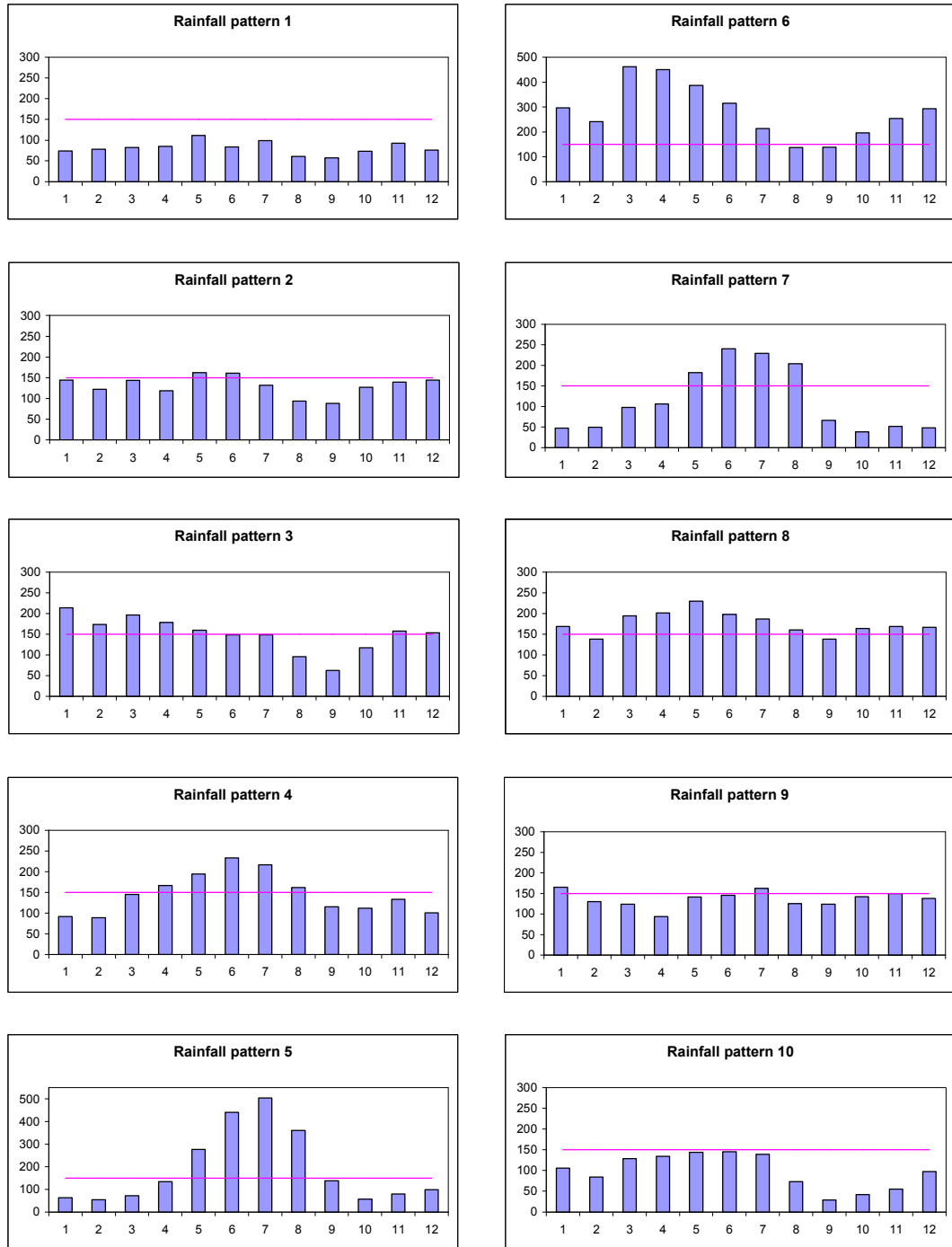


Figure 2.5: The average rainfall pattern for each cluster from 33 rainfall stations in Central Sulawesi. The graph attributes are the same as in Figure 2.4.



Table 2.3: Wet and dry season periods in 6 seasonal rainfall patterns in Central Sulawesi

Rainfall Pattern	Locations	Dry season period	Length of dry sason	Wet season period	Length of wet season
2	Ongko, Tampiala, Mantikole	July - April	10	May - June	2
3	Kamba, Lamadong, Lambunu, Toaya	June- October	5	November - May	7
4	Hek Bunta, Parigi, Kolonodale	September - March	7	April - August	5
5	Songkoyo	September - April	8	May - August	4
6	Mayoa, Pandayora	August - September	2	October - July	10
7	Waru	September - April	8	May - August	4

From Table 2.3, we can examine that the period of the seasons vary quite largely from 2 to 10 months. There are two rainfall patterns that have a length of wet (dry) season of 4 (8) months and each of the four rainfall patterns has a length of wet (dry) season of 2,5,7 and 10 months.

#### 2.4. Discussion

The ten rainfall patterns of rainfall courses within a year resulted from the Hierarchical Cluster Analysis, can be grouped into three patterns generally found in Indonesia. The monsoon rainfall pattern is associated with the Asian-Australian monsoon circulation. Indonesia and its surrounding regions, in the context of monsoon discussion, is also referred to as the Maritime Continent which was introduced by Ramage (1968). The Maritime Continent and northern Australia is a region of strong seasonal variation in wind and rainfall regimes, which consists of a prevailing easterly wind and dry conditions during the boreal summer and prevailing westerly winds and wet conditions during the boreal winter (Chang, 2004). Rainfall pattern 3 and 6 can be grouped into the monsoon pattern, although the dry period is not so clear because the amount varies slightly below 150 mm and only three months show a clear dry period in pattern 3. In the clear monsoon area such as in South Sulawesi or Java Island (BMG, 2002) the monsoon pattern are divided clearly into two seasons more or less in the same period of a year.

Rainfall pattern 2 (although it only has a small difference of wet season), pattern 4, pattern 5 and pattern 7 are grouped into the anti-monsoon pattern. They have the wet season in the period of April to August or it coincides with the Australian monsoon. The remaining months from September to March are the dry season period, which coincides with the Asian monsoon. The season of the anti-monsoon pattern is the opposite to the monsoon pattern, that means the period of wet season in the monsoon pattern is the period of dry season in the anti-monsoon pattern. There is strong evidence of the possibility of an ocean influence in the anti-monsoon pattern which is found only around Maluku and eastern part of Central Sulawesi (Aldrian, 2003). The Maluku is along the eastern route of the Indonesian Through Flow (ITF) (Gordon and Fine, 1996). The ITF flows mainly through the Makassar Strait with a small part flowing through the Maluku Sea (Gordon et al., 1999). The ITF in Maluku brings sea water from the warm pool area, which is located northeast of Irian Jaya Island (New Guinea). Hence, the SST over Maluku is determined mainly by the condition over the warm pool. During the dry season of anti-monsoon pattern (September to March) the sun's position is in the southern hemisphere. The ITF brings cooler surface water from the warm pool to the Maluku Sea. This cooler SST inhibits the formation of a convective zone. On the other hand, during the wet season of anti-monsoon pattern (April to August) the warm SST enhances the convective zone.

The rainfall patterns 1 and 10 are not match into one of the three main patterns commonly found in Indonesia because all months are dry period. Rainfall pattern 8 can be grouped into the bimodal pattern with two small peaks in May and November. Rainfall pattern 9 has only 2 months slightly above the 150 mm as its peaks. Overall the rainfall patterns 1, 8, 9 and 10 are most affected by local factors such as the geographical position, instead by monsoon circulation. Rainfall pattern 1, for instance, most of its stations are located in lowland of the Palu Valley. The valley is surrounded by mountains chain from three directions i.e. west, south and east. Therefore the westerly wind of the Asian monsoon and the easterly wind of the Australian monsoon reach the valley as the leeward and

bring less moist air. This position was reported by Braak (1929) that the Palu Valley is the driest region in Indonesia.

## 2.5. Conclusion

The Hierarchical Cluster Analysis to group rainfall patterns in Central Sulawesi has been performed using rainfall data from 33 rain gauge stations over Central Sulawesi.

Due to steeped topography within a short distance, the rainfall pattern changes accordingly and contributes to a more local effect of rainfall pattern. Therefore the classification of rainfall obtains 10 rainfall patterns. From this classification, one can differentiate the average position of dry and wet seasons, here being distinguished with the threshold rainfall rate of  $150 \text{ mm month}^{-1}$ .

In the study area of Central Sulawesi, 3 of the 10 rainfall patterns are anti-monsoon (the peak of wet season occurs between April and August) with a contrast monthly rainfall amount during dry and wet season. The monsoon pattern with only two to three months of dry period is found in two rainfall patterns. There are the two patterns having rainfall less than  $150 \text{ mm month}^{-1}$  over the year, therefore they do not match the three main patterns. The remaining three rainfall patterns also do not match the three main patterns. One pattern has a slightly above of  $150 \text{ mm month}^{-1}$  over the year, but it is interrupted by slightly below  $150 \text{ mm month}^{-1}$  in February and September. Two patterns are slightly below  $150 \text{ mm month}^{-1}$  over the year but it is interrupted by two months of slightly above  $150 \text{ mm month}^{-1}$ .

The Central Sulawesi is a part of the anti-monsoon pattern areas. The other part is Maluku Island. These patterns cover only a small part compared to the monsoon pattern which is a general pattern found in Indonesia. Overall, the most frequent of the ten patterns in Central Sulawesi the local patterns as the consequence of complex terrain in relatively short distance and the second most frequent is the anti-monsoon pattern.

---

In a practical way, the duration of the dry and wet season period in each rainfall pattern can be used to in general determine the onset of a planting date and to plan the irrigation schedule so that the farmers can use this information directly for their activities. Monitoring of climate impact and variability will also be more appropriate if it applied to each rainfall pattern. The study of the dominant mode responsible in rainfall variability will be assessed in Chapter 5. In the next chapter the rainfall variability will be studied using the regional atmosphere model REMO.

## CHAPTER 3

# **SIMULATION OF RAINFALL VARIABILITY USING THE REGIONAL ATMOSPHERIC MODEL REMO AND COMPARISON WITH RESULTS OF GROUND-BASED RAINFALL MEASUREMENT**

### **Abstract**

*The regional atmospheric model REMO has been applied for the study of rainfall variability in Sulawesi, Indonesia, by comparing modelled and observed monthly rainfall data from two sub domains. During the period of 1979 to 1993 the correlation coefficients between modelled and observed data were 0.64 and 0.52 for the South Sulawesi sub domain and for the Central Sulawesi sub domain respectively. A higher correlation (more than 0.80) was obtained for the year 1987 which was an El Niño year. For La Niña year 1988/1989, the results of the REMO simulation underestimated the observed data. The annual rainfall differed considerably between El Niño years and La Niña years. The modelled patterns of rainfall variability related to ENSO phenomena were similar to that of observed patterns. Rainfall in the dry season during an El Niño year was lower than the averaged of non-ENSO year while it was higher during the La Niña year than the averaged of non-ENSO year, whereas the rainfall during the wet seasons did not vary significantly between ENSO and non-ENSO years.*

### 3.1. Introduction

The inter annual climate variability in Indonesia is caused by the El Niño Southern Oscillation (ENSO) which is a rather global factor, occurring periodically every two to seven years. In Indonesia the ENSO causes severe drought during El Niño events or heavy rain during La Niña events (Ropelweski and Halpert, 1987). Hendon (2003) studied the impact of the ENSO and local air-sea interactions on rainfall variability in Indonesia. The high correlation between Indonesian rainfall and some ENSO indices such as the sea surface temperature anomaly in the NIÑO3.4 region or the Southern Oscillation Index (SOI) are well known and have been investigated by several researchers (Malcolm and McBride 2001; McBride et al., 2003; Hendon, 2003; Aldrian, 2002; Gunawan and Gravenhorst, 2005a).

Rainfall variability with respect to space and time can be analyzed by observed data or by using simulation data from atmospheric models. Atmospheric model studies for Sulawesi Island are still unavailable. Aldrian et al. (2004) used the MPI-M regional model REMO to study long-term rainfall over the Indonesian Archipelago. Roswintiarti and Raman (2003) used the MM5 model to simulate the transport of air pollutants during the 1997 forest fires in Kalimantan. In global circulation models (GCM) several authors have focused on the Indonesian region in their research (Ju and Slingo 1995; Soman and Slingo 1997; Smith et al., 1997; Slingo et al., 2003). Advantages of models are that they can be used for the study of large areas and also of remote areas which are usually not covered by dense meteorological networks. A model should be tested and verified to simulate any meteorological parameters under question. For this purpose, the model output should be validated with observed data. An atmospheric model for the Indonesian region should accommodate at least the local physical influences. Therefore the spatial resolution of the model has an important role for recognizing the local topography. For this reason, the regional atmospheric model REMO was used to simulate monthly rainfall amounts. The results were compared with ground based measurements on Sulawesi Island.

## 3.2. Material and Methods

### 3.2.1. Data on ground-based measured rainfall amounts

The measured rainfall data was obtained within this dissertation from a network of meteorological stations belonging to the Meteorological and Geophysics Agency (BMG) of Indonesia. Additional data was collected from rain gauge and climate stations operated by institutions such as the Department of Agriculture and the Irrigation Section of Department of Public Works. The Cressman objective analysis (Cressman, 1959) was performed on these stations data to yield a gridded result representing the station data. On a global scale, the Global Rainfall Climatology Center, GPCC, has gridded all available observed data to 0.5 degree horizontal resolution (Beck et al., 2005). Both this gridded data was used for comparison. It should be remember that spatially compared rainfall data from point measurement do not necessary represent the true area rainfall amounts. The local topography and wind pattern can not always be included in the extrapolation and interpolation procedures.

In the Cressman method the radius of influence is defined as the maximum radius from a grid point to a station by which the observed station value may be weighted to contribute to the value at the grid point. Stations beyond the radius of influence have no bearing on a grid point value. For each run, a new value is calculated for each grid point based on its correction factor. This correction factor is determined by analyzing data from each station within the radius of influence. For each such station an error is defined as the difference between the station value and a value derived by interpolation from the grid of that station. A distance-weighted formula (equation 1) is then applied to all such errors within the radius of influence of the grid point to arrive at a correction value for that grid point. The correction factors are applied to all grid points before the next pass is made. Observations nearest the grid point carry the most weight. As the distance increases, the observations carry less weight. The *cressman* function calculates the weights as follows:

$$W = (R^2 - r^2)/(R^2 + r^2) \quad (1)$$

where R = influence radius and r = distance between the station and the grid point.

### 3.2.2. Description of the model

The regional atmospheric model, REMO (*REgional MOdel*), applied in this study was originally developed for the Numerical Weather Prediction and operationally by the German Weather Service (DWD). It was formerly named EM (Europa Modell). A complete description of the EM model can be found in Majewski (1991) and DWD (1995).

The development of REMO as an atmospheric research tool has been conducted in a collaboration between DWD and Max Planck Institute for Meteorology (MPI-M) in Hamburg as well as German Climate Computing Center (DKRZ) in Hamburg resulting in the REMO model operated in a "climate mode". The development in a collaboration between DWD and GKSS Research Centre Geesthacht resulting in the REMO as a research tool operated in a "forecast mode" (Jacob and Claussen, 1995; Karstens et al., 1996; Jacob and Podzun, 1997). Both REMO models have been used in the BALTEX project for studies of the water catchments around the Baltic Sea (Jacob, 2001; Jacob et al., 2001) using the GCM of the MPI-M Hamburg (ECHAM-4).

Some parameters were changed to represent the tropical meteorological characteristics from the original of the GCM of MPI-M Hamburg (ECHAM-4) parameterization when REMO was applied to the Indonesian region. The minimum cloud thickness for the start of the rainfall process over land (ZL) and over sea (ZO) were changed to 1500 m each. This thickness values were chosen because the BMG meteorologist often experienced these cloud thickness to be both at this height above sea level in Indonesia. The original ECHAM-4 parameterization used 3000 m and 5000 m for ZL and ZO, respectively. The minimum humidity threshold for the onset of condensation in a grid volume was also changed. This parameter influences two rainfall processes, the convective (ZRTC) and the large-scale rainfall (ZRTL). The parameters were set to 80% whereas originally they were set to 60%. These two parameters were changed to the new values because Aldrian



(2003) showed a resulting better agreement between measured and modelled rainfall rates for the main island of the Indonesian Archipelago.

REMO is a hydrostatic model with 20 vertical layers in the hybrid coordinate system. A hydrostatic model is an atmospheric model in which the hydrostatic approximation replaces the vertical momentum equation. This implies that vertical acceleration is negligible compared to vertical pressure gradients and vertical buoyancy forces, a good approximation for synoptic and subsynoptic scales of motion. This is not realistic if one goes to small scale space resolution. In addition if the topography is rather structured and steeped the hydrostatic approach will have difficulties to be realistic.

The hybrid coordinate system is a combination of both a theta coordinate system above the boundary layer and a sigma coordinate system within the boundary layer. It has a horizontal resolution of  $\frac{1}{2}^\circ$  like the EM model formerly used by the DWD. For the research in the Sulawesi domain, the horizontal resolution has been increased to  $1/6^\circ$  or to a grid size equal to 18 by 18 km<sup>2</sup> which was nested into REMO  $\frac{1}{2}^\circ$  (see Figure 3.1).

The input data used for REMO  $1/6^\circ$  simulations has been obtained from the output of the same model running with  $\frac{1}{2}^\circ$  horizontal (55 km) resolution (Aldrian, 2003). In turn, REMO  $\frac{1}{2}^\circ$  used input data from ECMWF Re-Analyses of its global circulation model or the so-called ERA-15 data (15 years period of ECMWF Re-Analyses from 1979 to 1993) (Gibson et al., 1997) and some extension years until 1999 used the data from the same centre (also known as ERA-40, the 40 years data period of ECMWF Re-Analyses from mid-1957 to mid-2002). According to the availability of the REMO  $1/2^\circ$  simulations (Aldrian, 2003), the rainfall in South Sulawesi is simulated from 1979 to 1999 in this study.

Air temperature, water vapour pressure and liquid water content as well as the horizontal wind components and surface pressure are prognostic variables in REMO. The time discretization uses a semi-implicit leapfrog scheme and the advection scheme is semi-Lagrangian. In this numerical scheme at every time step the grid-points of the numerical

mesh represent the arrival points of backward trajectories at the future time (Untch and Hortal, 2002). To quantify the lateral boundaries, Davies (1976) method is used, where the lateral boundary relaxation zones extend to 8 grid rows.

The grid scale rainfall is based on the solution of the mass budget equations with the bulk schemes from Kessler (1969). Kessler assumed that the rate of autoconversion increases with the cloud water content but is zero for some values below a threshold value, where cloud conversion does not occur. The cloud conversion is the autoconversion rate of cloud droplets to rain drops which depend on the liquid water content (Lohmann and Roeckner, 1996).

The description of the sub grid scale rainfall processes follows the Tiedke (1989) method, with deep convection adjustments due to Nordeng (1994). Condensation parameterization follows Sundqvist (1978) and the gravity wave drag is quantified using the proposal of Palmer et al., (1986). The closures (both triggering conditions and entrainment/detrainment rates) are based on surface evaporation and large-scale water vapor convergence rates. The evaporation rate for the precipitating water in the atmosphere is computed according to Kessler (1969).

In REMO, three types of convection are considered: penetrative, mid-level, shallow and deep convection. Only one scheme is allowed in one grid cell and no different layers of convection. Penetrative convection is assumed if both the cloud base is within the planetary boundary layer and large-scale convergence occurs in the lower troposphere. During shallow convection clouds are formed in conditions of slightly divergent flow and are often driven by high evaporation rates at the surface. A mid-level convection is associated with the situation in which cloud base is formed in the free atmosphere and with large-scale lifting in the vicinity of fronts in regions of thermal instability. Deep convection is assumed if advective humidity transport predominates, while shallow convection is assumed if evaporation from the surface (land or ocean) is of a larger importance.

### 3.2.3. Model setup

The model domain for this study includes Sulawesi (Celebes Island), the eastern part of Kalimantan (Borneo Island) and Maluku Island (Figure 3.1).

The borders of the model domain in the left corner is  $117^{\circ}$  E;  $7^{\circ}$  S and in the right corner is  $129^{\circ}$  E;  $3^{\circ}$  N. The total of the  $1/6^{\circ}$  grid size are 73 by 61 or 4453 grids points. The model domain is divided into several sub domains according to the availability of the observed data. In the South Sulawesi area, observational data is quite well distributed in comparison to other regions in Sulawesi. REMO is run on a supercomputer in the same manner as the numerical weather prediction model. With the fast development of personal computer technology and the existence of a relatively new operating system named Linux, new computer architecture with the name Linux Cluster is available nowadays. In principle the Linux Cluster is a combination in a parallel way of several PCs with a Linux as the operating system which has a similar function as the UNIX operating system on a supercomputer. Wyser (2001) reported the results of a regional climate model's simulation using several computer architectures including Linux Cluster. REMO  $1/6^{\circ}$  for the Sulawesi domain runs on both platforms; a box PC with Linux as an operating system and the IBM p690 series supercomputer with 32 CPU.

### 3.3. Results and discussion

Sulawesi Island has, as the main REMO model domain, different topographical conditions. In South Sulawesi the topography is relatively flat whereas Central Sulawesi is a mountainous region with steep topography, i.e. changing strongly within short distances. The discussion of the time series of a REMO model simulations will focus on these two regions representing two different topographical conditions (see Figure 3.2).

Results of the monthly rainfall simulation and observed data for South Sulawesi are shown in Figure 3.3. During the 15 years of simulation, the monthly rainfall of the model agrees well with the observed data, with a correlation coefficient of 0.64.

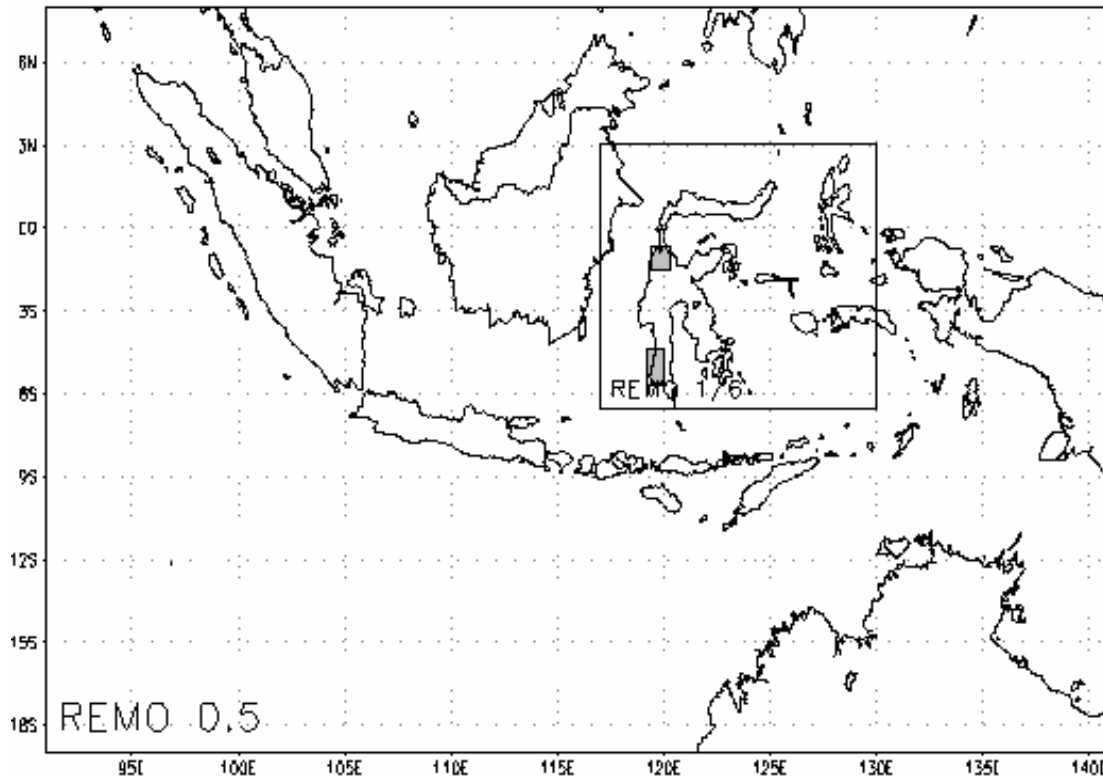


Figure 3.1: The REMO model domain including the down scaling scheme from REMO  $\frac{1}{2}^\circ$  (Indonesia region, the outer box) to REMO  $\frac{1}{6}^\circ$  cover Sulawesi Island (the inner box). The shaded areas are the South Sulawesi and Central Sulawesi sub domains which are used for comparison with ground-based rainfall measurements.

The rainfall rates measured and modelled for the Central Sulawesi sub-domain are shown in Figure 3.4. The monthly rainfall in Central Sulawesi sub domain is smaller compared to the South Sulawesi sub domain. The averaged rainfall in Central Sulawesi sub domain is smaller, because it includes the Palu Valley which is the driest region in Indonesia (Braak, 1929). The simulated maximum rainfall for the entire sub domain is 363 mm/month and occurred in November 1988, whereas from observation the maximum value is 381 mm/month and occurred in May 1992. Comparing with the results from two different topographic situations shows that in the structured mountainous area of Central Sulawesi, a lower correlation  $R$  0.52 found between simulated and observed and up

scaled data. The reason for the lower correlation is probably a more structured rainfall distribution in space and time, which makes it difficult both to model and to upscale the rates from point rainfall measurements. The maximum correlation for all modelled and measurement-based rainfall values is 0.85 (Figure 3.4). In this flat sub domain, REMO overestimates the monthly rainfall.

To investigate the correlation in greater detail, the correlation has also been analyzed in one month step running window of 12 months over 15 years (Figure 3.5). It can be seen that most of the correlation coefficient (86% from all the 12 months correlated) have a higher value than 0.50 for the South Sulawesi time series. In the El Niño years 1982/1983 and 1986/1987 the correlation coefficient value was 0.80. During this time, El Niño events had the highest intensity. The ENSO index (SOI) as an indicator of ENSO was on average -19.5 during this period. In normal year the SOI falls between -5 and 5, in moderate El Niño (La Niña) years the SOI is between -5 and -10 (5 and 10). The SOI values of -19.5 for the year 1982/1983 and 1986/1987 indicates the very strong and severe El Niño (past values of the SOI can be looked up at <http://www.bom.gov.au>). It can be seen that REMO can simulate extreme low rainfall amounts as for the years 1982, 1987 and 1992 which are the years of high El Niño intensity. In contrast, in the La Niña event (1988/1989) the results of REMO simulation are lower than the observed data (Figure 3.3b). The maximum modelled rainfall rate during the simulation period is 336 mm/month and occurred in March 1989, whereas from rain gauges the maximum rainfall is 473 mm/month and occurred in December 1987.

### 3.3.1. REMO model Climatology

The long-term simulation during the years 1980-1999 gives the monthly rainfall distribution pattern which also characterizes the rainfall climatology for the Sulawesi Island. Here the simulated distribution of rainfall is described and discussed in terms of the monsoon circulation. The simulated rainfall field will also be compared with the up-scaled rainfall data.

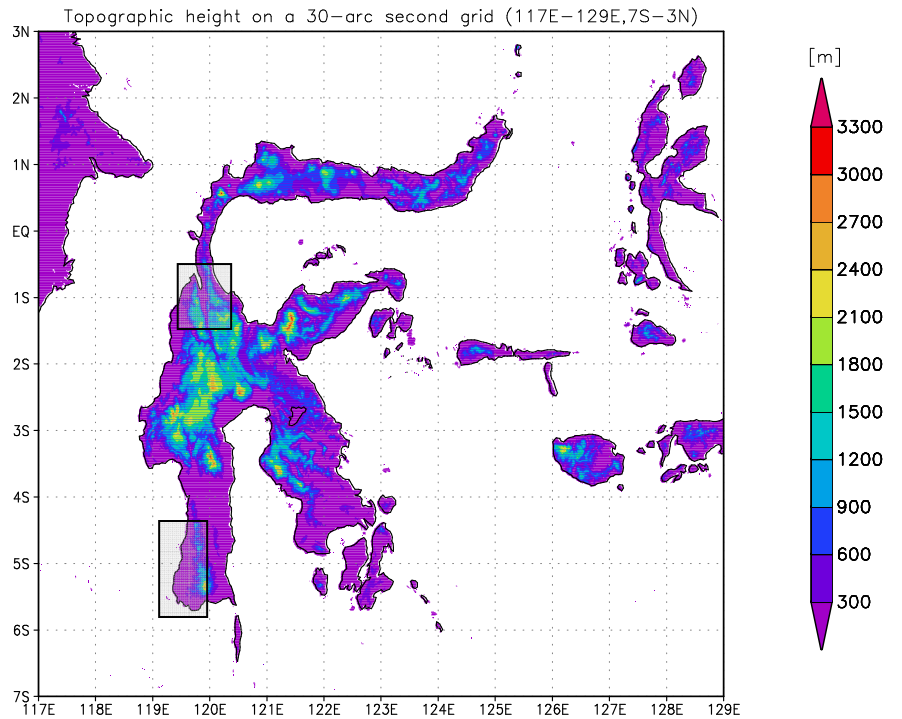


Figure 3.2: Topography of the REMO  $1/6^\circ$  model domain. The two framed boxes indicate the model sub domains in South Sulawesi province and in Central Sulawesi province.

The spatial distribution of the simulated rainfall is shown in Figure 3.6. It is shown that the spatial and temporal distributions of monthly rainfall agreed well with the monsoon circulation. This means that during the Asian monsoon (November to March) high rainfall occurs in the west of South Sulawesi province. This can be explain that the Asian monsoon is rather humid and the mountain ridges increase convection are causing more stop up lifting and therefore cloud and rain formation. During the Australian monsoon (April to October) the high rainfall occurs in the eastern and south eastern part of the model domain, because the warm sea surface of the ocean surrounding the south east Sulawesi initiating vertical instability of the atmosphere. Figure 3.6 also shows that the REMO  $1/6^\circ$  model simulated much higher rainfall over the sea compared to the land. The same results are obtained by Aldrian (2003), in REMO 0.5 for the Indonesian region.

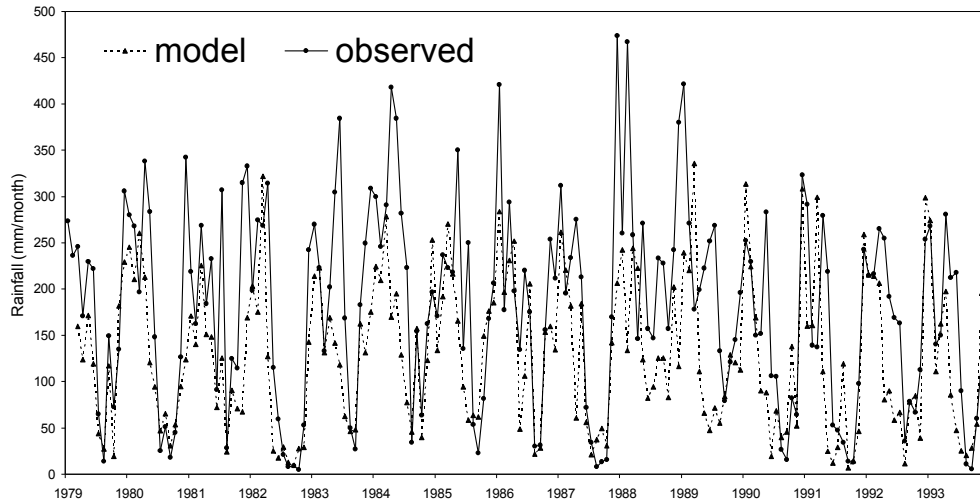
The REMO model rainfall rate has been compared with the data of GPCC gridded observed rainfall over the land as depicted in Figure 3.7. The spatial and temporal rainfall distribution looks similar.

### 3.3.2. The rainfall simulated by REMO related to the ENSO phenomenon

The long-term REMO model simulation results are used to study the rainfall variability in relation to the ENSO phenomenon. The ENSO years are identified based on the occurrence of cold and warm episodes, which are defined by the National Oceanic and Atmospheric Administration (NOAA) with the so-called Multivariate ENSO Index (MEI). Positive values of MEI indicate a warm episode of ENSO (El Niño) and negative values indicate a cold episode (La Niña). More details about the MEI can be found at [http://www.cdc.noaa.gov/ENSO/enso.mei\\_index.html](http://www.cdc.noaa.gov/ENSO/enso.mei_index.html). The MEI used in this paragraph instead of SOI as it used in the previous section is to adapt the definition of warm and cool episodes. It obtained based on the six main observed variables over the tropical Pacific. These six variables are: sea-level pressure (P), zonal (U) and meridional (V) components of the surface wind, sea surface temperature (S), surface air temperature (A), and total cloudiness fraction of the sky (C).

With this definition, intensive El Niño events took place in 1982, 1987, 1992 and 1997 and La Niña events occurred during the years 1988, 1989, 1990 and 1999-2000. The graphs of modelled and observed mean monthly rainfall during the El Niño years, La Niña years and during the Non-ENSO year for the South Sulawesi sub domain are shown in Figures 3.8 a and 3.8 b, whereas Figures 3.9 a and 3.9 b represent the Central Sulawesi sub domain.

a)



b)

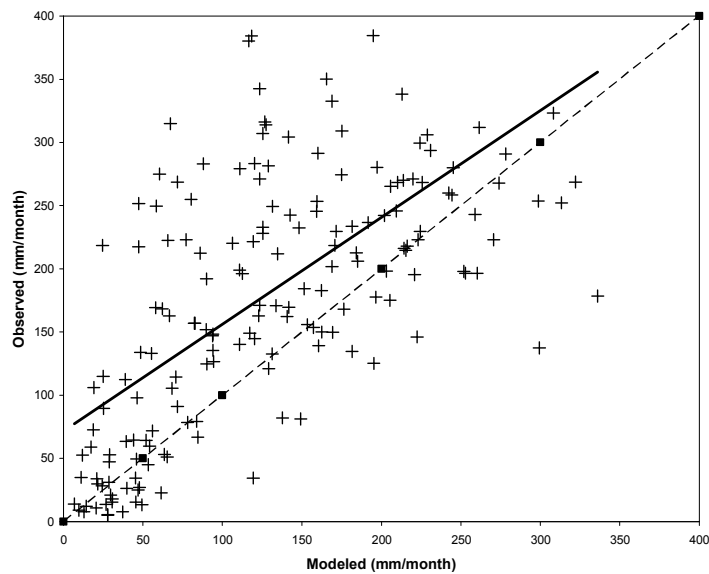
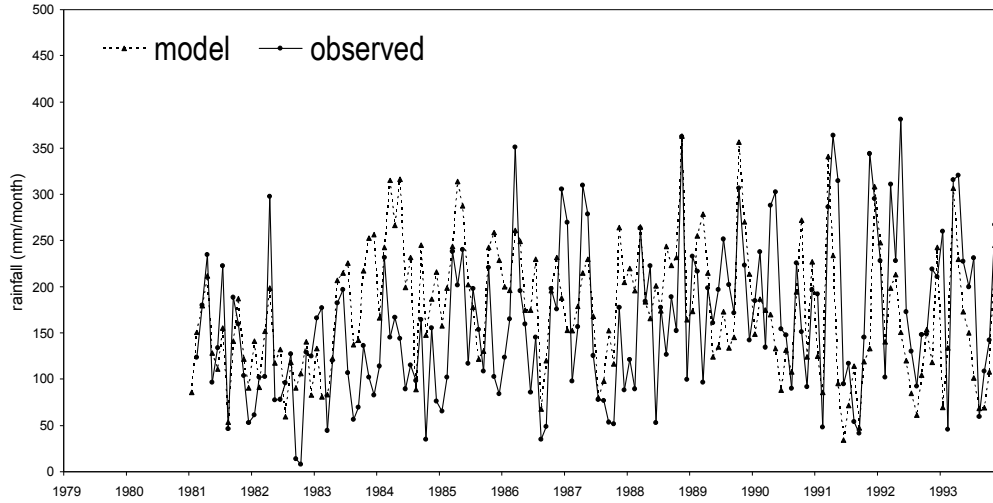


Figure 3.3: Monthly rainfall (mm/month) in South Sulawesi sub domain as simulated by REMO and as observed by rain gauges, in line graph (a) and scatter diagrams (b). The dashed line in the scatter diagram (b) is a 1:1 line and the solid line is a linear trend line.



a)



b)

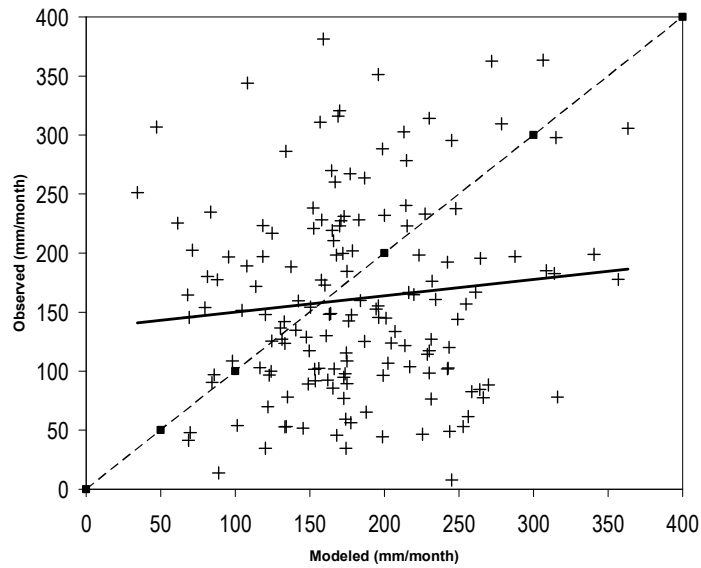


Figure 3.4: Same as in Fig.3.3 but for the Central Sulawesi sub domain

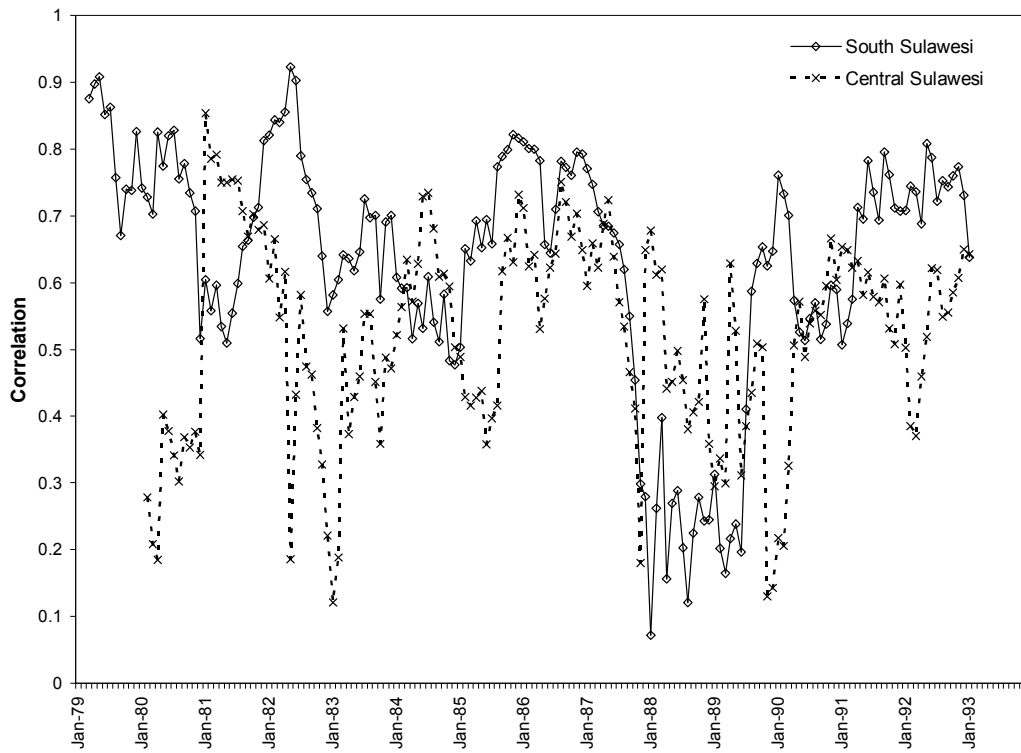


Figure 3.5: The correlation coefficient of monthly rainfall between the REMO model and data observation for the sub domain area rainfall amounts in the South Sulawesi sub domain (solid line) and the Central Sulawesi sub domain (dashed line). The value of running window is put in the first month of the window of period. The reason for this approximation is to show the ENSO events.

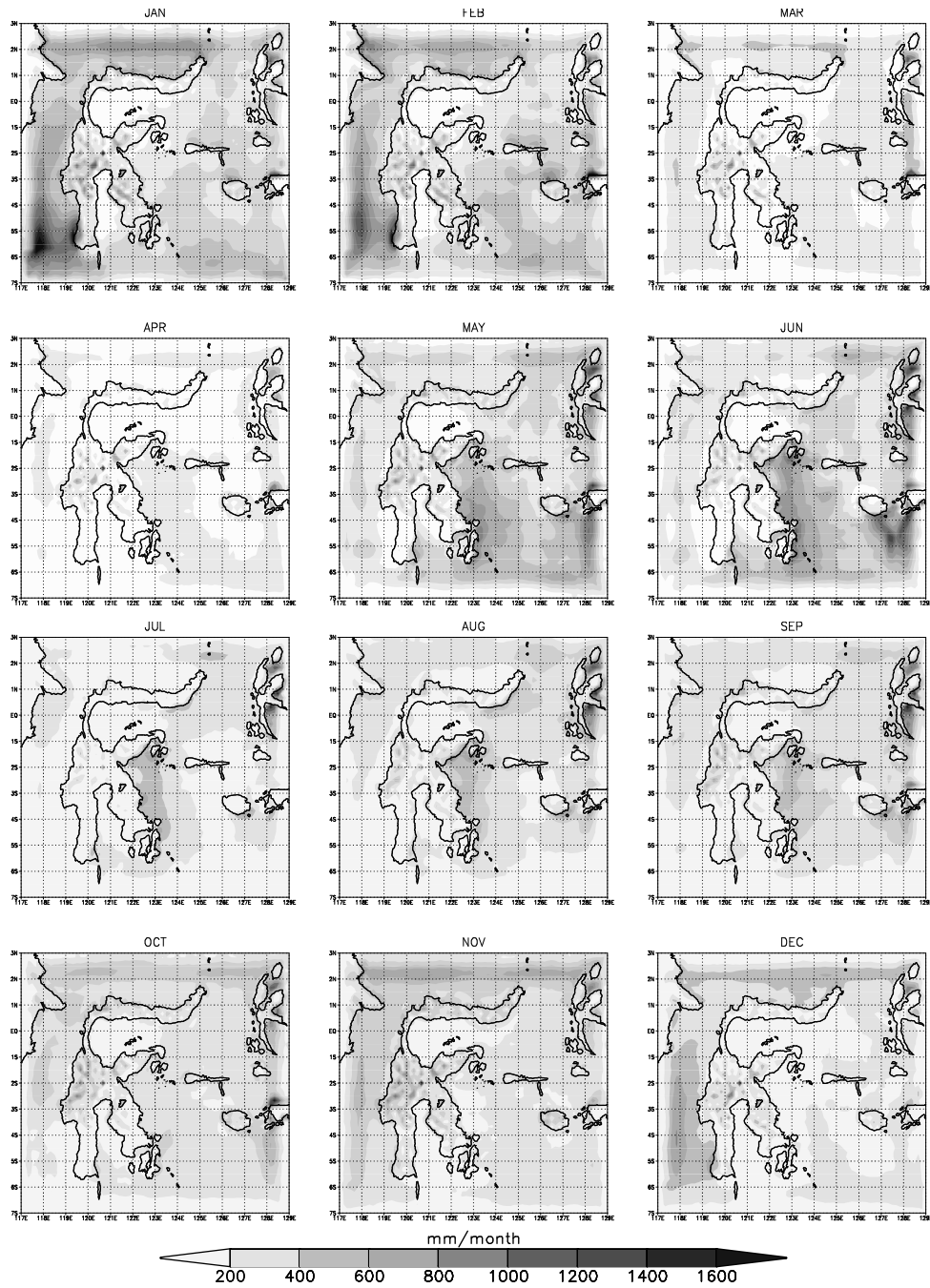


Figure 3.6: REMO 1/6 modelled monthly mean rainfall rate derived from accumulated 6-hour rainfall rates. The time period for monthly mean rainfall is 1979 to 1999.

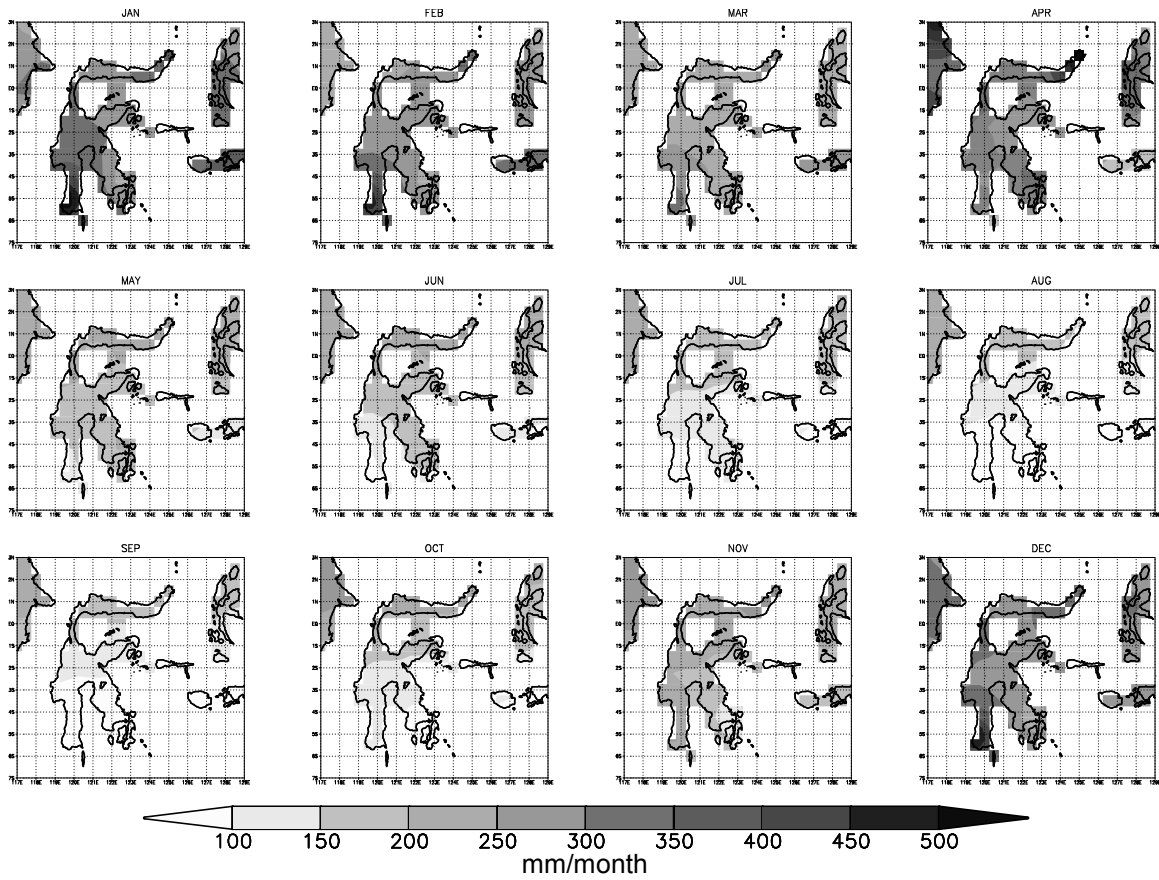
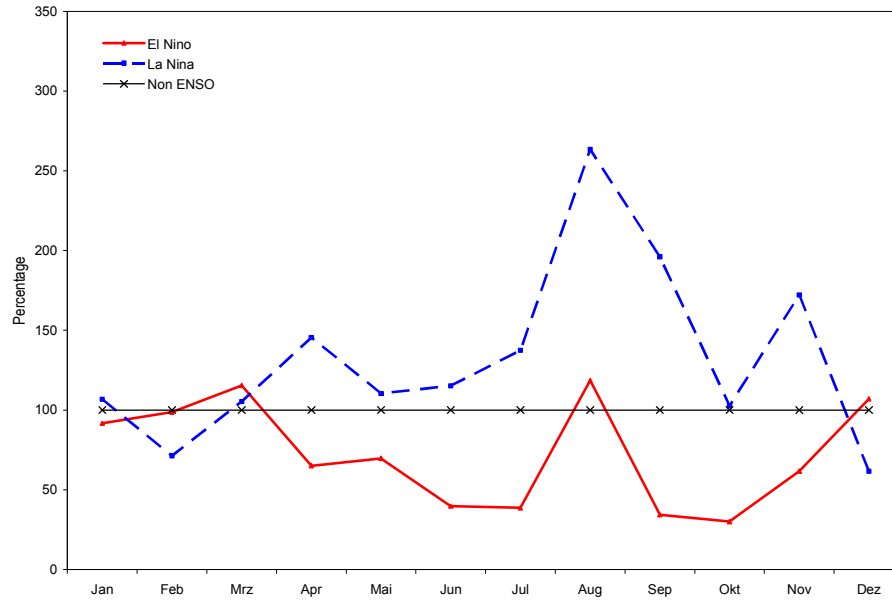


Figure 3.7: As in Fig.3.6, but for GPCP monthly mean (1980 -1999) rainfall.

a)



b)

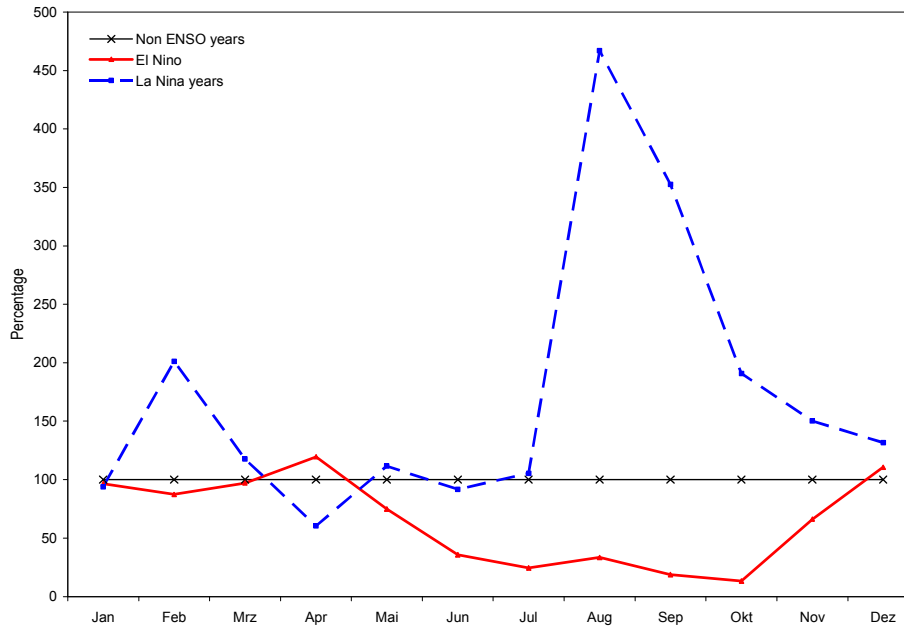


Figure 3.8: Monthly relative rainfall rates in South Sulawesi (1979 to 1993) during El Niño-, La Niña- and Non-ENSO years in % of Non-ENSO year rates. a). REMO model, b) measured.

The two pair of graphs indicates the similarity of the modelled and measured rainfall pattern: low rainfall during the dry season of the El Niño years and high rainfall during the dry season of the La Niña years. The months that are affected by ENSO events fall in the period of the Australian monsoon. In South Sulawesi the lower rainfall periods as an impact of El Niño simulated by REMO (Figure 3.8a) occurred from April to November, while observed data (Figure 3.8b) show that the low rainfall occurs from May to November. The relative higher rainfall as an impact of La Niña is simulated between May to November whereas as observed between May to October. In Central Sulawesi the low rainfall during the El Niño years occurs in the period of April to November as simulated by REMO (Figure 3.9a) whereas according to observation it occurs during the period of May to October (Figure 3.9b). In the La Niña years, the high rainfall occurs in the period May to October as simulated and in the period of July to November as obtained from rain gauges. In general, the ENSO events are only related to the rainfall variability during the Australian monsoon including the transitional period and do not show any correlation pattern to the rainfall during the Asian monsoon or during the wet season. An exception is observed in Central Sulawesi where some regions have a rainfall pattern of the anti-monsoonal type season (see Chapter 2). In such regions the Australian monsoon causes a wet season. Haylock and McBride (2001) have shown that the rainfall is spatially coherent with ENSO forcing during the dry-transitional seasons [June-July-August to September-October-November (JJA-SON)] for the entire Indonesia region but the rainfall is spatially incoherent during the wet season [December-January-February (DJF)], where there is no significant correlation with ENSO events. Similar results are reported by Kirono and Tapper (1999); McBride et al. (1998); Aldrian (2002); Chang et al. (2004); Gunawan and Gravenhorst (2005b); Juneng and Tangang (2005).

Spatial distributions of REMO model rainfall anomaly during El Niño and La Niña for selected ENSO events are depicted in Figure 3.10 and Figure 3.11 respectively. An El Niño event is represented by the year 1987 whereas La Niña is represented by the year 1999. Since most periods affected by ENSO are between April to October as discussed in previous paragraphs, the monthly evolution of ENSO-affected rainfall distribution is

displayed for this period only. Rainfall anomalies due to ENSO events are represented by the relative different of the rainfall amounts during an ENSO event and during the entire simulation period. Thus rainfall deviation/anomaly in any month in a year is calculated as follow:

$$RainAnom_{m,y} = \frac{rain_{m,y} - rain_{m,ave}}{rain_{m,ave}} \times 100$$

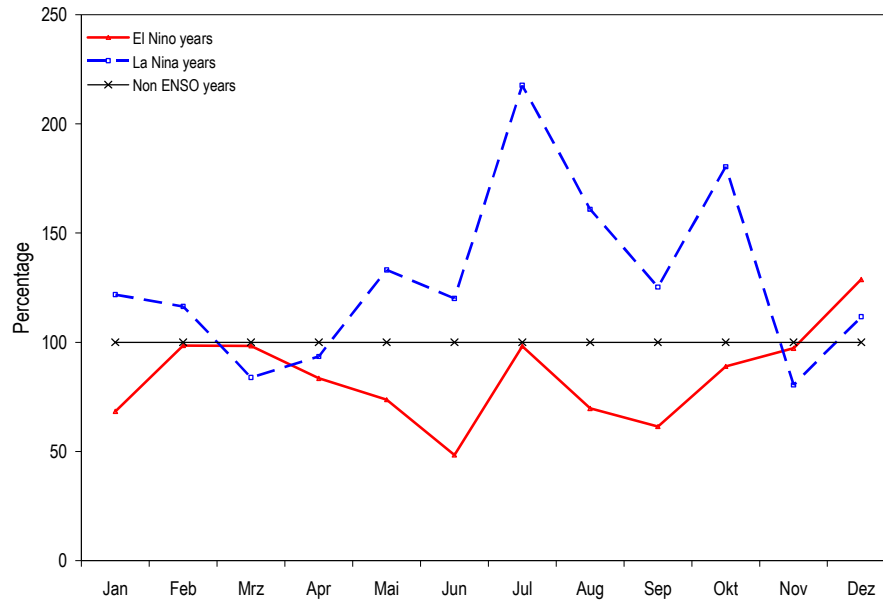
where,

$RainAnom_{m,y}$  = rainfall anomaly at month m of ENSO year y,

$rain_{m,y}$  = monthly rainfall at month m of ENSO year y

$rain_{m,ave}$  = monthly rainfall at month m averaged over REMO simulation period.

a)



b)

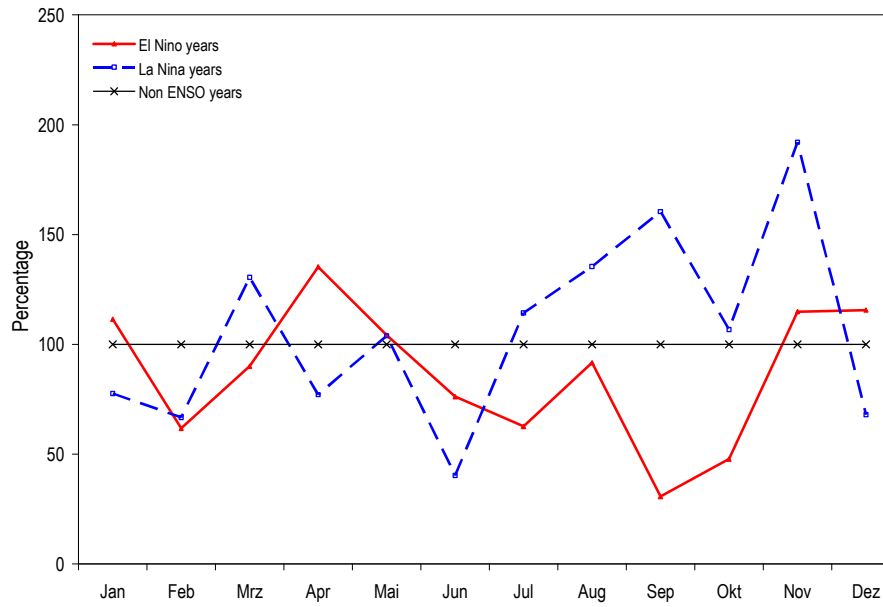


Figure 3.9: Same as Figure 3.8 but for Central Sulawesi.



From Figure 3.10 it is obvious that during an El Niño event the rainfall has a negative deviation and reduces to 80%. Figure 3.11 represents the monthly evolution of the REMO model rainfall for the same period as in Figure 3.10 and additionally for the year 1999 as a representation of a La Niña year. Positive deviations reach up to more than 70% occurring during the period from May to October. It is first detected in some areas of Central Sulawesi, and then spread out to the east, south and south east of the island in June. These situations were maintained until October and afterwards the positive deviation decays in November and in December.

The rainfall anomaly in the ENSO-impact period affects the interannual variation. It is the typical impact of the ENSO on rainfall. The ENSO events characterize the atmospheric for more than half a year because it not only changes the intensity of rainfall decrease, but also prolong the dry season period. Therefore it is justified to compare rainfall amount for entire years. The variation of annual rainfall for the REMO simulation and GPCC within the period 1986 to 1999 over Sulawesi Island is displayed in Figure 3.12. Interannual rainfall variation due to the impact of ENSO is well observed in this figure. The La Niña year 1999, for instance, is the wettest year among the La Niña events such as in 1988 and in 1996 and appears in both the REMO and GPCC datasets. The dry years associated with El Niño events took place during the years 1987, 1991-1994 and 1997.

A large difference in the amount of rainfall for entire Sulawesi between REMO and GPCC occurred in 1994. For this period REMO predicts up to 700 mm/year more than GPCC. The same situation occurred for the El Niño year 1997 with a difference of 341 mm. The smallest difference occurred in 1996 with a difference of 12 mm. The REMO model underestimated most of the annual rainfall during the period 1986 to 1999 (see Table 3.1).

Table 3.1: The difference of annual rainfall (mm) between the GPCC and the REMO model rainfall.

Year	GPCC	REMO	REMO-GPCC
1986	1910	1940	29
1987	1714	1628	-86
1988	2531	2152	-379
1989	1940	1919	-22
1990	1569	1529	-40
1991	1461	1270	-191
1992	1171	1442	271
1993	1542	1456	-86
1994	1543	2243	701
1995	2384	2553	169
1996	2498	2486	-12
1997	1489	1830	341
1998	2448	2352	-96
1999	2724	2598	-126

It is calculated from Table 3.1, the mean annual rainfall during the entire simulation period (1980 – 1999) is 1957 mm from the REMO model and 1923 mm from observed data (GPCC). The mean annual rainfall during the El Niño years composite is 1714 mm for the REMO model and 1574 mm for observations respectively. Within the La Niña years composite the mean annual rainfall simulated by REMO is 2412 mm and from observations is 2584 mm. In other words we conclude; on El Niño (La Niña) year the REMO model rainfall is higher (lower) than the GPCC observed data. All situations of rainfall variability corresponding to ENSO events are summarized in Figure 3.13. In the relatively dryer El Niño years the REMO model overestimated the rainfall amount compared to the GPCC. During the relatively wet La Niña years the REMO model was underestimated the rainfall amount compared to the GPCC rainfall distribution. This shows that the REMO model is able to catch the trend from year to year correctly; however it may tend to underestimate the degree of the rainfall anomaly due to ENSO events compared to the ground-based point measurements extended to large areas. It probably the parameterization of precipitation does not catch the extreme wet and dry situations in the adequate manner.

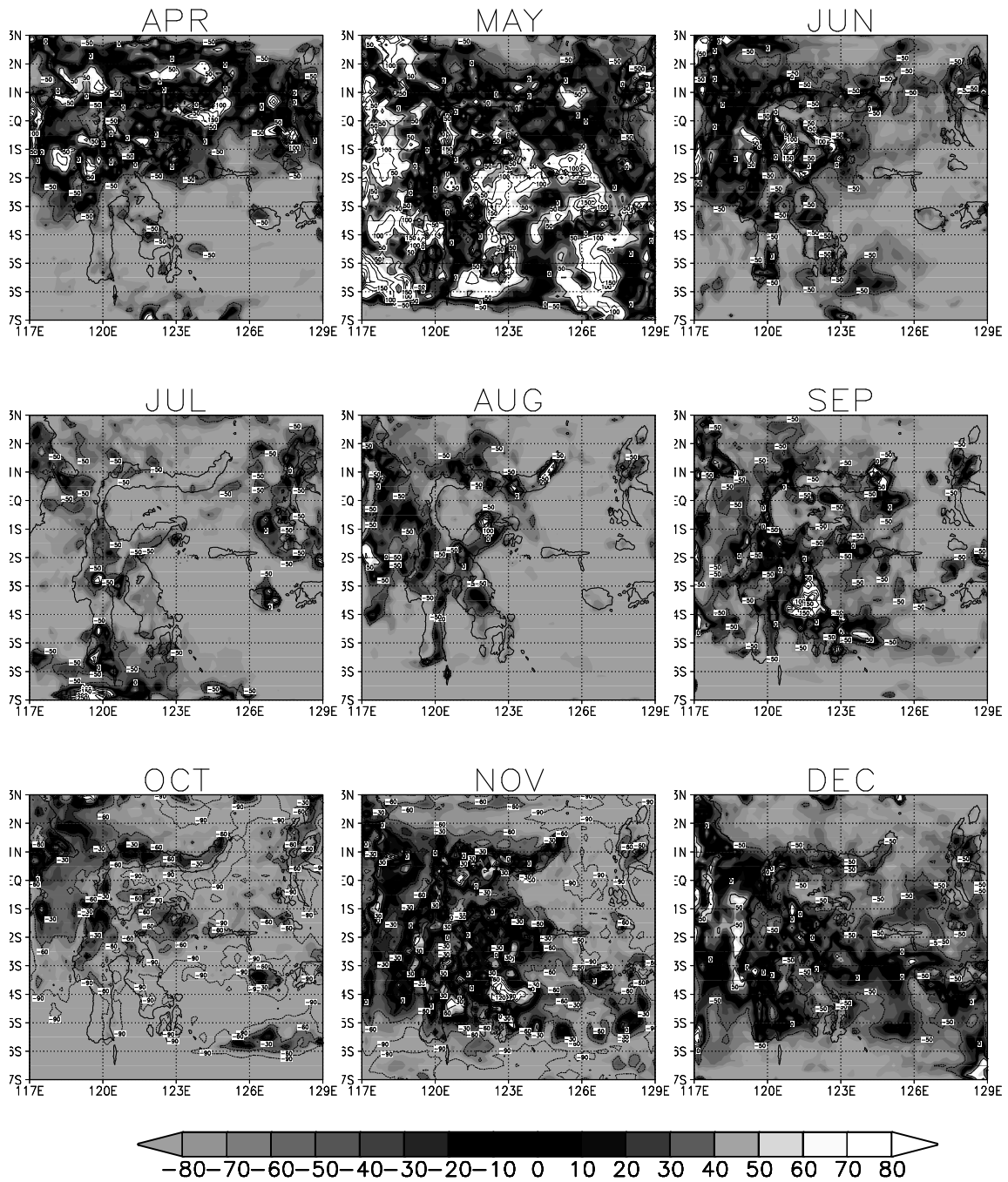


Figure 3.10: Monthly deviation (percentage) of all year average rainfall of REMO model during a strong El Niño event. The figure only displays data from April to December 1987.

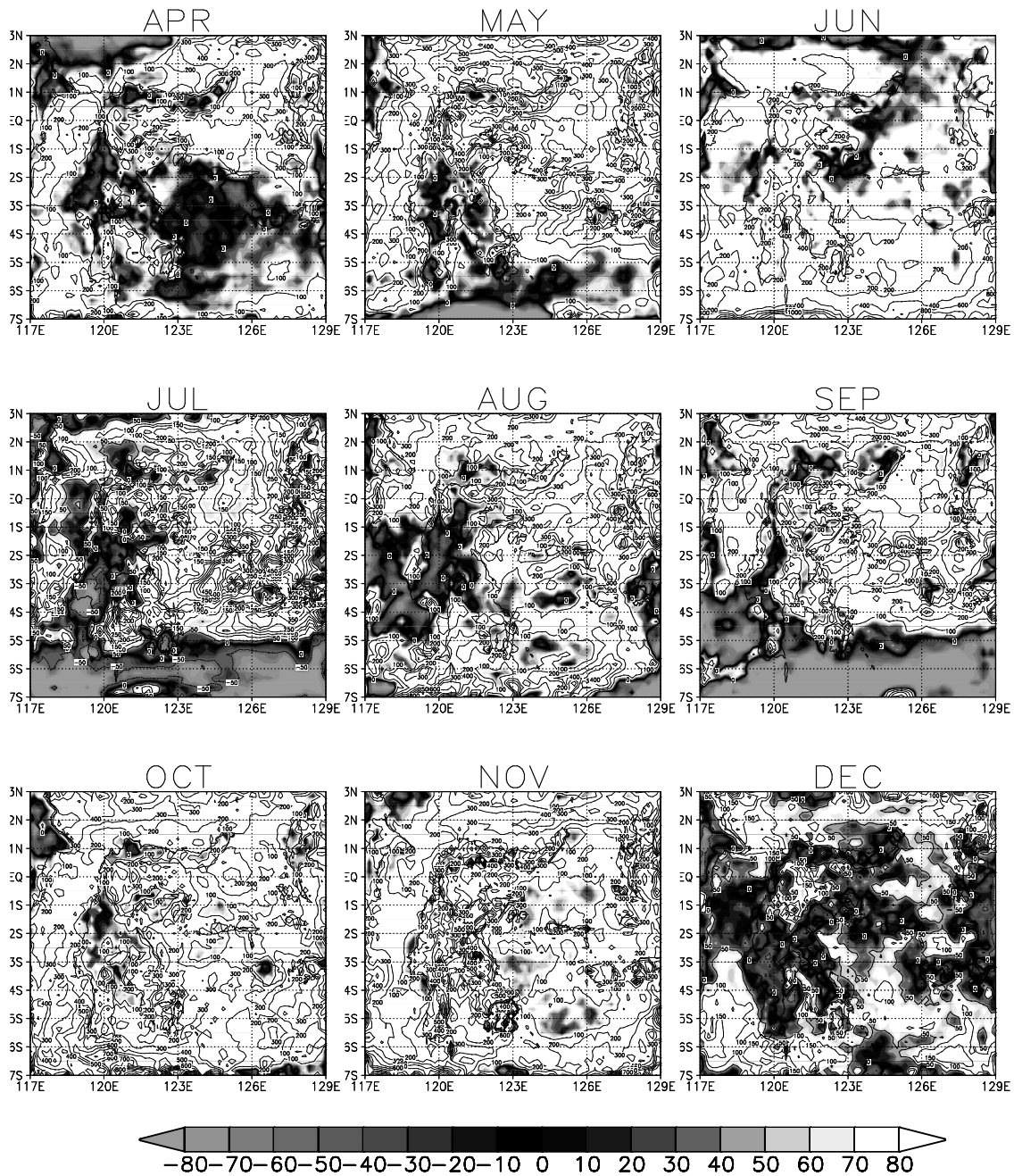


Figure 3.11: Same as Fig. 3.10, but for a strong La Niña event in the year 1999.

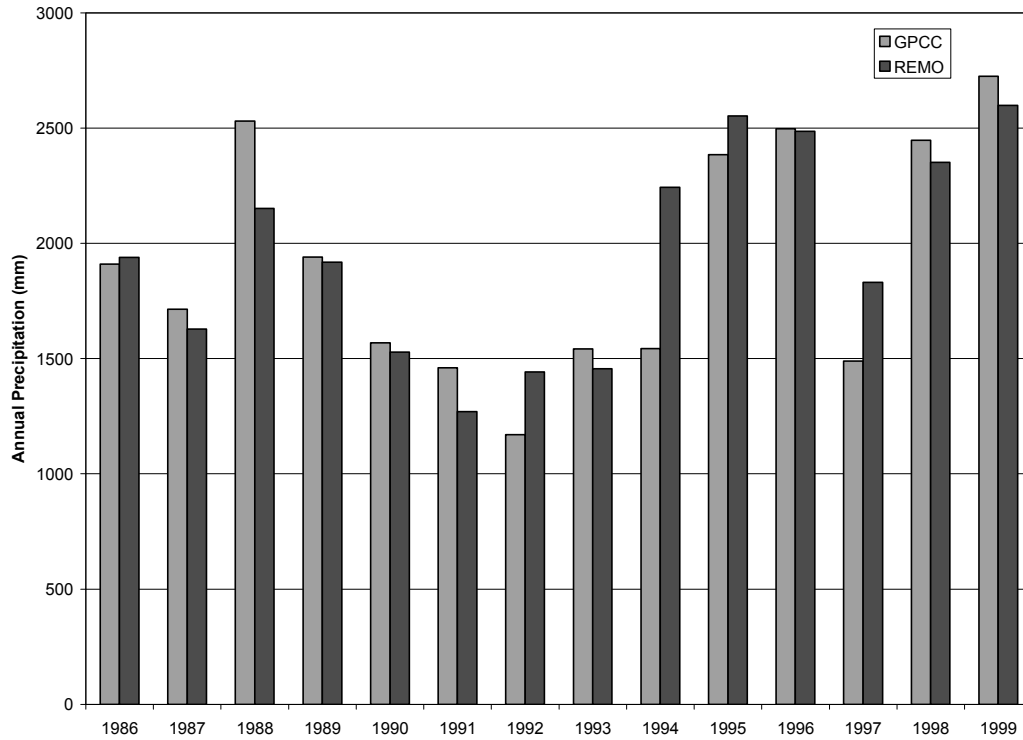


Figure 3.12: Annual rainfall rates ( $\text{mm year}^{-1}$ ) simulated by the REMO model (dark grey) and measurement derived rainfall amounts (GPCC, light grey) for the period 1986 to 1999 over the land area of the REMO model domain (entire Sulawesi).

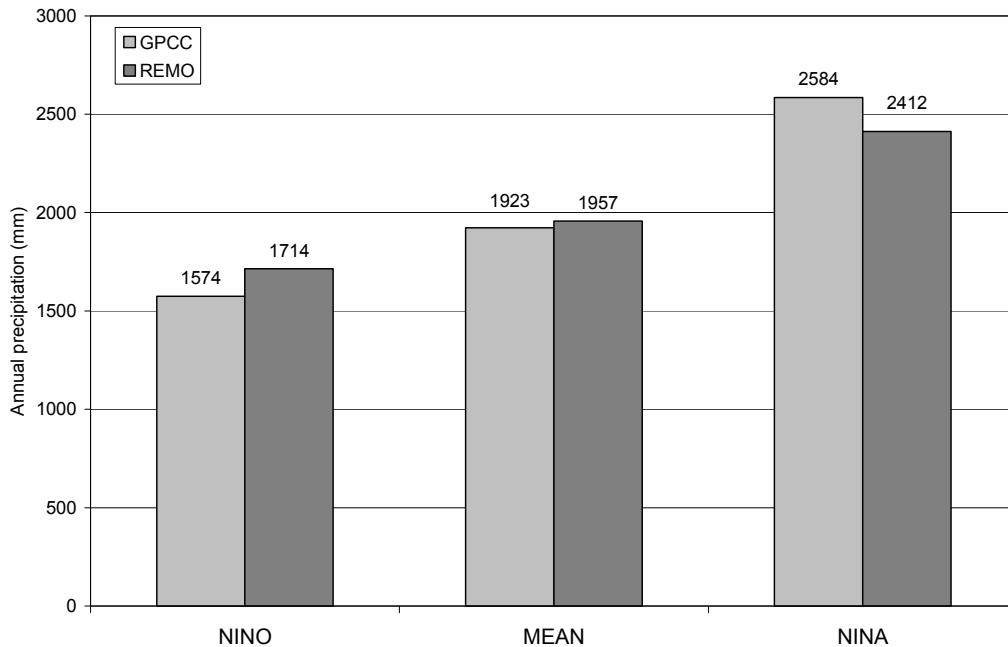


Figure 3.13: Annual rainfall rates in millimetres per year over the land area of the REMO model domain during different types of ENSO events and on average. Left bars are in El Niño years, centre bars are averaged over simulation period and right bars are in La Niña years. The dark grey bars represent the REMO model results and the light grey bars represent the GPCC rainfall values.

As a hydrostatic model, REMO 1/6° does not consider the vertical acceleration in updraft air masses to form rainfall. The vertical acceleration should be a significant factor in intensive convection processes, occurring at extreme conditions such as La Niña events. In South Sulawesi the onset of the lower rainfall period caused by the El Niño in the REMO model is one month earlier than the measured rainfall. The high rainfall period indicated by the La Niña in the REMO model is one month longer than the period of observed data. In Central Sulawesi, the REMO model data has a clear monthly pattern with low (high) rainfall as the impact of El Niño (La Niña) during the dry season whereas from the observed data, the pattern of impact only appears in a short period during the dry season.

### 3.4. Concluding remarks

In this chapter the Regional Atmospheric Model REMO with 1/6 degree or about 18 km horizontal resolution was used to simulate the rainfall amount during the period of 1979 to 1999 for Sulawesi domain (Figures 3.10 to 3.12). The time resolution of model output is hourly. The hourly values are accumulated to a daily rate and finally summed up to get monthly amounts. These monthly rainfall values were related to ENSO events. The REMO model rainfall climatology was compared with the GPCC rainfall climatology for the land part of the study area. The results showed a general agreement in terms of spatial and time distribution pattern.

It is shown from this study that the regional atmospheric model REMO 1/6° simulated monthly rainfall variation in agreement with observed data. Rainfall amount can, therefore, be looked upon as a successful indicator of the model performance. In the South Sulawesi sub domain the 12-month running correlation gave higher values compared to the Central Sulawesi sub domain. By comparing results of rainfall between the two sub regions which are topographically different showed that model REMO simulated the rainfall closer to the observations in the relatively flat region such as in South Sulawesi compared to the topographically complex area such as in Central Sulawesi. The mismatch in the topographically more complex region can be caused by an oversimplification of the topography in the REMO model but can also be caused by the difficulties arising from the lack of sufficiently representative observational data.

During the El Niño events, the rainfall rates were lower than that of non-ENSO year seasons. This was true in the two investigated sub domains. With respect to the annual amount evaluated from years 1986 – 1999, the REMO 1/6° simulation results were lower than measured in 9 years out of the 14 years period. These occurred in years 1987-1991, 1993, 1996, 1998 and 1999 (Table 3.1). This nine ENSO years are therefore well represented in the trend but not represented in absolute values.

ENSO phenomena are extreme events. In the El Niño years which are dryer than average, the REMO model overestimated (9%) and in the La Niña years which is wetter than average the REMO model underestimated (7%) the rainfall amount compared to the measured and extrapolated GPCC rainfall amount.

In the next Chapter, the study of rainfall variability using other sources of data i.e. satellite-based estimate will be performed. Inevitably some repetition may occur in the REMO and ground-based data description and usage.



## CHAPTER 4

### COMPARISON OF LONG-TERM SIMULATED, GROUND-BASED AND SATELLITE –BASED RAINFALL ESTIMATES FOR INDONESIA AND SULAWESI

#### *Abstract*

*This chapter describes the comparison of a long-term REMO model simulation rainfall amounts, ground-based observed and satellite-based estimate rainfall amounts over the Indonesian continent as well as over Sulawesi Island. The simulation period includes some ENSO events, which are the focus of this comparative study.*

*Monthly temporal and spatial rainfall amounts agree well among the three datasets during the Australian monsoon periods. High correlations are obtained in the period August to November which in general makes up the dry season period.*

#### 4.1. Introduction

Rainfall in the tropics is an interesting weather parameter due to its high variation in space and time. In a practical way, this parameter also plays an important role in biotic and abiotic processes in terrestrial ecosystems like agriculture crops and natural rainforest. To study the rainfall variability in Central Sulawesi, Indonesia is in particular interesting because this area is located at the equator. And, due to orographic factors, the climate regime varies very strongly over a short distance from a semi desert climate to tropical rain forest climate in the Palu area.

Several methods exist to analyze station rainfall data for their spatio-temporal distribution. The cluster analysis is a method to group rainfall data at different sites spatially and temporally according to their pattern. This has been done in Chapter 2. The Global Rainfall Climatology Centre, GPCC (Rudolf et al., 1994) performed a rainfall regionalization using the Cressman method to obtain rainfall data in several regular grid resolutions (0.5°, 1° and 2.5°). The GPCC used station data collected from all available data over the globe but for this study the data for Indonesia was used. In a similar way but using data from satellite-based measurements the Global Rainfall Climatology Project, GPCP (Huffman et al., 2001) estimate also rainfall amount in time and space. Both these centres closely collaborate in order to provide the gridded data sets for validation of atmospheric models as well as for monitoring rainfall variability.

The satellite-derived rainfall estimate has a big advantage over a network ground-based rain gauges distribution in Central Sulawesi. Satellites can cover and observe the entire cloud and rain covered surfaces. Another way of studying rainfall variability is using an atmospheric model which has the same advantage of the coverage area as the satellite observation. Both the satellite and atmospheric model data sources could be use as a tool to study rainfall variability in remote area which can not be covered by ground-based observations in inaccessible areas. Before it is applied to such a

study, data has to be verified with the rain gauge observations; since rain gauges remain the standard source of rainfall estimates (Margulis and Entekhabi, 2001). This chapter is addressed to the study of rainfall data comparison derived by satellite sensors, the output of numerical regional atmospheric model, REMO and ground-based observation. The non-existence of a dense rain gauge network in Central Sulawesi as is mentioned in the Chapter 2 was the reason for using satellite data as a complement data for the study of rainfall variability.

A hypothesis was made for this chapter that the rainfall estimate based on the satellite borne instruments can represent the rainfall at any time in Central Sulawesi. The ground-based rainfall measurement is considered as the reference data in this comparison study.

## 4.2. Material and methods

### 4.2.1 Data sources

There are two classes of information that have been inferred from satellite radiation measurements. The Global Rainfall Climatology Project (GPCP): infrared and microwave algorithms (McCollum et al., 1999). Infrared algorithms are based on the relationship between the rainfall rate and cloud-top temperature, as low temperatures are usually associated with deep convective clouds, which account for much of the rainfall in the tropics. The GPCP infrared algorithm, the GOES Rainfall Index (GPI; Arkin and Meisner 1987), is primarily based on infrared data from geostationary satellites, which have the advantage of high temporal resolution, i.e. 3-hour sampling. Data from the NOAA Advanced Very High Resolution Radiometer (AVHRR) is used, if necessary, to fill the gaps of missing geostationary satellite data.

The second class of satellite algorithms used by GPCP is based on the data of the Special Sensor Microwave Imager (SSM/I) aboard the Defence Meteorological Satellite Program (DMSP) satellites. The GPCP uses both an emission (Wilheit et al., 1991) and a scattering algorithm (Ferraro, 1997). The emission algorithm is used over

the ocean only, because it is based on the microwave emission of microwave radiant energy by raindrops, which can be detected over the low-emissivity ocean surface. The scattering algorithm is based on the depletion of the upwelling radiation due to scattering by large ice particles. This scattering algorithm is applicable over land and ocean, but the GPCP applies it only over land where the emission algorithm is not useful because of the lack of emissivity contrast between the surface and rain clouds. The microwave algorithms have the disadvantage of less frequent temporal sampling than the infrared algorithm because the SSM/I data is collected by the polar-orbiting DMSP satellites, which observe a point on the earth at most two times per day. The satellite-based rainfall data used in this study has been obtained from the NOAA/NESDIS/Office Research and Application/Atmospheric Research and Application Division/Hydrology Team. The one degree gridded monthly datasets are available online at <ftp://orbit.nesdis.noaa.gov/pub/corp/scsb/rferraro/ncdc>. An overview of these data products can be found in Ferraro et al. (1996).

The Global Rainfall Climatology Centre (GPCC), which is operated by the Deutscher Wetterdienst (DWD/National Meteorological Service of Germany), is a component of the Global Rainfall Climatology Project (GPCP) with the main emphasis on the evaluation of global ground-based rainfall observations. The GPCC simultaneously contributes to the Global Climate Observing System (GCOS) and other international research and climate monitoring projects (e.g. ISLSCP, 2004). This data set of ground-based measurements was acquired from the GPCC and resampled to 0.5 degree grid boxes for use in the International Satellite Land Surface Climatology Project (ISLSCP) Initiative II. The GPCC collects rainfall data which is locally observed at rain gauge stations and distributed as CLIMAT and SYNOP reports via the Global Telecommunication System (GTS) of the World Weather Watch of the World Meteorological Organization (WMO). The Center acquires additional monthly rainfall data from meteorological and hydrological networks which are operated by other national services. Observed rain gauge data from Central Sulawesi is included in the datasets of the Center (Rudolf, 2004 pers.comm.). The rain gauge analysis is produced

by interpolating the data to a 0.5 degree mesh using the Cressman method (Rudolf et al., 1994; ISLSCP, 2004; Beck et al., 2005). These data are used for comparison with REMO model results and GPCP satellite-derived rainfall data.

The REMO 0.5° rainfall data that is used for this comparison over Indonesia is available at the MPI-M Hamburg (Aldrian, 2003 pers.comm) and explained in Aldrian et al. (2004). Data from the REMO 1/6° model is used here as they have been described in Chapter 3.

#### 4.2.2 The regional atmospheric model (REMO)

The regional atmospheric model, REMO (Regional Model) 0.5° was developed from a Numerical Weather Prediction model used operationally by the German Weather Service (DWD). It was formerly named EM (Europa Modell). The REMO model has been explained in Chapter 3.

#### 4.2.3 Statistical methods

Spatial correlations were performed using GrADS software and the calculation was conducted on line at <http://climexp.knmi.nl/>. The ground-based gridded rainfall, GPCC and the satellite-derived gridded rainfall, GPCP data sets have the grid resolution of 0.5° and the REMO model has the grid resolution 1/6°. The spatial correlation was confirmed with the REMO model resolution. In order to obtain the time series for temporal correlation, all data sets are aggregated to the REMO 1/6 model domain i.e. in the area of 117°E-129°E ; 7°S – 3°N.

### 4.4. Results

A comparison of monthly rainfall amounts over Indonesia for August 1992 between the three data sets is shown in Figure 4.1. The REMO model rainfall value agrees

more with GPCC data set than Satellite data. Over the sea REMO is only compared with the Satellite data set. Figure 4.1 shows that rainfall rate agree up to 300 mm/month values and are not comparable at values greater than 300 mm/month, especially over the sea area southwest of Sumatra Island.

Spatial correlation of monthly rainfall between REMO 1/6° and GPCP (Satellite) and between REMO 1/6° and GPCC over Sulawesi Island are shown in Figure 4.2 and Figure 4.3 respectively. A high correlation mainly occurs in the period from August to November. The period coincides with the Australian Monsoon and which is normally at this time the dry season period. Correlation between REMO 1/6° and satellite include the sea region is shown in Figure 4.2. The temporal and spatial correlation pattern over the land is similar to the GPCC correlation. Over the sea, the high correlation is almost surrounding the archipelago.

The time series of regionally averaged data for Sulawesi Island from REMO 1/6°, GPCC and Satellite datasets are shown in Figure 4.4. The large variation between the three data sets occurs at the rainy season (November to February) which reaches differences of up to 200 mm/month in comparison to the REMO and satellite data set. The result is consistent with the report of Rudolf (2000) which compared the GPCP-Version 2 and CMAP (The Climate Prediction Centre Merged Analysis of Rainfall) data set the over of the south equator the eastern Indonesia/tropical Pacific. In the dry season (between July to September) comparison of the three pairs of dataset has a good agreement.

The comparison between REMO and Satellite data results in a correlation coefficient of 0.70. The comparison between REMO and GPCC has a correlation coefficient of 0.72, and the comparison of the measurement between satellite and rain gauge (GPCC) data has correlation coefficient of 0.86. The comparisons of these three data sets are plotted in Figure 4.5. As they are examined from time series (Figure 4.4) and

scatter diagram (Figure 4.5), the satellite yields lower values than in comparison with REMO and GPCC.

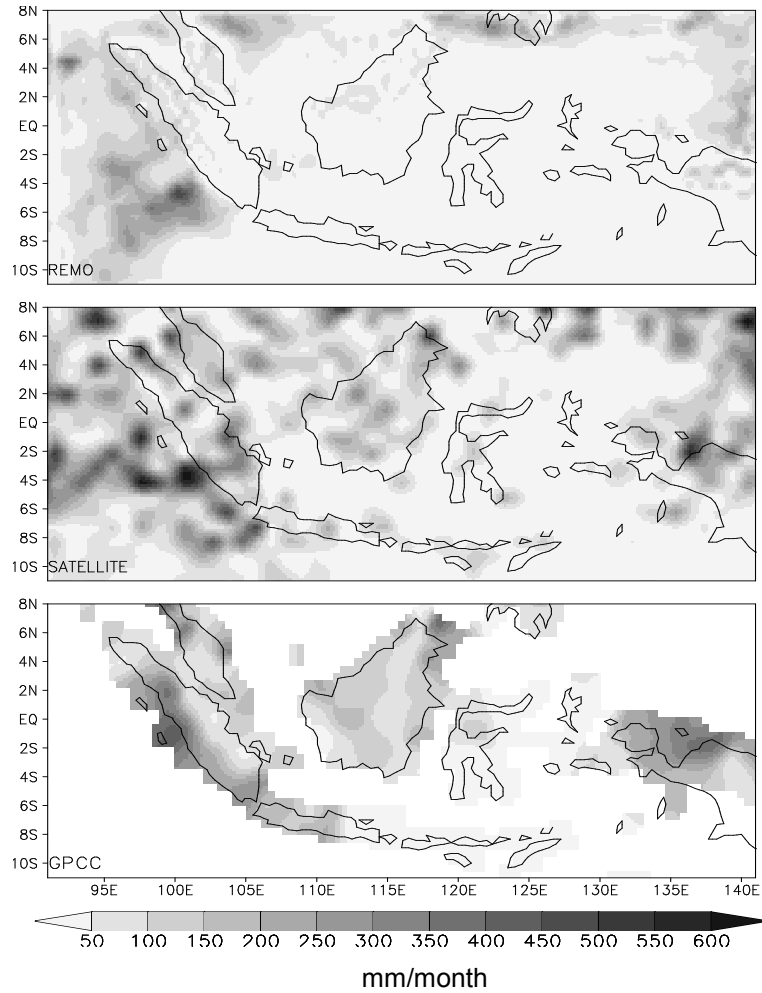


Figure 4.1: Spatial comparison of rainfall rates for August 1992 between model REMO 0.5° results (upper), satellite derived values (middle) and values derived from ground-based measurement by GPCC (bottom) for Indonesia Maritime Continent. Unit is in mm/month. Pixels size is 0.5° by 0.5°.

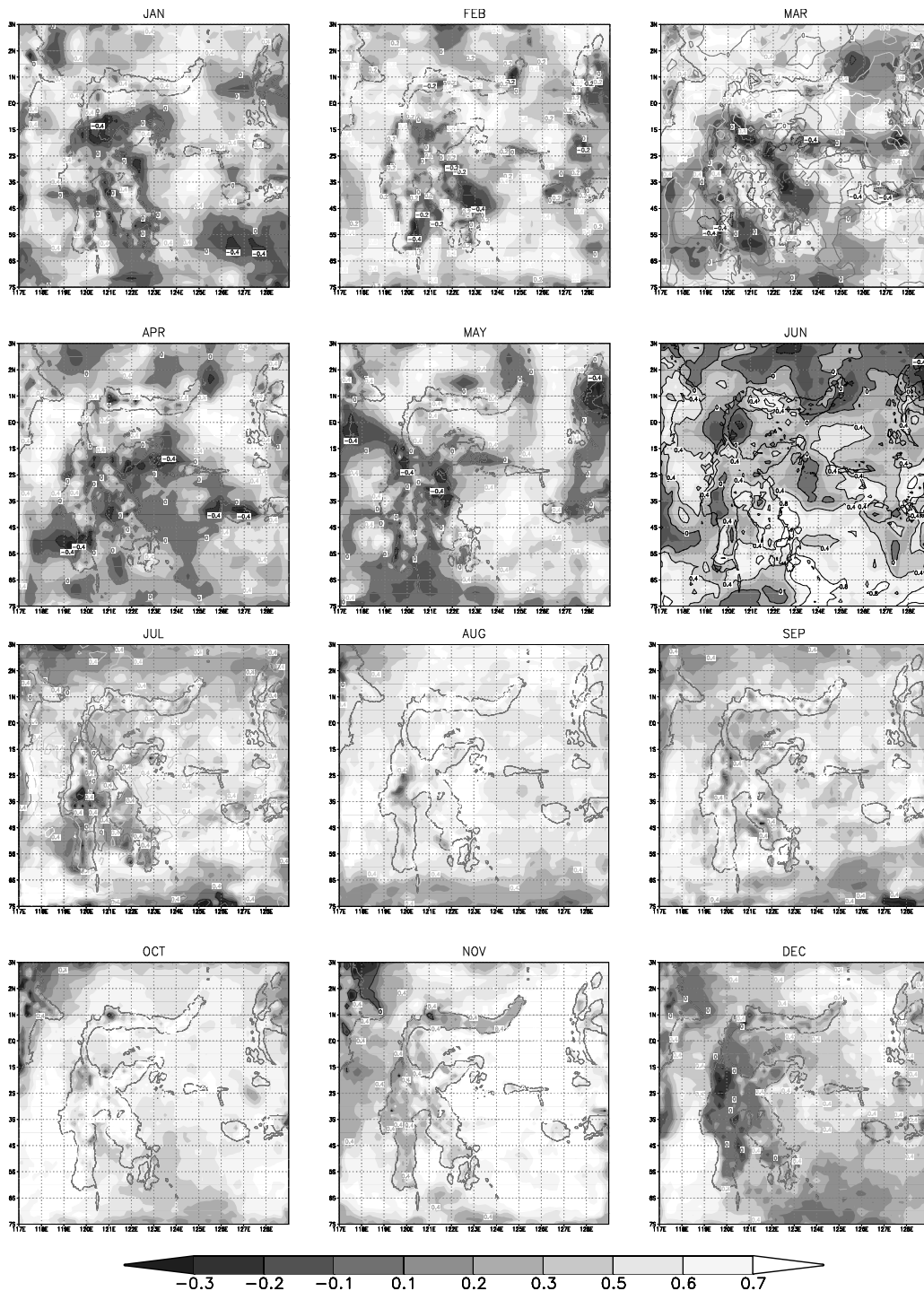


Figure 4.2: Correlation coefficient between the REMO 1/6° model rainfall and the satellite-based estimate for Sulawesi Island. The years 1986 to 1999 were used for the correlation analysis.



The simulated rainfall data is used to study rainfall variability in relationship with ENSO. For this purpose, modelled data from REMO and observed data from GPCC are plotted in time-longitude slice (Hovmöller diagram) as are shown in Figure 4.6.

The evolution of the ENSO impact is analyzed for the REMO 1/6 domain, i.e. the entire Sulawesi Island (117°E-129°E; 6°S-3°N). The left panels of Figure 4.6 are time-longitude contour plots of REMO rainfall data and the right panels depict the GPCC data, respectively. During the El Niño event 1982/1983 all regions receive less than 100 mm/month in the REMO 1/6° simulation, i.e. less than the average rainfall. In all other prominent El Niño events (1986/1987, 1991/1992, 1993, 1994 and 1997/1998) both the REMO simulated rainfall and the GPCC ground-based rainfall correspond very well with significant negative SOI. Negative values of SOI, i.e. indication of El Niño events, correspond to decreases in monthly rainfall down to less than 100 mm/month.

Using GPCC 1° by 1° rainfall data from 90°E (through 180°) to 90°W, Kidd (2001) illustrated the effects of El Niño/La Niña in the zonal evolution of rainfall on the global scale. For the longitudes between 120°E and 130°E, which is close to our study area, he noted that the general seasonal pattern of rainfall can be characterised as relatively wet from November to February and as relatively dry between March and October. This pattern is interrupted in 1983, 1988, 1992, 1993 and 1998 by El Niño episodes.

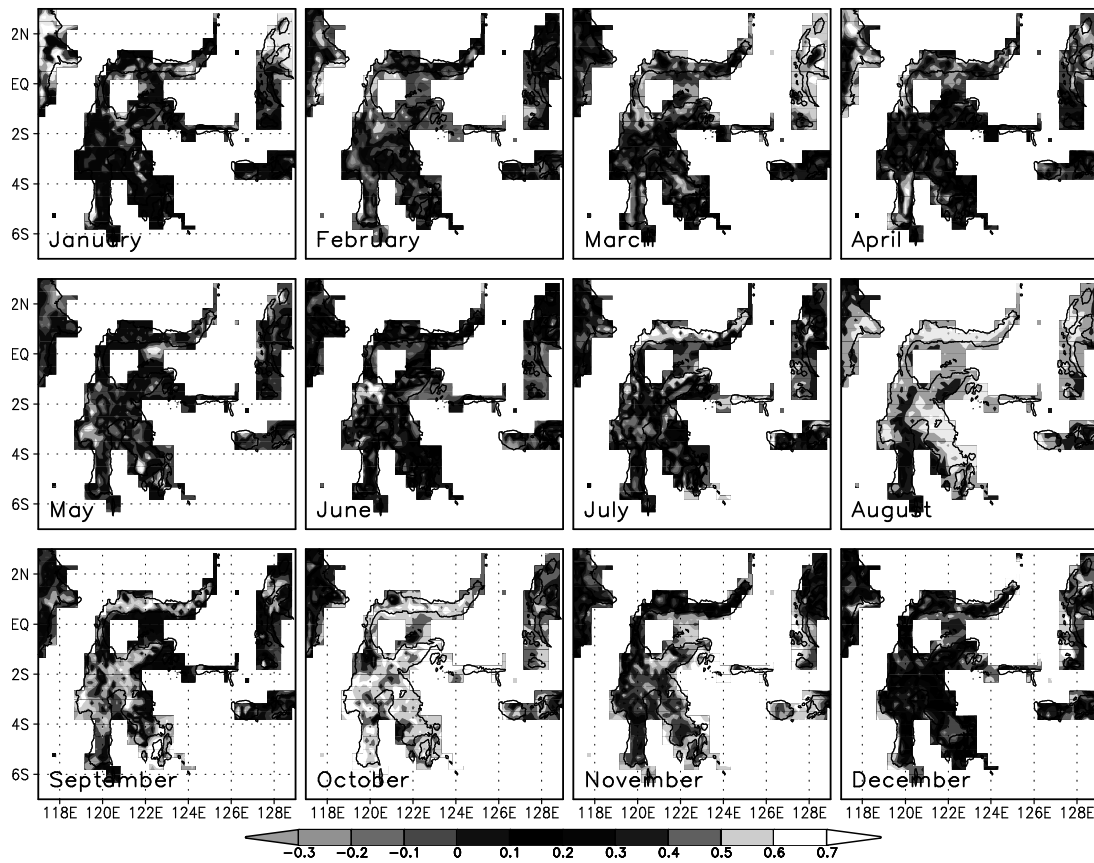


Figure 4.3: Correlation coefficients between the REMO 1/6° model rainfall and the GPCP ground-based rainfall over Sulawesi Island. The comparison period extends over the years 1986 to 1999.

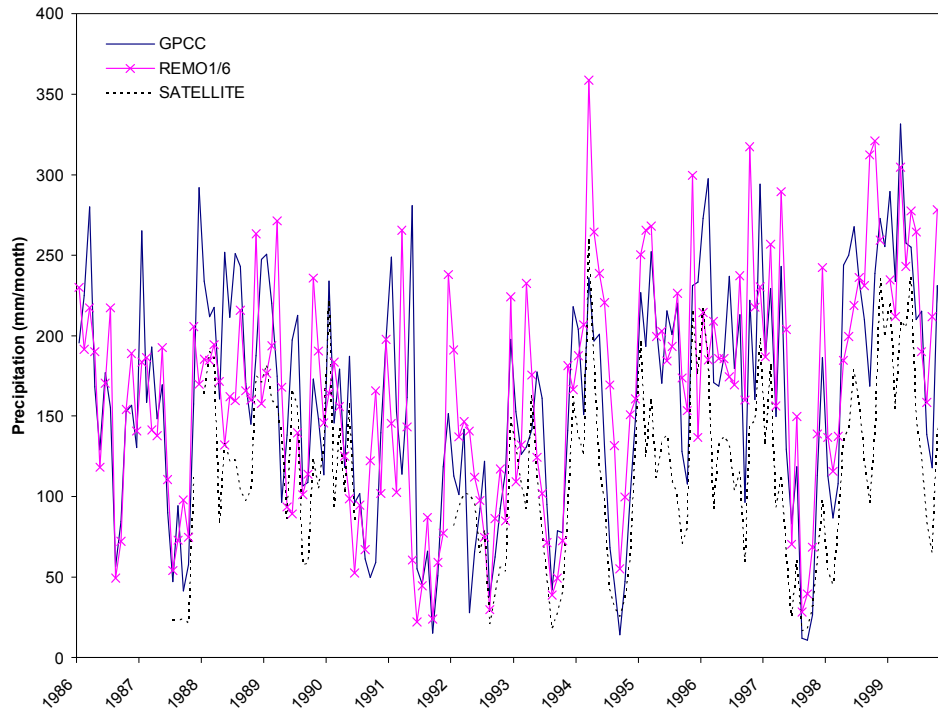


Figure 4.4: Time series of area averaged monthly rainfall over entire Sulawesi area derived from ground-based measurements (GPCP), model simulations (REMO 1/6°) and satellite-derived (GPCP) data.

Figure 4.6 (middle panels) is the time-longitude of monthly rainfall that was simulated by REMO 1/6° and assembled by GPCP 0.5° by 0.5° for the strong El Niño 1987/1988 and the normal years 1989/1990 (Figure 4.6 bottom panel, see [http://www.cpc.ncep.noaa.gov/products/analysis\\_monitoring/ensostuff/ensoyears.shtml](http://www.cpc.ncep.noaa.gov/products/analysis_monitoring/ensostuff/ensoyears.shtml) for the time series and definition of the ENSO years). One can see that from May to October during the El Niño year 1987, rainfall of less than 100 mm/month occurred in the region from 118°E to 129°E. In comparison with the normal year 1989, shows that the zonal average is greater than 150 mm/month. Figure 4.6 (middle panel) shows lower monthly values both in the REMO and in GPCP rainfall data in all meridional sections ranging between 118°E and 129°E during the strong El Niño event of 1987.

Evolution of the ENSO impact in meridional direction on the same area and the same ENSO year cases as in Figure 4.6, are shown in Figure 4.7. Both the REMO model and GPCC data show that during the El Niño events in 1986/1987, 1991/1992, 1993, 1994 and 1997/1998 monthly rainfall was less than 150 mm. Decreased monthly rainfall during these El Niño years was mainly concentrated at latitudes between 2°S and 1°N.

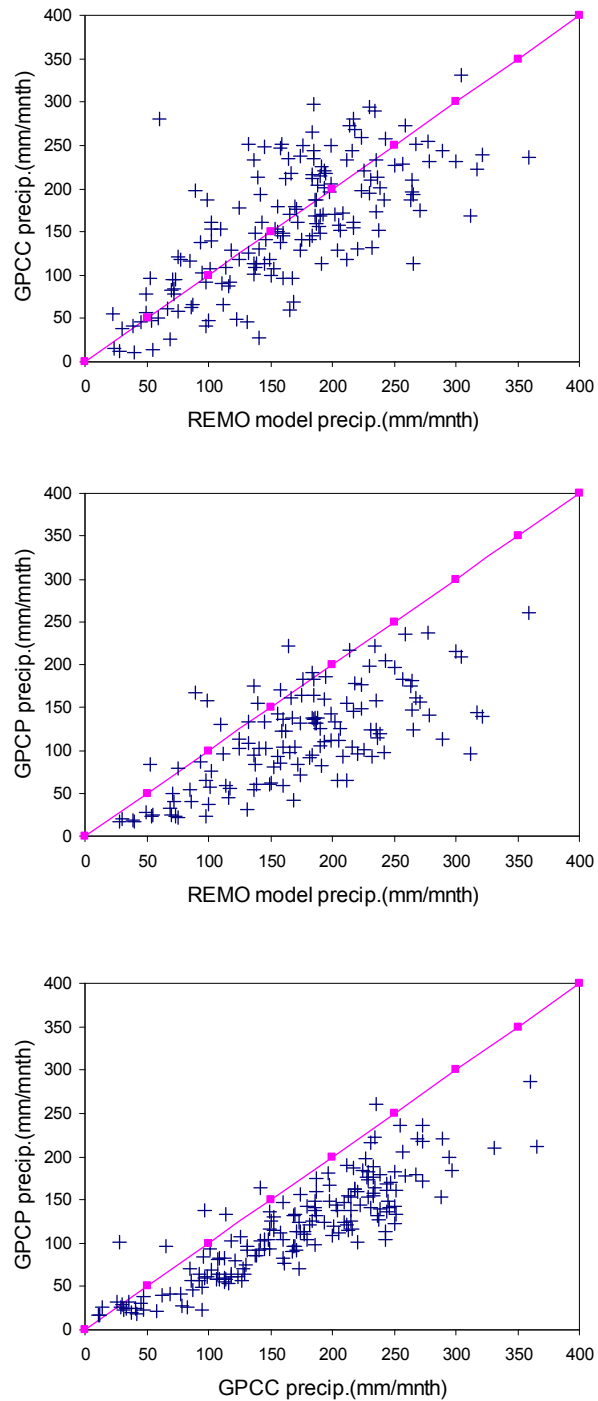


Figure 4.5: Scatter plots between REMO 1/6° model rainfall results and ground-based observed rainfall rates, GPCC (upper), the REMO results and satellite-based estimates (middle) and the observed GPCC rainfall rates and satellite-based estimates (bottom)

for monthly average rates in the time period 1986 to 1999 for the entire Sulawesi Island area.

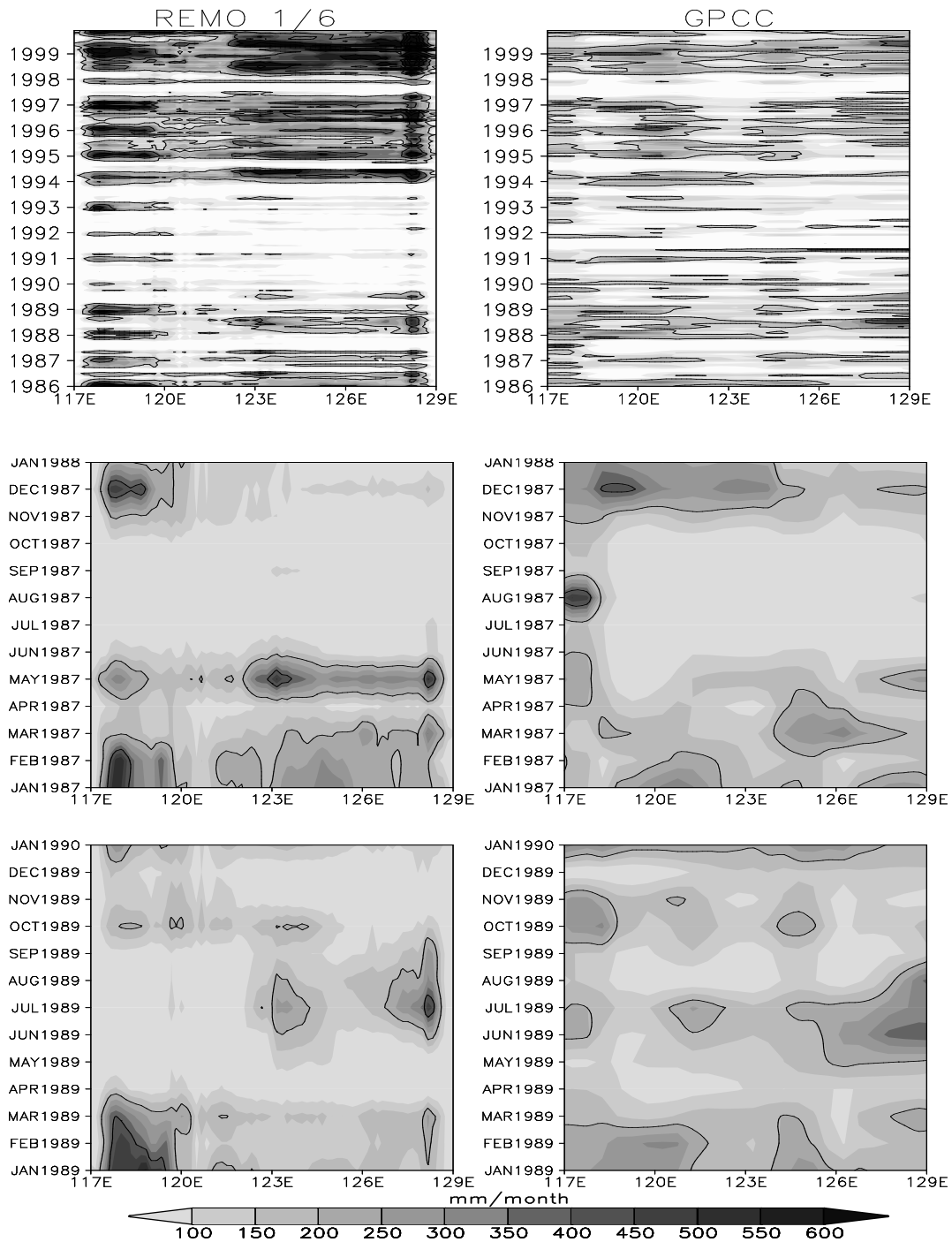


Figure 4.6: Time-longitude diagram (averaged over 6°S-2°N latitude) of monthly rainfall as simulated by REMO 1/6° (left panels) and GPCP gridded observed rainfall (right panels). The upper panel shows the results of the REMO simulation (1986 – 1999, left) and from GPCP (1986 – 1999, right). The middle panel depicts the same but only for the El Niño year 1987/1988 and the bottom panel displays the data for the normal years 1989/1990.

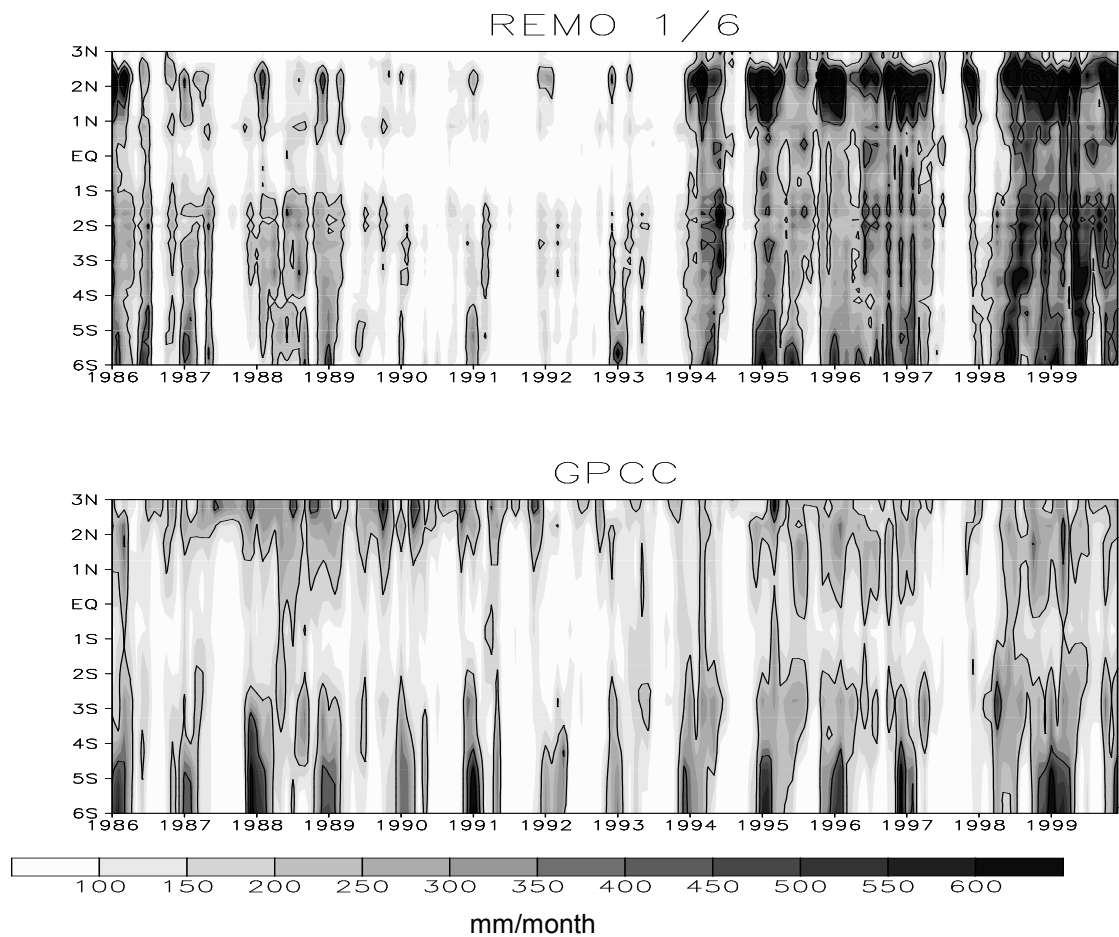


Figure 4.7: Time-latitude diagram of monthly rainfall average over Sulawesi (117°E –129°E) as simulated by the REMO 1/6° (upper) and GPCP gridded rainfall (lower) for the period of 1986 to 1999.

#### 4.4. Discussion

In this study rainfall variability in time and space in mesoscale resolution,  $0.16^\circ$  by  $0.16^\circ$ , regional rainfall data as simulated with the atmospheric model REMO, gridded observed rainfall data and satellite-based estimated data were compared. Within the study area, the three datasets show the agreed well. Temporal variations of rainfall show a high degree of correlation during the period from April to October. At this period correlation coefficient between 0.5-0.7 spatially spreads over the Sulawesi Island and its surrounding seas. During this time, the dry season or the Australia monsoon prevails. The less congruence in the rainy seasons can be due to a methodical effect with the remote sensed rainfall estimate. Because the satellite does not measure the rainfall rates directly (Gruber et al., 2000), the accuracy of the rain data depends on conversion from the measured parameter (cloud top temperatures) to rainfall rates. The larger the clouds vary as in rainy season, the larger are the possible errors of the rainfall estimate and hence, the less correlation to the observations.

Temporal comparison could be used for the ENSO impact study on rainfall variability. From data series available in three datasets, the impact of ENSO on rainfall variability is examined.

The impact of ENSO on the rainfall variability study using REMO  $1/2^\circ$  model for the Indonesian region and REMO  $1/16^\circ$  model for the Sulawesi Island show that rainfall decreases here more than usual in the dry period from April to October. These results are well in agreement with several studies based on ground-based rainfall observations [see Ropelweski and Halpert (1987); Haylock and McBride (2001); Hamada et al. (2002); Aldiran (2003), van Oldenburg et al. (2003)]. Comparison of model, satellite-based estimate and ground-based rainfall data agree well. On average, the REMO rainfall rates agree with ground based extrapolated rain gauge values within 89% ( $0.8\sigma$ ). But REMO and gridded rain gauge values overestimate satellite



derived data by 30% ( $0.7\sigma$ ). Model as well as satellite-based estimate could be useful to study the impact of ENSO on rainfall rates at the ground notably, as is found from this study, for the period of April to October. The atmosphere–ocean interaction plays an important role in the evolution of significant ENSO-related rainfall impact that occurs in this period over the Indonesian region. Juneng and Tangang (2005) explained that the evolution of the dominant mode of the South East Asian Rainfall (SEAR) anomalies is in tandem with the evolution of ENSO-related sea surface temperature (SST) anomalies. The strengthening and weakening of the “boomerang-shaped” SST in western Pacific, the changing sign of anomalous SST in the Java Sea and the warming in the Indian Ocean and the South China Sea are all part of ENSO-related changes and all are linked to the SEAR anomaly. Furthermore Juneng and Tangang (2005) explained that the anomalous low-level circulation associated with ENSO-related SEAR anomaly or Asian-Australian Monsoon anomaly [Wang et al. (2003); Tim et al. (2005)] indicates the strengthening and weakening of two off-equatorial anticyclones, one over the Southern Indian Ocean and the other over the western North Pacific.

#### 4.5. Conclusions

A comparison of REMO model simulated, ground-based and satellite-based rainfall estimate has been performed. The comparison showed that it is possible to realistically simulate local patterns of rainfall with a regional atmospheric model. During the rainy period the simulation seems even superior to gridded ground-based measurements. With the simulations a detailed spatio-temporal overview over rainfall at the  $1/6^\circ$  and monthly time scale is obtained. The results also showed that ENSO had only the effect to reduce rainfall in a certain period, when usually rainfall was also low. This temporal effect follows from April to October and the spatial distribution of rainfall anomaly spreads out gradually from southeast of the island to whole island and its surrounding seas.

The satellite-based rainfall estimate can be used to complete ground-based rainfall measurement in order to have well-distributed spatially datasets for climate monitoring and analysis. In the case of ENSO-related rainfall anomaly study the satellite-based rainfall are useful mainly for the period of April to October when the correlation with the ground-based measurement is considerably high.

## CHAPTER 5

# SPECTRAL ANALYSIS OF RAINFALL VARIABILITY IN SULAWESI

### *Abstract*

*The Maximum Entropy Method (MEM), the Multi Taper Method (MTM) and wavelet spectral analyses have been used to study the dominant mode of rainfall variability in South Sulawesi and Central Sulawesi sub domain as determined by the model REMO as well as by the observed data.*

*It is evident from the spectral analysis with all methods that in the South Sulawesi sub domain the dominant mode of rainfall variability is caused by the annual cycle of the Asian-Australian Monsoon; indicated by the maximum of the power spectrum at frequency around one cycle per 12 months. The ENSO event represents the second prominent mode in rainfall variability in South Sulawesi indicated by periodicities between 2-7 years in the power spectrum. The Asian-Australian Monsoon does not play an important role in the rainfall variability in the Central Sulawesi sub domain. This is shown by the maximum spectral power which corresponds to characteristic frequencies of ENSO events. Coherency as a measure of correspondence between the spectra for two signals showed the correlation between rainfall and ENSO indices (SOI and SST anomaly in NIÑO3 region).*

*The advantage of wavelet analysis is to decompose time series into a time-frequency space. Both the dominant modes of variability and how those modes vary in time can be, therefore, determined.*

### 5.1. Introduction

Time series analysis detects dominant periodicities or *modes* in climatic data. The monthly rainfall amounts, both the simulated by the REMO model and the observed, can contain several dominant frequencies, which can physically be interpreted as a dominant mode governing the climatic variability. Indonesia's climate is strongly influenced by the seasonal cycle of the monsoon and its intra seasonal oscillation, the so-called Madden-Julian Oscillation (MJO) (Madden and Julian, 1971). At larger time scales the inter annual variation is governed by ENSO events. A discussion concerning the monsoon mode of variability can be found, e.g. in (Kim and Chung, 2001; Kim, 2002; Kim and Kim, 2002; Lim et al., 2002). Lim et al. (2002) concluded that the first mode of seasonal variation the Asian summer monsoon, describes the typical seasonal evolution of the spatial patterns that are associated with the Indian monsoon from late May, mei-yu (China) in June, baiu (Japan) from mid-June to mid-July and changma (Korea) from late June to late July. The "meiyu" in Chinese, "baiu" or "tsuyu" in Japanese and "changma" in Korea refers to the frontal rainfall caused by mei-yu and changma front, a persistent east-west zone of disturbed weather during spring which is quasi-stationary and stretches from the east China coast, across Taiwan, eastward into the Korean Peninsula and the Pacific south of Japan (Chung et al., 2004; Wikipedia, 2006).

Several mathematical and statistical methods, from classic to modern, have been applied by some researchers to analyze several key features of climatic time series, in order to understand the climate variability and the dominant factors driving this variability. Wang et al. (2003) developed an extended singular value decomposition analysis to analyze the changing characteristics of Asian-Australian Monsoon anomalies during El Niño (La Niña) from its development to its eventual disappearance. Lim (2004) performed the cyclostationary EOF (CSEOF) analysis to decompose and separated dominant factors of the Asian Summer Monsoon variability.

One of the powerful tools to analyze the time series and extracting its information is the spectral analysis with numerous variants of this method. The Maximum Entropy Method (MEM) is one of the spectral analysis methods based on approximating the time series under study by linear Auto Regression (AR) process of order  $M$ , AR ( $M$ ). An example of MEM is given by Ghil et al. (2002) for the SOI time series. Pederson et al. (2001) showed the MEM analysis of the periodicities of rainfall in Mongolia which is composed of 18.2 and 21.3 years periodicities. Tomic and Unkasevic (2004) applied MEM and MTM to analyze the rainfall series of Belgrad.

The Multi Taper Method (MTM) is one of the spectral analysis method widely applied to problems in geophysical signal analysis, including analyses of atmospheric and oceanic data (Ghil and Vautard, 1991; Kuo et al., 1990; Lall and Mann, 1995; Mann et al., 1995; Thomson 1995; Mann and Park, 1996), paleoclimate data (Berger et al., 1991; Chappellaz et al., 1990; Mann and Lees, 1996; Mommersteeg et al., 1995; Park and Maasch, 1993; Yiou et al., 1994). MEM and MTM only describe the spectrum without knowing the time of occurrence. The more recently developed method, wavelet analysis, can detect the localized spectral signal in time and frequency space (e.g., Torrence and Compo, 1998; Gu and Zhang, 2001). Torrence and Webster (1999) and later Tiwari and Rao (2004) used the multiple spectral techniques (e.g. multi-taper method (MTM), maximum entropy method (MEM), wavelet and cross spectra) to identify the coherent cyclic and non-stationary modes in the signature of ENSO signals in the Coral Growth Rate Record of the Arabian Sea and the Indian Monsoons. Jevrejeva (2003) used the wavelet approach to study the influence of ENSO and Arctic Oscillation on ice condition in the Baltic Sea. Another wavelet application is to analyze the tropical convection (Weng and Lau, 1994) and the El Niño Southern Oscillation (ENSO) (Gu and Philander, 1995; Wang and Wang, 1996). A practical guide to wavelet analysis with the SST NIÑO3 and SOI time series as examples of analysis can be found in the work of Torrence and Compo (1998), whereas Ghil et al. (2002) described completely the application of spectral methods for climatic time series. There is no best spectral estimate (Kay, 1988) thus it is

advisable to apply several independent estimation procedures. This chapter will address the application of several spectral analysis methods to study the dominant mode of the rainfall variability in two sub domains of the REMO model on Sulawesi Island.

## 5.2. Data and methods

### 5.2.1. Data

Data used to perform these spectral analyses is the rainfall time series that are either simulated by the REMO model or ground-based observed from two sub domains of the REMO  $1/6^\circ$  model, i.e. the regions of South Sulawesi and Central Sulawesi. The investigated period spans from 1979 to 1993. The data is also used in Chapter 3 and some explanation about the data can be read in that chapter. Two ENSO indices i.e., Southern Oscillation Index (SOI) and Sea Surface Temperature Anomaly in NIÑO3 region will be used to correlate rainfall time series with these two indices.

### 5.2.2. Methods

Several spectral methods were applied to study dominant modes responsible for rainfall variability. The methods enable us to isolate statistically significant periodicities of rainfall time series. The methods are Maximum Entropy Method (MEM), Multi Taper Method (MTM) and wavelet analysis. Within the frequency domain the correlation of two signals is performed by cross coherency analysis. The MEM, MTM and the wavelet theory are presented here briefly.

#### Maximum-Entropy Method (MEM)

The purpose of MEM is to obtain the spectral density by determining the most random (i.e. with the fewest assumptions) process, with the same auto-correlation coefficients as  $X$ . In terms of information theory, this is the notion of *maximal entropy*, hence the name of the method (Ghill et al., 2002)

### Multi Taper Method (MTM)

The MTM revolves around calculating  $k$  tapers independent spectral estimate with a given bandwidth  $w$  for a time series  $x$  and product of each tapers. The number of relevant taper's is then proportional to the bandwidth so that a cutoff between the resolution (small  $w$ ) and confidence (large number of tapers) has to be found by trial and error. The MTM is appropriate for monitoring the significant modes in such distinct variability because it has low variance, high spectral resolution and accurate statistical significance for the detected spectral peaks (Mann and Lees, 1996).

### Wavelets method

This method revolves around decomposing given time series into scale components for identifying oscillations occurring at fast (time) scale and others at slow scales. Mathematically, the continuous wavelets transform of a time series  $f(t)$ , can be given as (Tiwari and Rao, 2004):

$$W_{\psi}(a, b) = \left[ \frac{1}{\sqrt{a}} \right] \int_{-\infty}^{\infty} f(t) \Psi[(t - b) / a] dt$$

Here  $f(t)$  represents signal,  $\Psi$  is the base wavelets function (in the present case, Morlet function), with a length that is much shorter than the time series  $f(t)$ .  $W$  stands for wavelet coefficients. The variable  $a$  is a scale factor that determines the frequency (or scale) so that varying  $a$  gives rise to spectrum. The factor  $b$  is related to the shift of the analysis window in time so that varying  $b$  represents the sliding method of the wavelet over  $f(t)$ . In several recent analyses complex Morlet wavelets have been found useful for geophysical time series analysis.

The complex Morlet wavelet can be represented by a periodic sinusoidal function with a Gaussian envelope. Morlet wavelet may be defined mathematically, as follows:

$$\Psi_{a,b}(t) = \pi^{-\frac{1}{4}} (ap)^{-\frac{1}{2}} e^{\frac{-2\pi i t}{a}} e^{\frac{-1}{2} \frac{(t-b)^2}{ap}}$$

The parameter  $p$  represents the relation between periodicity and time resolution.

The MEM method was applied using the free statistical package KyPlot, the MTM method was implemented using free software program The Singular Spectrum Analysis–Multi Taper Method (SSA-MTM) Toolkit. It is available at URL <http://www.atmos.ucla.edu/tcd/ssa/> and the wavelet software used in this analysis was provided by C. Torrence and G. Compo, and is available at URL: <http://paos.colorado.edu/research/wavelets>.

### 5.3. Results

Monthly averaged rainfall values for the entire sub domain averaged from 1979 to 1993 from the REMO model simulation and from observations are depicted in Figure 5.1 for two sub domains. In the South Sulawesi sub domain the absolute maximum of an averaged monthly rainfall amount of  $288 \text{ mm month}^{-1}$  (December) and a minimum of  $48 \text{ mm month}^{-1}$  (August) were observed. In Central Sulawesi the maximum and minimum rainfall is  $239 \text{ mm month}^{-1}$  (April) and  $94 \text{ mm month}^{-1}$  (August) respectively. The rainfall pattern in South Sulawesi reveals the monsoon pattern indicated by a clear and large difference between dry and wet seasons. The seasons have roughly the same duration. In contrast the rainfall in the Central Sulawesi sub domain, slightly varies during the year and the existences of two different seasons are not obvious. The nature of the variability is investigated with spectral analysis and the results are described below.

#### 5.3.1. Maximum Entropy Method

The MEM spectral analysis of the monthly rainfall simulated by REMO  $1/6^\circ$  modelled and observed for the two sub domains are displayed in Figure 5.2. In the South Sulawesi sub domain, the maximum peak of MEM analysis appears at frequency  $0.08 \text{ month}^{-1}$  or 12.5 month periodicities. This is consistent with the annual cycle of the Asian Australian Monsoon. Therefore the first mode of rainfall variability



in the South Sulawesi sub domain is most probably caused by the monsoon circulation. The second peak exists at frequency  $0.3 \text{ month}^{-1}$  or 3.3 months in REMO and at frequency  $0.2 \text{ month}^{-1}$  or 5 months in the observed data. These frequencies are related to the intra seasonal variability.

In the Central Sulawesi sub domain time series both modelled REMO rainfall amount and observed rainfall amount by rain gauges are decomposed into several peaks and the maximum peak appears at the frequency  $0.011\text{--}0.02 \text{ month}^{-1}$  corresponding to 4.1 to 7.5 years periodicities (Figure 5.2 lower panel). This time scale is similar to the well-known ENSO periodicities of 2 to 7 years (Torrence and Compo, 1998; Torrence and Webster, 1999; IPCC, 2001; EL-Askary et al., 2004). The four-year mode of rainfall variability can be attributed to ENSO events. The other peak has less power spectral density and appears in the frequency  $0.15$  or 6.7 months periodicities both in REMO and observed data. This is similar to the period of a seasonal cycle of the Asian Australian Monsoon. There still exist the frequencies  $0.26 \text{ month}^{-1}$  (3.8 months) and  $0.43 \text{ month}^{-1}$  (2.3 months) in REMO and  $0.3 \text{ month}^{-1}$  (3.3 months) in the observed data. All the frequencies are related to the intra seasonal variability. To investigate, whether other pronounced frequencies exist in the time series, the MTM method is applied.

### 5.3.2. Multi Taper Method (MTM)

In the South Sulawesi sub domain, the results of the MTM spectral analysis are shown in Figure 5.3 (upper panel) for the REMO model and Figure 5.3 (bottom) for the data observed. In this sub domain the spectral peak with highest significance (99% confidence interval, CI) is in the frequency of  $0.09 \text{ month}^{-1}$  or in the period of 12 months and is observed in both time series. These periods reveal the annual cycle of Asian Australian Monsoon. The second significant spectral band (99% CI) for the REMO model is in the frequency of  $0.28$  (3.6 months). The next significant (95% CI) for the REMO model and data observed are within the frequencies of  $0.30$  to  $0.45$  (3.3 – 2.2 months). With 90% CI there is still a signal in the frequency of  $0.18 \text{ month}^{-1}$  or

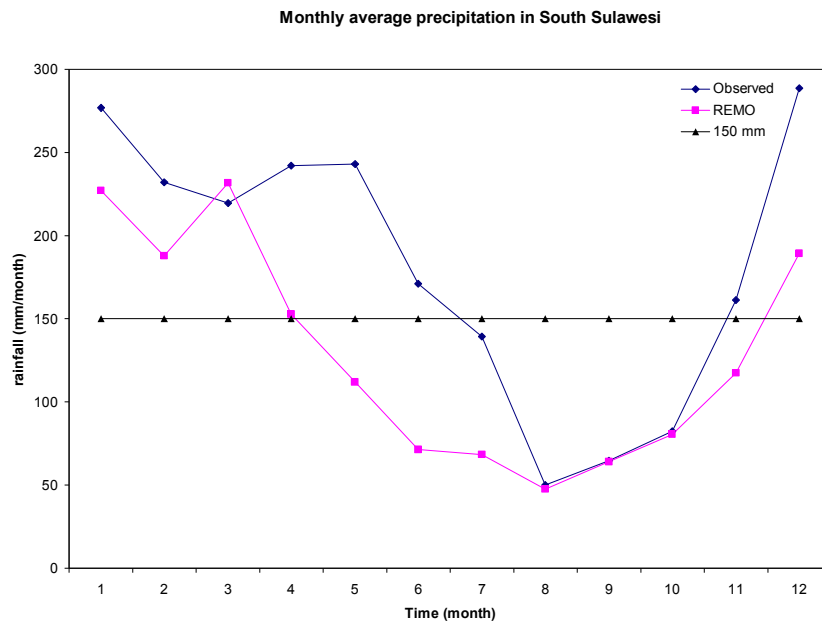
5.2 month of periodicities. The REMO simulations show a spectral peak at 95% CI within the period of 4.5 years, which is similar to average periodicity of ENSO events, whereas in the data observed time series such a significant signal is not apparent.

Results of the spectral analysis using Multi Taper Method (MTM) for the sub domains Central Sulawesi (Figure 5.4) show that the power spectrum has a higher statistically significance (at 99% CI) in the frequency ranges of 0.15 to 0.02 month<sup>-1</sup> or in the period of 4 to 6 years. This is also the period of ENSO events. The next stronger power spectrum (95% CI) is in the frequency range 0.25-0.29 month<sup>-1</sup> (period 3.4 – 4.0 month). The last significant peak of the power spectrum (90% CI), is in the period 2.0 to 2.5 month. Comparison between the REMO simulations and the observational data (Figure 5.4) show similar pattern of periodicities, i.e. peaks of significant spectral power are in the same frequency range.

### 5.3.3. Wavelet Method

The wavelet analysis shows that the annual cycle of the monsoon circulation has a dominant influence on rainfall variability in South Sulawesi (Figure 5.5.b). As in the MTM method, comparison of the REMO simulations values and observed data show close agreement in periodicity in this time period. The second highest values of wavelet power spectral density occur in the period of 2 to 7 years. This is the period of ENSO events. This confirms ENSO being the second mode of rainfall variability in South Sulawesi. Again we compare the REMO model simulation with observation data (Figure 5.6.b). Both time series have periodicities within the ENSO event period, i.e. 2 to 7 years.

(a)



(b)

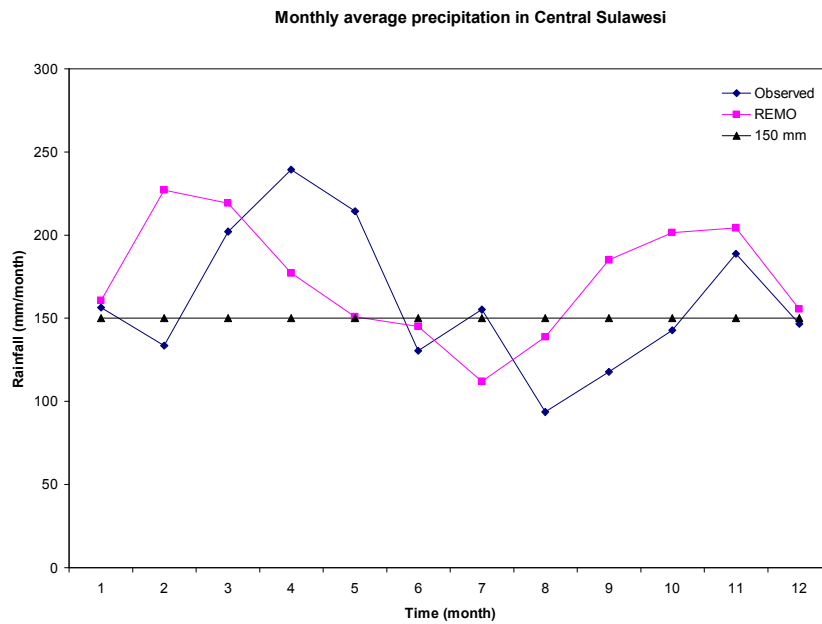


Figure 5.1: Monthly averaged (1979 to 1993) rainfall as modelled by REMO  $1/6^\circ$  and observed for the South Sulawesi (a) and the Central Sulawesi (b) sub domain.

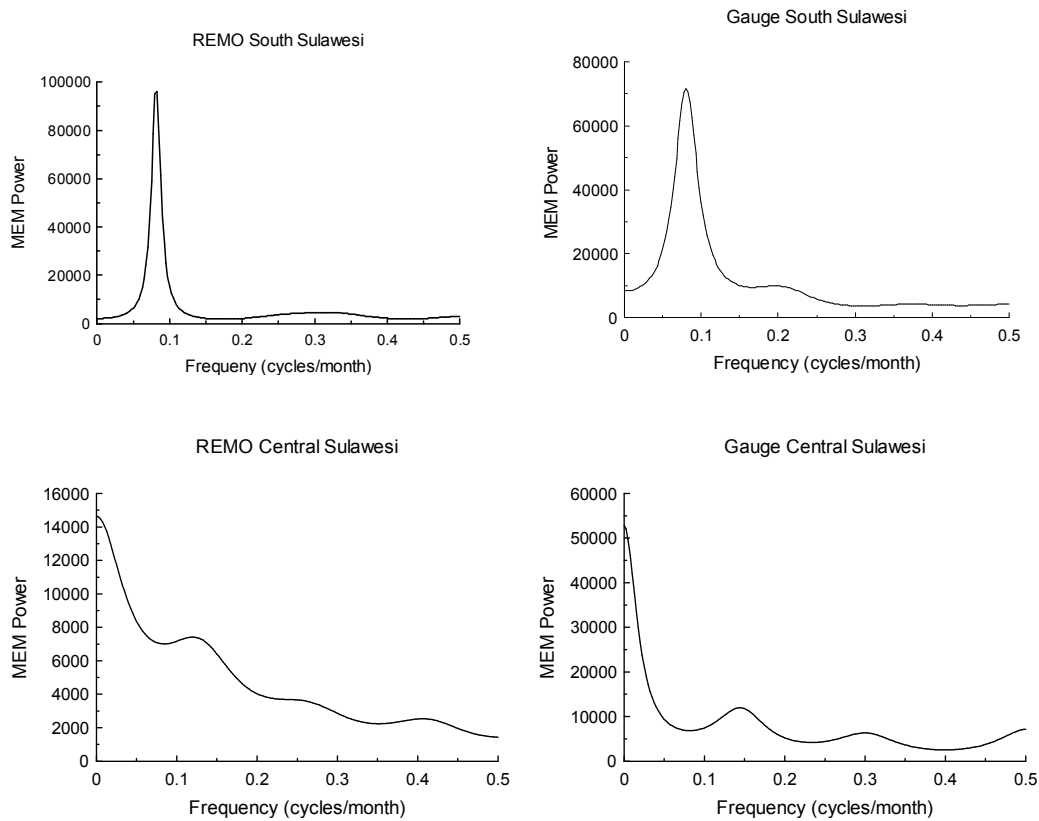


Figure 5.2: Maximum entropy method (MEM) power spectrum of rainfall time series as modelled by REMO  $1/6^\circ$  and observed in the South Sulawesi sub domain (**above**) and the Central Sulawesi sub domain (**bottom**).

The advantage of wavelet analysis is to localise the variability timescale in the course of the time (Torrence and Compo 1998; Torrence and Webster, 1999; Gu and Zhang, 2001). It is obvious from the evolution of periodicities that the annual cycle of a 12 month period occurs almost during the entire data period. This situation is valid in both simulated and observed data (Figure 5.5 and 5.6). The ENSO events, as the second mode to rainfall variability in South Sulawesi, occur within the period of 2 to 7 years as indicated by the second strong of spectrum power. Time evolution of this period is, however, divided into several distinct time periods. In the observed data, the period of the ENSO event mode is within 2 to 3 years and occurs in the time period from 1981 to 1987.

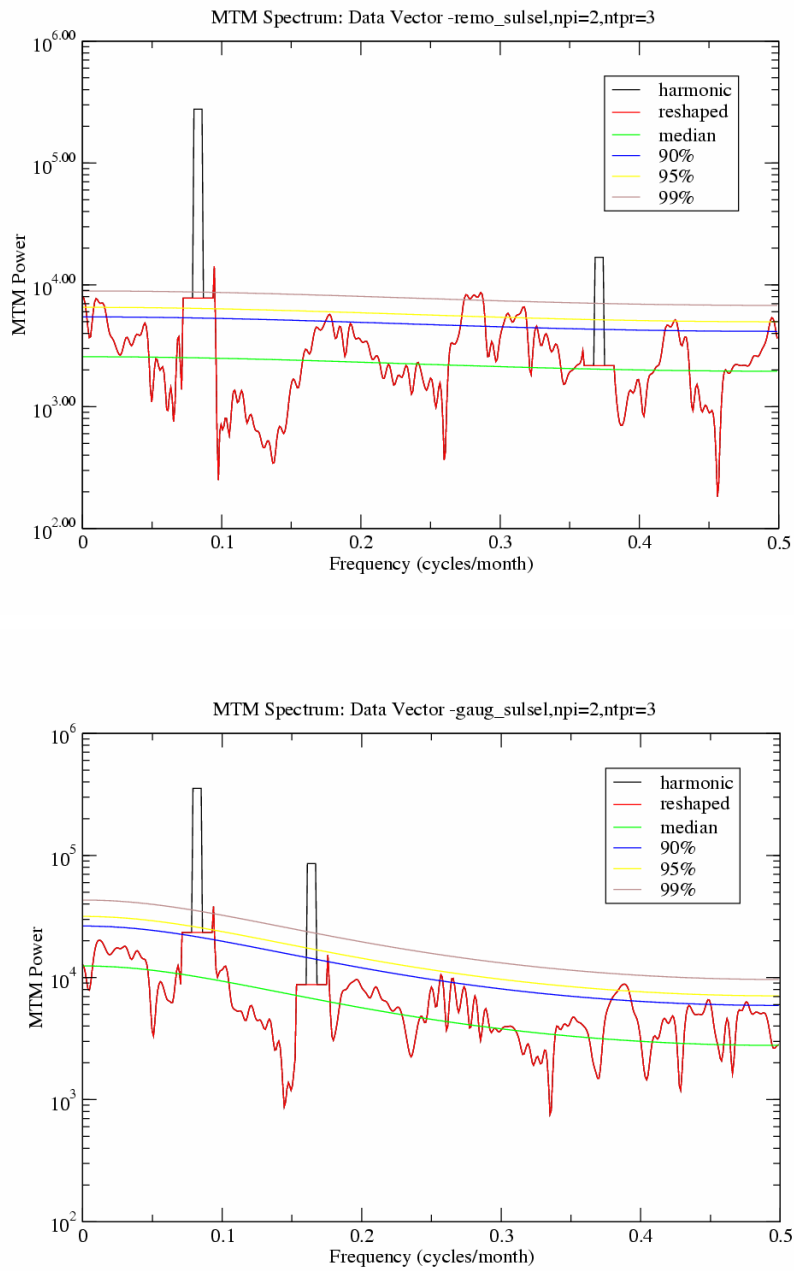


Figure 5.3: Multi Taper Method (MTM) power spectrum of rainfall time series as modelled by REMO  $1/6^\circ$  (upper) and observed (bottom) in South Sulawesi sub domain. The first three lines from the top are significant levels 99%, 95% and 90% respectively; fourth line is the median of the power.

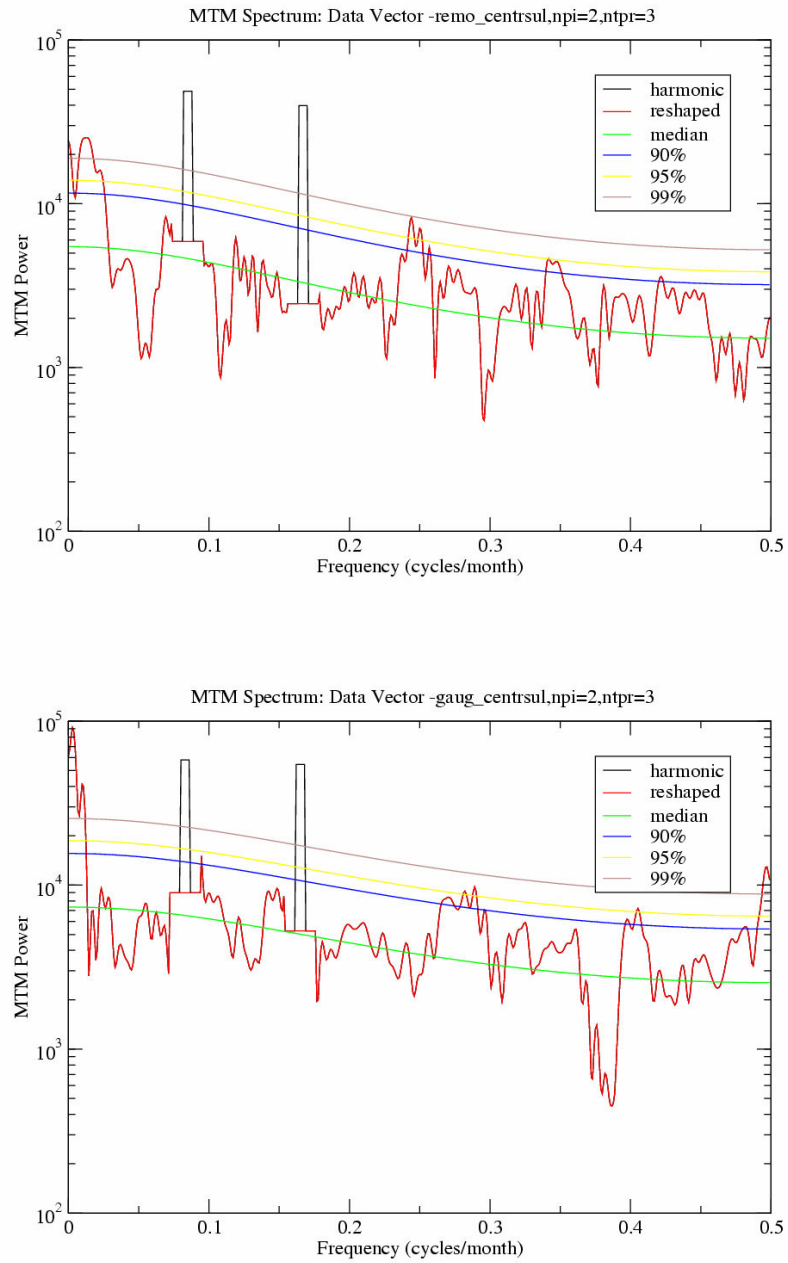


Figure 5.4: As Figure 5.3, but for the Central Sulawesi sub domain

The period between 5 to 7 years occurs between 1982 and 1993. By the REMO model, the period of ENSO events mode is similar to the observation, i.e. 2 – 7 years and the time sequence of ENSO event mode are 2 years period occurring in 1979 to 1993 with some levels of spectrum power decrease in the period of 1989 to 1991. There exist the periodicities of 5 – 7 years in the years 1979 to 1993. The period is divided into 5 years between 1979 -1981 and between 1991 - 1993. The period of 5 - 7 years appears in the years 1982 to 1983.

In Central Sulawesi, the situation is again different compared to the South Sulawesi sub domain. In this region, the monthly rainfall varies less than in Central Sulawesi (See Figure 5.1b). From the REMO modelled rainfall (Figure 5.7), the strongest power spectral density (90% CI) can be found at periodicities between 5 and 7 years and occurs within the time period from 1979 to 1988 (Figure 5.7) and again in 1993. The situation can be seen in both data time series, i.e. modelled and observed (Figures 5.7 and 5.8).

The monthly observed rainfall analyzed by wavelet (Figure 5.8) shows that within 90% of confidence level (the black contour line in figure) the power spectrum is in the period 3 to 9 years. It occurs during the periods of 1980 until 1984 and 1990 until 1993. The strongest power spectral density occurs in the periodicities of 4 to 8 years in the years from 1980 to 1982, whereas in whole period of time series, the highest densities occur at periodicities of 8 years. The second strongest spectral density can be also found in the periodicity of 6 to 12 months which occur in the years 1988 to 1989.

The shorter period of 2 -3 months (intra seasonal) are found by three methods with the higher power spectrum in Central Sulawesi compared to South Sulawesi and appear in both REMO modelled and observed data.

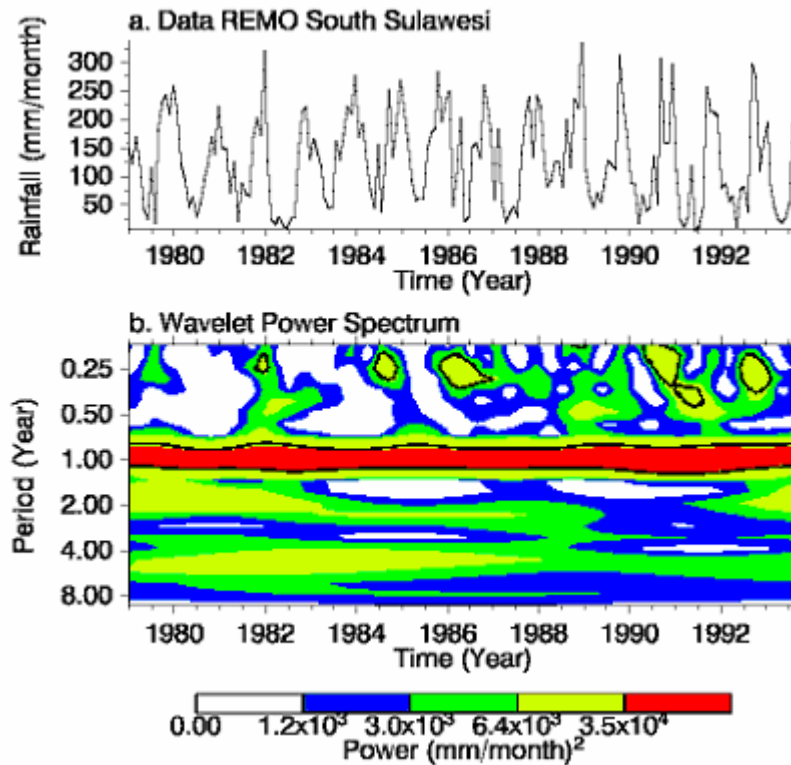


Figure 5.5: Data REMO South Sulawesi (a) and the wavelet power spectrum (b). The contour levels are chosen so that 75%, 50%, 25% and 5% of the wavelet power is above each level, respectively. The black contour is the 10% significance level, using a red-noise (autoregressive lag 1) background spectrum.

#### 5.3.4. Coherency Analysis

The cross-spectrum calculation between ENSO indices and rainfall (modelled and observed) showed the impact of ENSO on rainfall variability which is indicated by high coherency in the ENSO period. In the South Sulawesi sub domain (Figure 5.9) the high coherency between two ENSO indices (SOI and SSTA NIÑO3) and REMO model rainfall as well as with observed data appear in the frequency 0.01 -0.02 or in the period of 8.3 – 4.2 years.



In the Central Sulawesi sub domain (Figure 5.10) the coherency between REMO modelled rainfall and ENSO indices shows the highest value at the same frequency as in South Sulawesi, i.e. at 0.01 – 0.02 or in the period 8.3 – 4.2 years. The coherency between observed rainfall and ENSO indices show that it occurs in several frequencies.

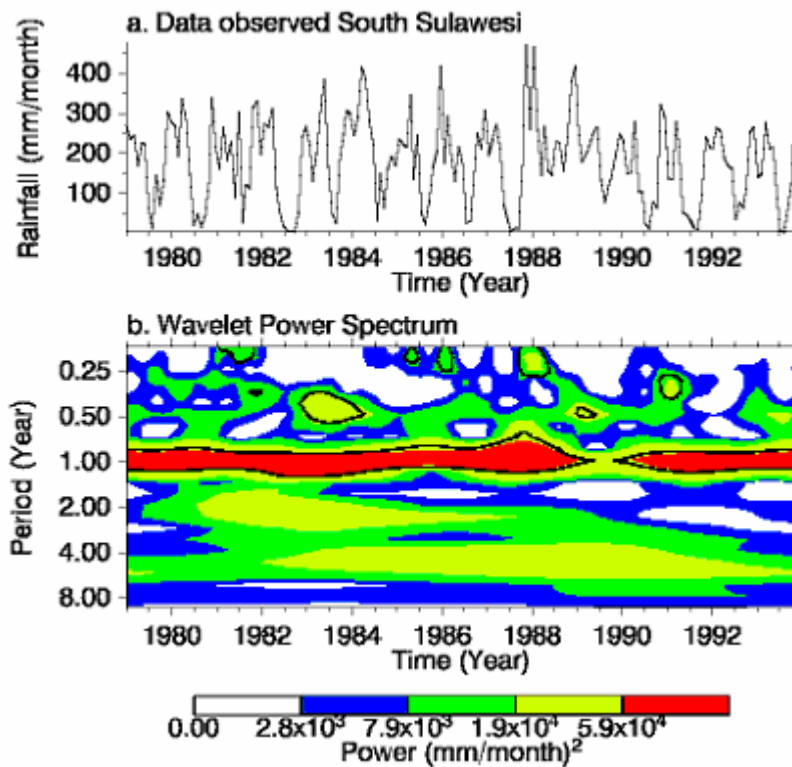


Figure 5.6: As Figure 5.5, but for observed rainfall.

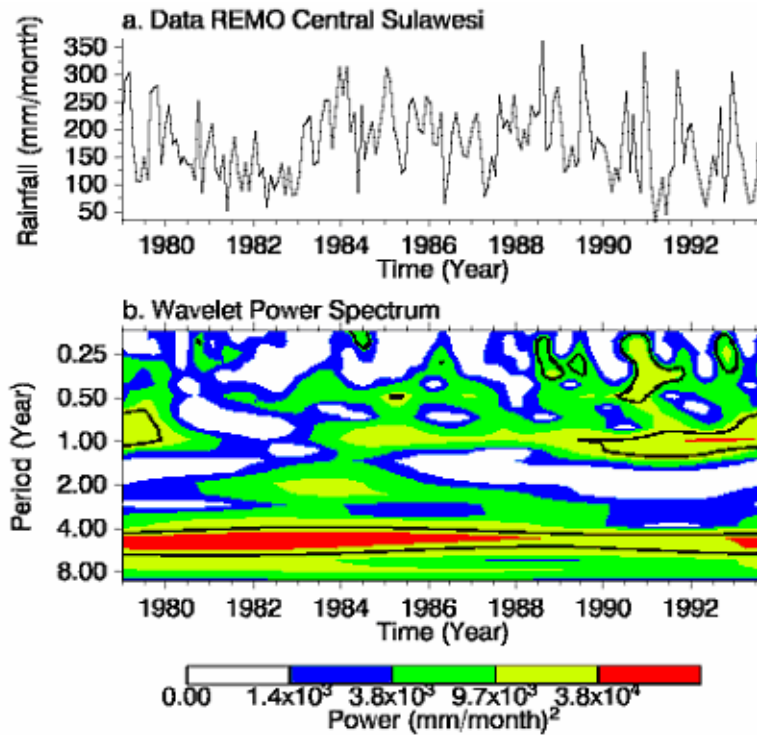


Figure 5.7: As Figure 5.5, but for the Central Sulawesi sub domain

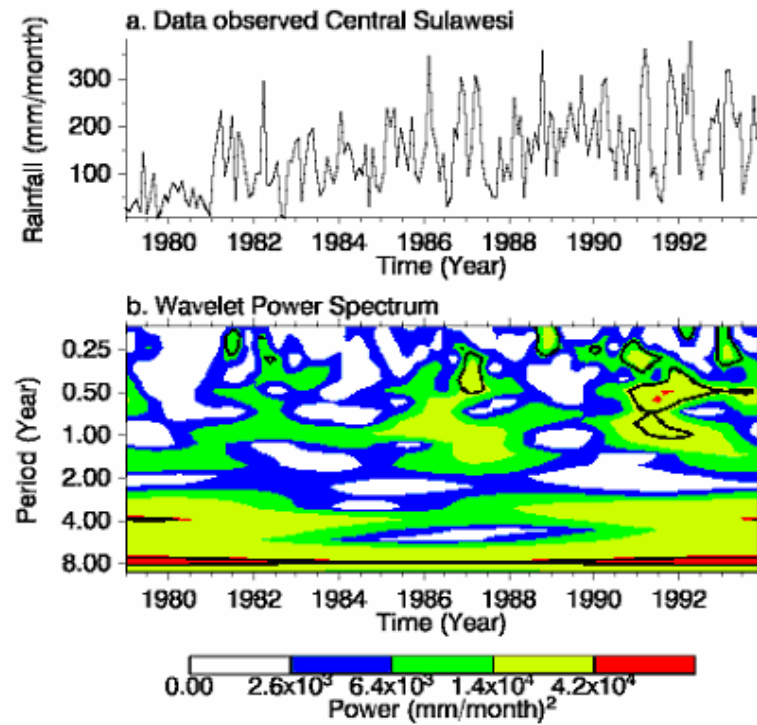


Figure 5.8: As Figure 5.6, but for the Central Sulawesi sub domain.

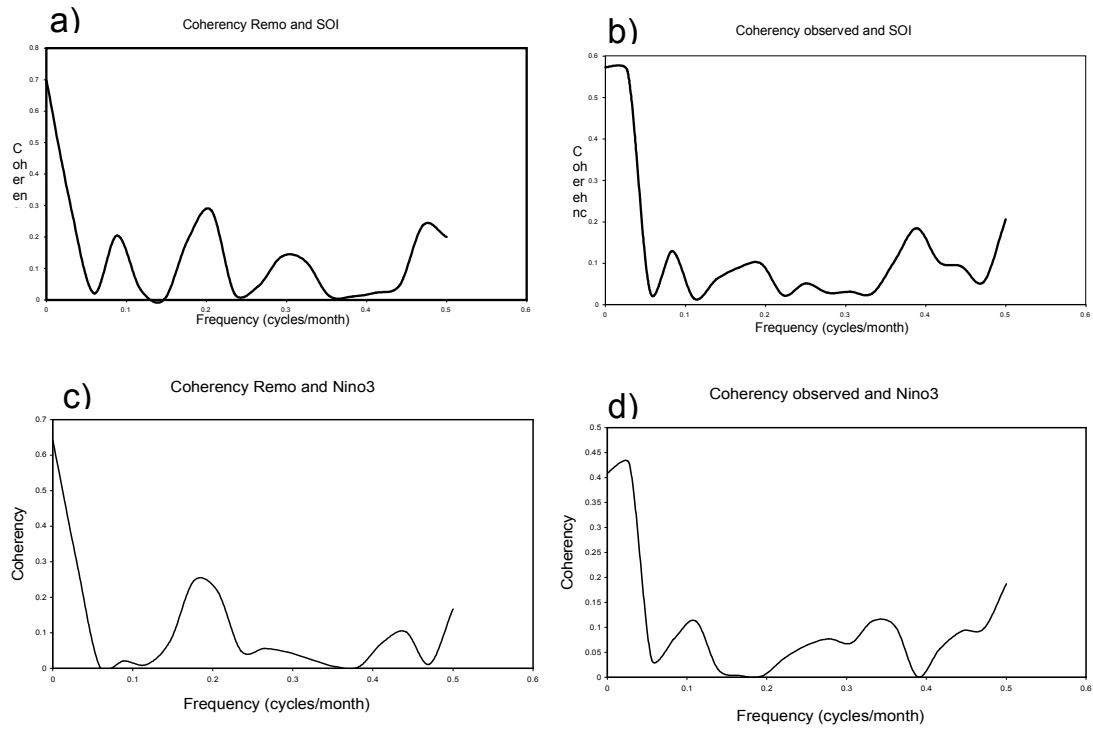


Figure 5.9: Coherency calculated between the REMO modelled rainfall and SOI (a), observed rainfall and SOI (b), modelled rainfall and NIÑO3 (c) and observed rainfall and NIÑO3 (d) for the South Sulawesi sub domain.

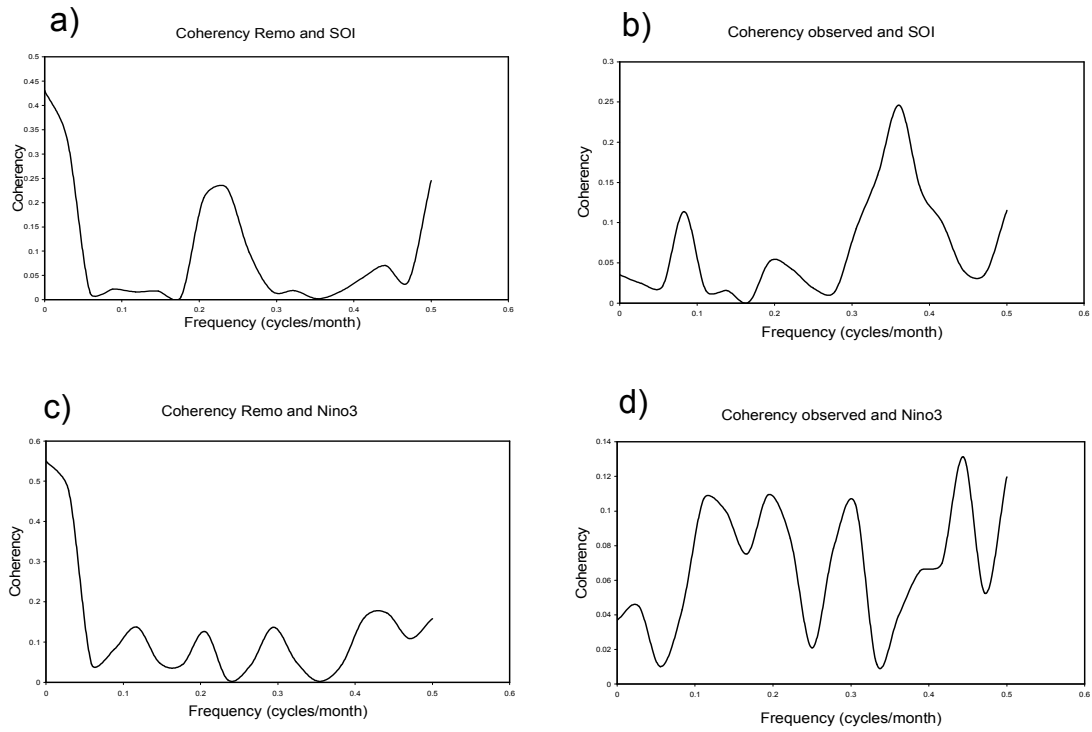


Figure 5.10: As Figure 5.9, but for the Central Sulawesi sub domain.

#### 5.4. Discussion

This chapter reports the use of three spectral methods and coherency analyses to analyse time series of REMO model simulations and observed rainfall data in two sub domains on Sulawesi Island. The two sub-domains are characterised by differences in the dominant modes of rainfall variability. These modes in respect to the time scale are inter annual, annual, seasonal and intra seasonal cycle.

In South Sulawesi the dominant mode of variability is the annual cycle indicated by the high power spectral density in a period of 12 months mostly along the data period in both time series. The annual cycle is related to the maximum convection (tropical rainfall) which can be viewed as the annual cycle in the movement of the inter tropical convergence zones, the regions of convergence of the large-scale moisture fluxes. Lau and Yang (1996) and Meehl (1997) have proposed that the tropical biennial oscillation (TBO) and the annual cycle of maximum convection are the main active participants in the link between the Indian monsoon, Indian Ocean and tropical Pacific. Torrence and Webster (1999) showed the annual cycle (1 year) variance time series of Nino3 SST and the Indian rainfall is negatively correlated with the inter annual ENSO signal.

The ENSO event influences the South Sulawesi region as the second mode of rainfall variability analyzed by MEM, MTM and wavelet methods. Using Cyclostationary (CSEOF) analyses, Lim et al. (2002); Lim (2004) also showed that ENSO is the second mode of variation in several Asia monsoon regions during the Asian Summer Monsoon. Cross coherency analysis applied to rainfall times series modelled and observed show the close correlation in frequency domain indicated by the high coherency values at dominant periodicities according to spectra analysis results (MEM, MTM and wavelet methods). Cross coherency with ENSO indices (SOI and of sea surface temperature anomaly in the NIÑO3 region) reveal the interaction between the monsoon circulation and ENSO events. In the South Asia monsoon, Torrence and Webster (1999); Tiwari and Lakshmi (2005) showed the coherency

between India Rainfall Index, IRF and NIÑO3 SST in periods of 10 years, 5 to 7 years and 2.8 years suggesting the ENSO as one part of the potential drivers of the Indian monsoon anomaly.

In Central Sulawesi the first dominant mode of rainfall variability is caused by the ENSO events. This evidence was proven by all three methods of spectral analysis. The range of periodicities differs from the three methods (4 – 6 years by the MTM, 4 – 7 years by the MEM and 5-7 years by the wavelets). The Asian Australian Monsoon does not play an important role for the rainfall variation in this region (see the rainfall patterns classification results in Chapter 2). This is a general trend in the spatial rainfall patterns in Indonesia (BMG, 2002; Aldrian, 2003): The further away from the equator, the clearer the monsoonal rainfall pattern becomes. In our case this is reflected by the absence of a monsoonal influence on the rainfall in Central Sulawesi (close to the equator) and the clear monsoon effect in South Sulawesi ( $6^{\circ}$  S).

During the period of the analysed data, the annual cycle as the first mode of rainfall variability in South Sulawesi and the inter annual (ENSO) events as the first mode of variability in Central Sulawesi are clearly indicated by REMO model time series and less clearly in the observed datasets. This is revealed for the average monthly rainfall amounts (Figure 5.1) more smoothly and more clearly in REMO modelled data than in the observed data. This feature appears in both of the regions. These features in the frequency domain appear especially in the MEM method (narrower band of frequency) and in the wavelets method (more continuously and small varies of frequency for the higher power spectrum). These differences between modelled and observed data because of the idealized of the model to calculate and to derive the parameter and produce small variations rather than the more complex variability that exist in the real world.

The three methods showed the existence of periodicities between 2-3 months which is the intra seasonal cycle. It appears mostly in Central Sulawesi and is not obvious in South Sulawesi. The Intra seasonal cycle is closely related to the so-called Madden

Julian Oscillation (MJO) (Madden and Julian, 1971; Hendon and Salby 1994; Jones et al., 2000; Waliser et al., 2003), i.e. an equatorial travelling pattern of anomalous rainfall. The MJO is characterized by an eastward progression of large regions of both enhanced and suppressed tropical rainfall, observed mainly over the Indian Ocean and Pacific Ocean. The anomalous rainfall is usually first evident over the western Indian Ocean and remains evident as it propagates over the very warm ocean waters of the western and central tropical Pacific. The reason of more pronounced of intra seasonal cycle in Central Sulawesi compared to the South Sulawesi is because the influence of the MJO more pronounced in the equatorial belt of 5 degree each to the north and to the south from equator.

The final remark of this chapter is that the frequency domain analysis is a helpful tool for detecting the periodicities which then can be interpreted physically as a dominant mode of variability of time series under evaluation. An additional comment is that the spectrum analysis can be applied for predicting a seasonal rainfall which is beyond this dissertation. A discussion about this issue can be found in Vautard and Ghil (1989); Penland et al. (1991).

### 5.5. Conclusions

The MEM, MTM and wavelet methods have been applied to perform spectral analysis of rainfall time series on two data sets: a data set modelled by REMO and an observed set of data by rain gauges. The evaluation has been done for two regions; South and Central Sulawesi. The methods showed that the data series contain certain dominant frequencies. Physically, such frequencies are related to the causes of the rainfall variability persistent in these regions. Two modes of rainfall variability are found, i.e. inter annual variability related to the ENSO events and the annual cycle which is related to the monsoon circulation.

In South Sulawesi the dominant mode of variability is the annual cycle of monsoon circulation and it is shown by all three methods. In Central Sulawesi also shown by three methods that the dominant mode is the inter annual variability of the ENSO event.

In this study it is found that the time evolution of ENSO periodicities varies along the course of the time. In the South Sulawesi sub domain, for instance, periodicities of observed data exist in a period of 2-3 years during the years 1981 to 1985 and in period of 5 – 7 years in the years 1986 to 1993. The rainfall variability corresponds to the period of ENSO events from the REMO model is similar to the observation, i.e. 2 – 7 years and the time sequence of ENSO event are 2 – 7 year period occur in 1980 to 1984 and from 1985 to 1993 the period is 5 - 7 year. The shorter period of 2 – 3 months which is known as the intra seasonal cycle was detected by the three methods. The power spectrums of these frequencies are higher in Central Sulawesi than in South Sulawesi. It revealed that the intra seasonal cycle influences most the rainfall variability in Central Sulawesi.

Cross coherency analysis between rainfall time series with ENSO indices show the correspondence of significant signals (at 2-7 years), reveal the correlation between ENSO and the monsoon circulation.



## CHAPTER 6

### THE LOCAL ATMOSPHERIC CIRCULATION IN CENTRAL SULAWESI

#### *Abstract*

*With the mesoscale atmosphere model MM5 (pixel size 5 km) the atmospheric motion in the boundary layer of the very structured Central Sulawesi (120°E,0.9°S) is described and compared with the results of field measurement. Rainfall, wind, temperature and humidity fields around the coastal city of Palu, at the airport of Mutiara close to Palu and the agricultural and forested region within and around the Lore Lindu National Park and of the entire watershed of the Palu River was analyzed, forecasted and parameterized. As a first step in this way the features of orographic rainfall and the land-sea breeze phenomenon were investigated. Rainfall in very structured topography is mostly generated by orographic lifting mechanisms whereas in lowland regions, especially in the west part of the ridges, the Asian monsoon still influences by lifting. This is evident from rainfall simulation, i.e. December and June representing two different seasons. In December 2003 the rainfall is much higher compared to June 2003.*

*There is a strong land-sea breeze along the entire coast of Central Sulawesi. In the Palu Bay the sea breeze penetrates about 70 km into the Palu Valley, between the two mountain ridges west and east of the Palu River. The maximum wind speed of about 7 m/sec is reached at 14.00 at the beach of Palu city; the maximum speed is reached at 350 m above ground level. The land breeze at night and in the early morning is much less pronounced (1 m/sec average) than the sea breeze.*

### 6.1. Introduction

Local atmospheric circulation plays an important role for the climate in a region with strong and heterogeneous topography. The research area in the Palu Valley region, for instance, is a region which has a unique geographic situation. It is surrounded by mountains chains from three directions so that this valley is a leeward region and hence as reported by Braak (1929) the rainfall amount in this region is very limited (600 mm/year). The north side of the Palu Valley faces to the bay and thus, the local atmospheric phenomenon of land sea-breeze circulation dominates the wind direction. A local atmospheric phenomenon, the land-sea breeze circulation in this special region, will be analysed with the mesoscale non-hydrostatic atmospheric model MM5. The non-hydrostatic model can represent atmospheric conditions in a very structured relief like in Central Sulawesi.

Some investigations showed that a complex topography plays an important role in the rainfall process (Rife, 1996; Kim and Soong, 2005; Roe, 2005). The dynamical response of the airflow to the presence of a structured orography as a lower boundary condition defines the three-dimensional pattern of condensation and cloud development from which rainfall results, which are sketched in Figure 6.1 (Roe, 2005).

To prove the hypothesis that a complex terrain in the Palu Valley and Lore Lindu National Park can govern an orographic rainfall, the mesoscale atmospheric model MM5 was applied to simulate some key atmospheric parameters such as rainfall amount and air temperature. A rainfall simulation in complex terrain using MM5 model has been conducted by Leung and Qian (2003) with a horizontal resolution of 13 km in the Rocky Mountains and Done et al. (2004) have applied the regional climate WRF (Weather Research and Forecasting) model of NCAR (the United States National Centre for Atmospheric Research) over the same region as Leung and Qian (2003) using a model horizontal resolution of 6 km.

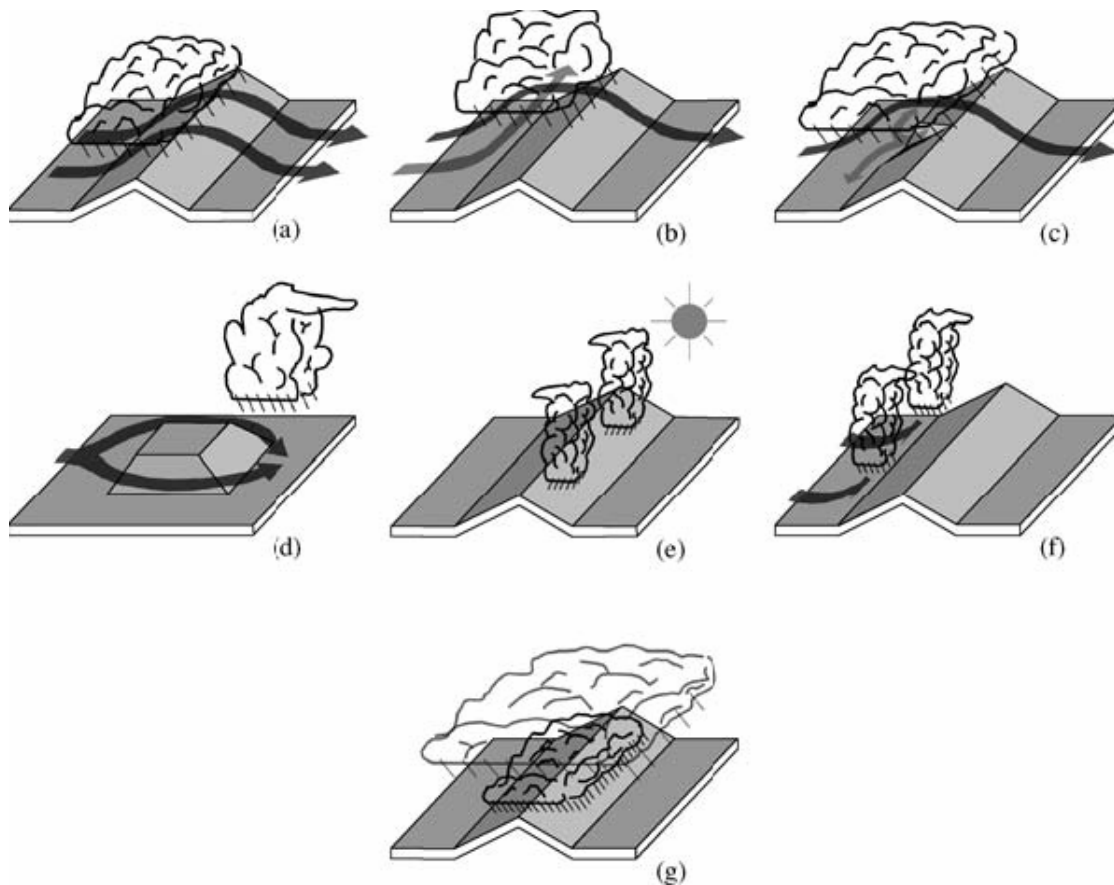


Figure 6.1: Schematic illustrations of different mechanisms of orographic rainfall. (a) stable upslope ascent, (b) partial blocking of the impinging air mass, (c) downvalley flow induced by evaporative cooling, (d) lee-side convergence, (e) convection triggered by solar heating, (f) convection owing to mechanical lifting above level of free convection, and (g) seeder-feeder mechanism (Roe, 2005).

The fifth generation mesoscale atmospheric model MM5 developed by Pennsylvania State University/National Centre for Atmospheric Research (PSU/NCAR) is widely used for atmospheric research and as an operational routine in numerical weather prediction. By the middle of 2005, 1224 users of MM5 working in 566 institutions all over the world have been listed on the model web site (<http://www.mmm.ucar.edu/mm5/>). The advantage of the MM5 model is that it is available on the web and freely downloadable and can be run on a large variety of computer platforms. Being completely documented on the web, following the online tutorial, one can implement the model at any region of interest on the globe. Beside the online tutorial, the development centre also routinely offers workshops on MM5

held in NCAR Boulder, Colorado. As the research tool of atmospheric science, the MM5 model has been applied as a single model but it could as well be coupled to another model according to the field to be studied. Some examples are given here: Coupling with a chemistry transport model has been done by Vautard et al. (2004); and by Klausmann et al. (2003), a hydrological model has been coupled by Tomassetti et al. (2005), and a land surface model was conducted by Xue et al. (1991) and Riley et al. (2003). In this chapter, MM5 is applied to study the local phenomenon of land-sea breeze circulation of Palu Bay, Central Sulawesi (Figure 6.2). By this MM5 was first used under the PC operating system Linux.

## 6.2. Material and Methods

### 6.2.1 Model Description

The numerical model used in this study is the non-hydrostatic MM5 version 3.6.1 (Dudhia, 1993; Grell et al., 1995). By May 2005 the version of this model has reached already version 3.7.2 and it was decided to be frozen (Dudhia, 2005). Originally the Penn State/NCAR Mesoscale Model has been hydrostatic, because the typical horizontal grid sizes in mesoscale models were comparable with or greater than the vertical depth of features of interest. When the scale of resolved features in the model, however, have aspect ratios close to unity or when the horizontal scale becomes even shorter than the vertical scale, non-hydrostatic dynamics can not anymore be neglected. The only additional term in non-hydrostatic dynamics is the vertical acceleration that contributes to the vertical pressure gradient so that hydrostatic balance is no longer exact.

The model has 23 vertical levels using sigma coordinates  $\sigma = (0.025, 0.075, 0.175, 0.225, 0.325, 0.375, 0.425, 0.475, 0.525, 0.575, 0.625, 0.675, 0.725, 0.775, 0.825, 0.87, 0.91, 0.945, 0.97, 0.985 \text{ and } 0.995)$  between the ground surface up to a height of 100 hPa (~15 km). The sigma coordinate is defined as the ratio of the pressure at a given point in the atmosphere to the pressure on the surface of the earth underneath it.

Several parameterization schemes are applied in this study. The schemes contain several options for selecting how the model represents different atmospheric processes, e.g. the planetary boundary layer (PBL), cumulus convection, radiation and microphysical processes. Many different configurations in the MM5 model are possible and the appropriate choice for simulating the local climate is not obvious (Tadross et al., 2006).

Parameterization of non convective rainfall use the simple ice scheme (Dudhia, 1989), whereas for the convective rainfall the scheme published by Grell et al. (1995) is used. The scheme, which is useful for smaller grid sizes 10-30 km, tends to allow a balance between resolved scale rainfall and convective rainfall. Shear effects on rainfall efficiency are considered. The planetary boundary layer (PBL) processes are parameterized using the MRF or Hong-Pan PBL (Hong and Pan, 1996) scheme. The scheme is suitable for high-resolution in PBL. For the radiation processes the scheme of cloud-radiation is used (Grell et al., 1994). The scheme is sophisticated enough to account for longwave and shortwave interactions with explicit cloud and clear-air. As well as atmospheric temperature tendencies, this provides surface radiation fluxes. The exchange processes on the surface are parameterized by a multi-layer soil temperature model scheme. Temperature predicted in 1, 2, 4,8,16 cm layers (approx.) with fixed substrate below using vertical diffusion equation. Thermal inertia, the same as force/restore scheme, but vertically resolves diurnal temperature variation allowing for more rapid response of surface temperature. See Dudhia (1996 MM5 workshop abstracts) for details.

The flowchart of MM5 modelling system is shown in Figure 6.2. Terrestrial and isobaric meteorological data are horizontally interpolated (programs TERRAIN and REGRID) from a latitude-longitude grid to a mesoscale, rectangular domain on either a Mercator, Lambert Conformal, or Polar Stereographic projection. Since the interpolation of the meteorological data does not necessarily provide much mesoscale detail, the interpolated data may be enhanced (program LITTLE\_R/RAWINS) with observations from the standard network of surface and rawinsonde stations using a successive-scan Cressman or multiquadric technique (see Chapter 3). Program

INTERPF then performs the vertical interpolation from pressure levels to the  $\sigma$ -coordinate of the MM5 model. After a MM5 model integration, program INTERPB can be used to interpolate data from  $\sigma$ -levels back to pressure levels, while the program NESTDOWN can be used to interpolate model level data to a finer grid to prepare for new model integration. Graphic programs (RIP and GRAPH) may be used to view modelling system output data on both pressure and  $\sigma$ -levels.

The model was run using 32 CPUs of the IBM p690 series for one month simulation, whereas the single PC Linux with PGI Fortran compiler was used to test the time to produce a 48 hour forecast.

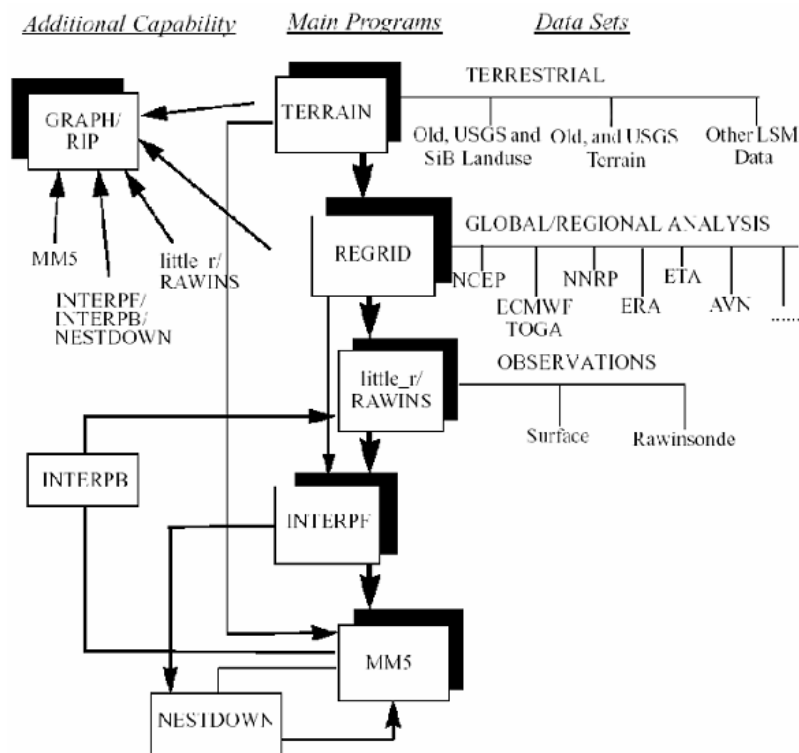


Figure 6.2: Flowchart of the MM5 Modeling system (Dudhia et al., 1995)

### 6.2.2 Representation of the study area in the simulations

Due to the complex terrain of the Central Sulawesi region, the atmospheric condition varies considerably in a relatively short distance. The variation is indicated mainly by

the rainfall regime, radiation and temperature differences between the Palu Valley and its surroundings. The valley is surrounded by mountains from three directions (west, south and east) and it faces the bay in the north which also surrounded by the mountains. As an overview of the complexity of this region, Figure 6.3 shows a three dimensional view of the topography of this region. It can be seen that the Palu Valley is surrounded by mountain chains with elevations reaching up to 2000 m in a distance of less than 10 km. In the more south and east directions the mountains gradually increase up to 2500 m.

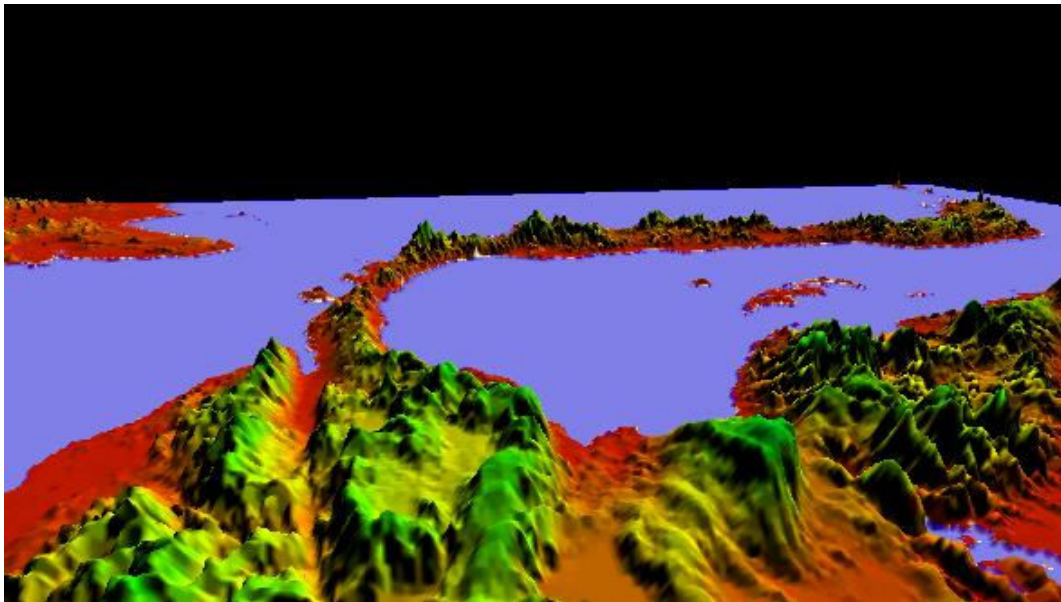


Figure 6.3: Three dimensional view of topography over Central Sulawesi. The elevation data are obtained from the Shuttle Radar Topography Mission - SRTM of the United State Geological Survey (USGS) at 90 m resolution.

The study area of the MM5 model is the Sulawesi region as the mother domain ( $116.1^{\circ}\text{E}$ - $125.9^{\circ}\text{E}$ ;  $6.3^{\circ}\text{S}$ - $2.7^{\circ}\text{N}$ ) with a 15 km horizontal resolution and the second domain covers Central Sulawesi ( $118.9^{\circ}\text{E}$ - $120.8^{\circ}\text{E}$ ;  $1.9^{\circ}\text{S}$ - $0.3^{\circ}\text{S}$ ) with a 5 km horizontal resolution. The study aspects are local phenomena such as the orographic rainfall in the complex terrain and the land-sea breeze circulation. Model domain for the coarse resolution (15 km) is similar to the one in Figure 3.2 of Chapter 3 and the

second domain (5 km horizontal resolution) appears in most of the panels of this chapter (see Figure 1.1).

### 6.2.3 Data

The external data required to characterise the model domain are the surface characteristics including terrain elevation, land use/vegetation (Leaf Area Index, LAI), land-water mask, soil types, vegetation fraction and deep soil temperature. They are available at six different resolutions: 1 degree, 30, 10, 5 and 2 minutes, and 30 second can be obtained from the USGS (United State Geographical Survey). The soil distribution type is obtained from FAO data base. The vegetation and soil physical parameters are explained in Dudhia et al. (2005). These data are available at <http://www.mmm.ucar.edu/mm5>.

The meteorological data of the NCEP GFS model final analyses, with the time interval every 6 hours, is used for initialization and lateral boundary conditions for monthly simulations. The data is available at ftp site [dss.ucar.edu](ftp://dss.ucar.edu). The time step of the coarse model with the resolution of 15 km by 15 km is 45 seconds. The grid point numbers for the mother domain (15 km horizontal resolution) are 40 in the x direction and 34 in the y direction or 1360 grid points and the nested domain (5 km horizontal resolution) has 42 grid points in the x direction and 36 grid points in the y direction or 1512 grid points.

## 6.3. Results

### 6.3.1 Rainfall simulation on complex terrain

In the Figure 6.4, the simulation results of selected monthly rainfall in 2003 to represent the Asian or Australian monsoon are depicted for the second model domain which covers the main research area of Lore Lindu National Park within the complex terrain. The Asian monsoon is represented by the model results for December and the Australian monsoon is represented by model results for June, respectively.

The spatial distribution of monthly rainfall is closely related to topography. High rainfall occurs in the mountains. In the Palu Valley, as is expected, the rainfall is low. The wind directions at the 800 hPa pressure level are overlaid on top of rainfall to



show the different effects of circulation of the two seasons. In December the wind comes mostly from the west and north-west, whereas at June the dominant wind directions are from east and south-east.

The rainfall formation processes in Central Sulawesi are determined by local topographical conditions which vary quite dramatically in the steep landscape. They are also affected by monsoon circulation which determines from where the air mass comes from. An analysis of the MM5 model results in zonal cross sections of  $1.0^\circ$  latitude to show the orographical rainfall (Figure 6.5). In December the air circulation corresponds to the Asian monsoon which brings moist air from the South China Sea (Langmann and Heil, 2004). The air mass reaches the Sulawesi Island from the west direction and in Central Sulawesi it is orographically lifted, condensation and rainfall take place. One can see from Figure 6.5 that during the Asian monsoon in December rainfall starts already before the air masses are lifted orographically. This is because the air masses is most humid during this time. This is different in June when the air flows from the Australian continent contain dry air masses.

The rainfall gradually increases according to elevation and after the peak of the mountain; air is moving down slowly and the air becomes warmer and the relative humidity decreases. The rainfall decreases accordingly as the elevation decreases, and the minimum rainfall values just occur in the valley. At the next ridge after the Palu Valley in the east direction, the air is again lifted orographically, the rainfall amounts increases gradually along the up slopes mountain and reaches a maximum at the top of the ridge and then decreases with lower elevation.

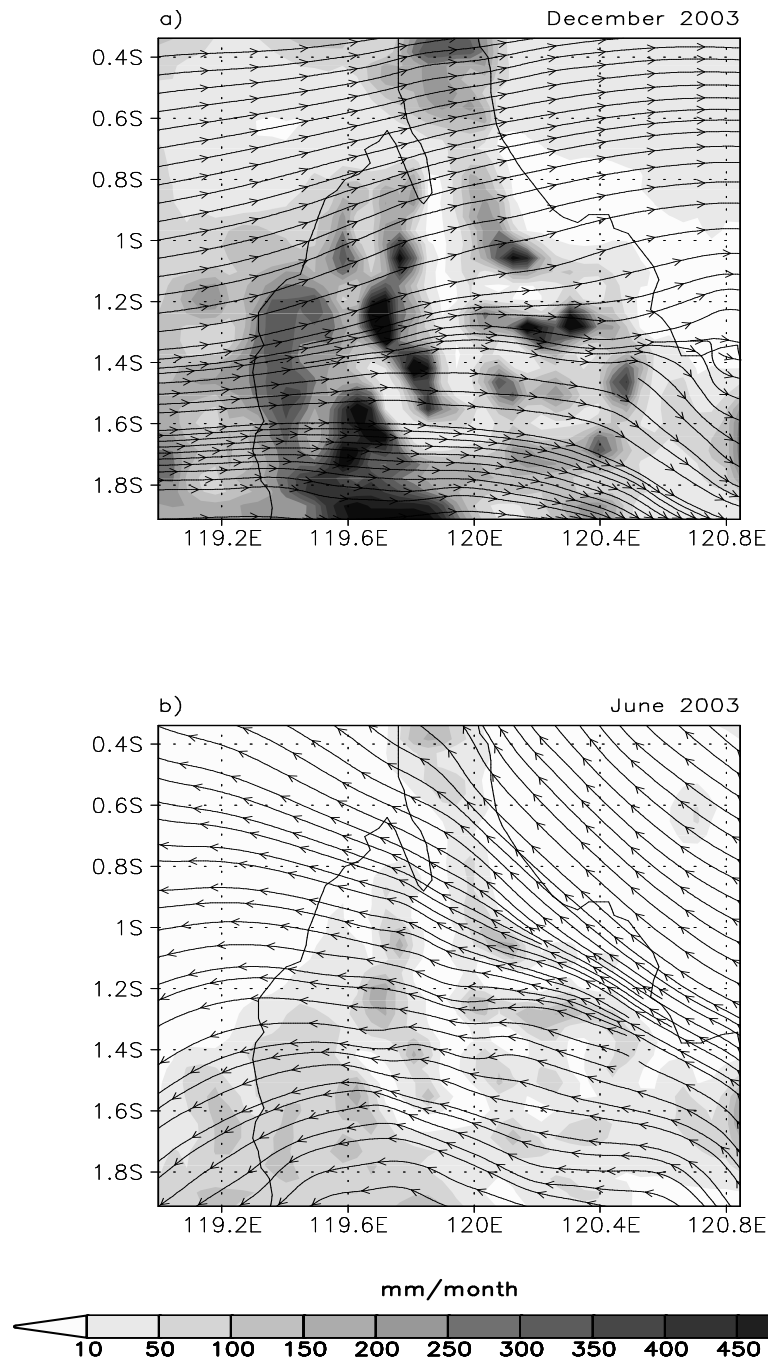


Figure 6.4: Spatial distribution of modelled monthly rainfall (shaded) and wind direction at the 800 hPa level (streamlines) for December 2003 (a) and June 2003 (b).

The pattern of orographic rainfall in June is similar to the December pattern. The monsoon circulation in June corresponds to the Australian monsoon and the air mass relatively dry and the wind direction mostly come from east/south east direction (see Figure 6.4). In this month, rainfall is formed purely orographically. The rainfall

amount at each elevation level is less in June compared to December hence, the total amount along this latitude also greater in December compared to June. Contrary to December the regions behind the ridges become leeward in June. The same case applies to the region behind the east ridges. The Palu Valley, on the other hand, faces leeward in both seasons and therefore, the monthly rainfall is always low.

Spatial comparison within the model domain of the monthly rainfall amount in these two seasons shows that in June 2003 (Australian monsoon) the rainfall amount is less compared to the December 2003 rainfall (Asian monsoon).

### 6.3.2 Land-Sea breeze circulation

The MM5 model is also capable to simulate the daily land and sea breeze circulation which dominated the surface wind velocity over this region. The wind analyses (wind rose) from the automatic weather station in Mutiara Palu as a coastal area show that the dominant wind direction is north/north-west (Figure 6.6). In the Gimpu region, which lies 75 km south from the Palu Bay, the analysis also shows that most of the time the wind comes from north/north east direction revealing that the sea breeze penetrates up to this area. The wind directions at the stations outside the Palu Valley reflect mostly the monsoon circulation. The mechanism and factors driving the land-sea breeze circulation over this region will be shown with the simulations of the MM5 model.

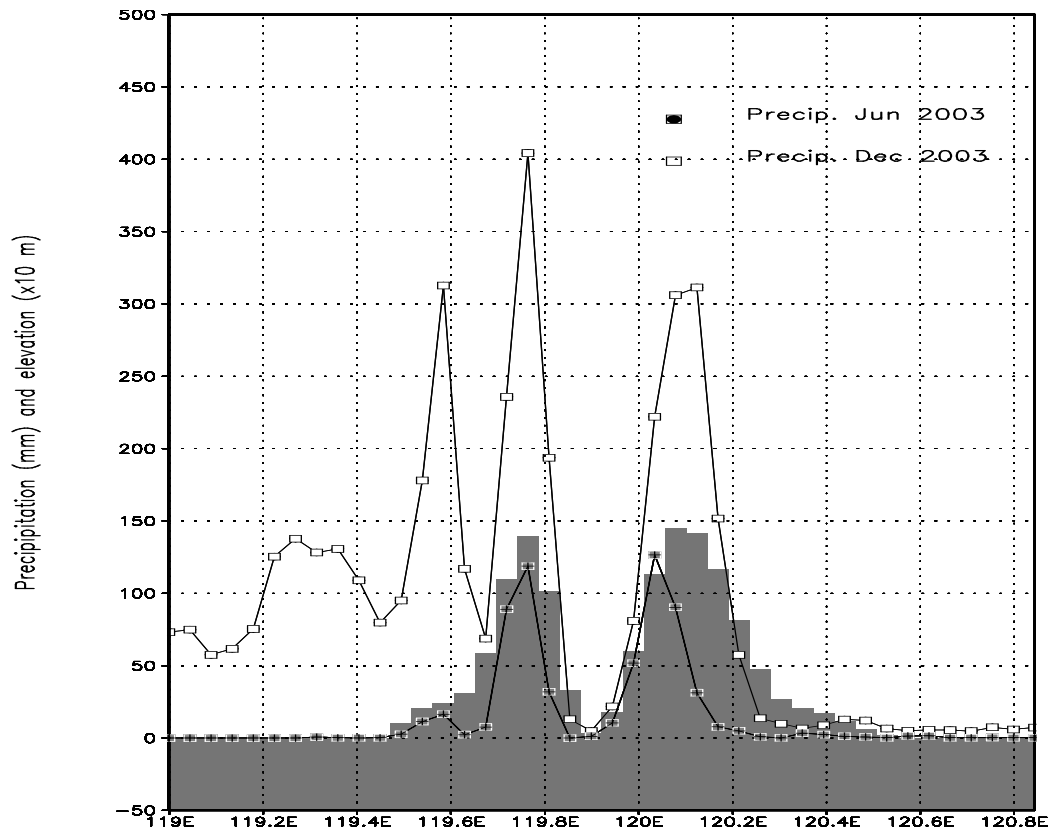


Figure 6.5: Zonally average modelled rainfall and altitude along the 1.0° S latitude. Orographic rainfall is shown for two months, December 2003 (open squares) and June 2003 (solid squares). The shaded bar graph shows the elevation in 10 meter units.

The monthly average wind circulation pattern showing the daily cycle of land-sea breeze simulated by the MM5 model for September 2004 can be seen in Figure 6.7. Six times are selected representing day and night time. The land-sea breeze circulations are well developed at these times, resulting from differences in atmospheric heating between land and sea surfaces. The sea breeze starts in the late morning at 10.00 local time and it pertains during daytime until about 16.00. The land breeze takes place from 19.00 to 08.00. During the daytime (at 12.00, 14.00, 16.00 local time, upper panels) the wind comes from Makassar Strait, Tomini Bay and Palu Bay onto the land. It can be seen from this figure that at Palu Bay the wind blows to the land from north/north west direction and the record from the automatic weather station in Mutiara Airport Palu shows the same results (see Figure 6.6). On the right

hand side of the lower panels of Figure 6.7, the elevation contour (in metre) is included.

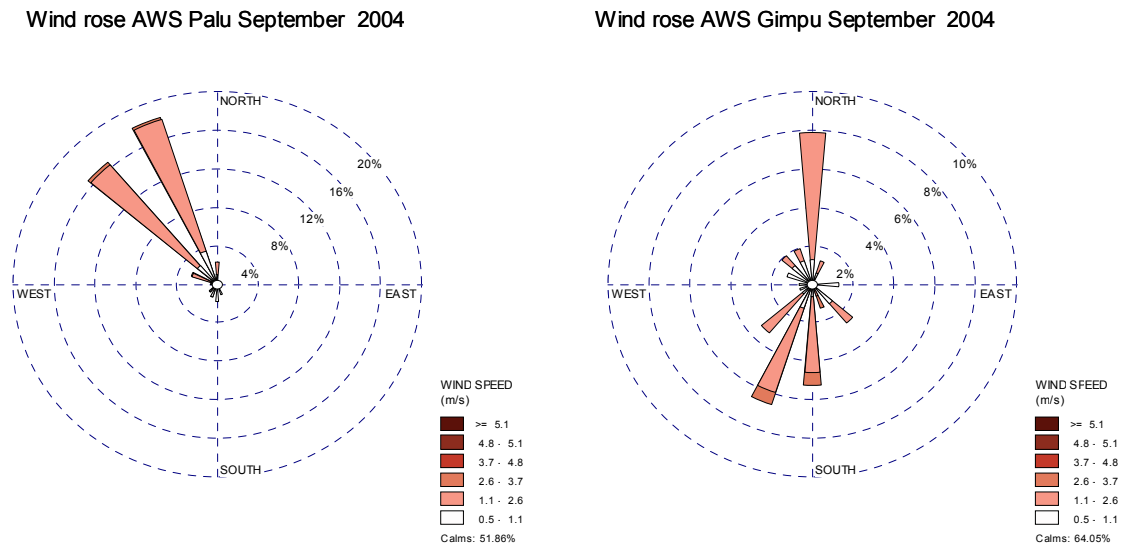


Figure 6.6: Wind analysis (wind rose) of the Automatic Weather Stations (AWS) Mutiara Palu (a) and Gimpu (b) in September 2004, showing the dominant wind directions (see stars in Figure 6.7 for the position of both locations).

The sea breeze follows along the bottom of the Palu Valley and blows to the south until it disappears at the edge of more complex terrain. The sea breeze propagation is pronounced all along the day and reaches far inland up to Gimpu (120.0°E, 1.6°S; 417.5 meters a.s.l) in the late afternoon (16.00 local time). The distance is about 75 km away from the coastal line in the Palu Bay.

Several studies (Hadi et al., 2002; Miao et al., 2003) have shown that the inland penetration distance of a sea breeze can reach 60-80 km. At night time (20.00, 00.00 and 04.00 local time, lower panels) the wind blows from the land on to the bay. The wind speeds far inland are weak, but around the coastal area such as around Palu and Tomini Bay the wind speed is continuously high with the direction opposite to the sea breeze. The low wind speeds at night time are consistent with the stable stratification of the atmosphere during night. The spatial distributions of atmospheric stability

during day and the night are represented by the so-called Total-Totals Index (TTI) in Figure 6.8 for the same six time periods as in the previous figures. The TTI is calculated from the sum of simulated air temperatures ( $T$ ) and dew point temperatures ( $T_d$ ) from different pressure levels as  $T_{850\text{hPa}} + T_{d,850\text{hPa}} - 2 T_{500\text{hPa}}$ .

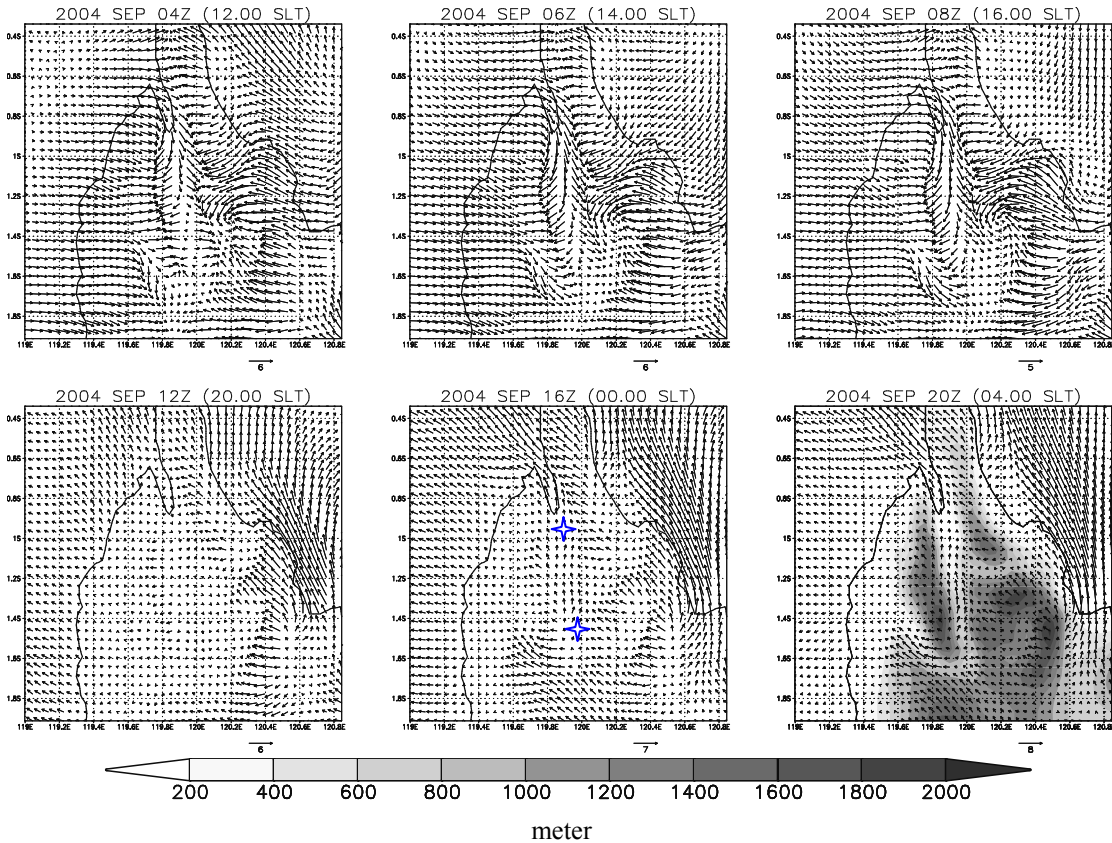


Figure 6.7: Horizontal distribution of the wind vector (m/sec) showing the sea-breeze circulation during the day (upper panels) and land-breeze circulation during the night (lower panels). The two stars on the middle lower panel mark the position of the automatic weather stations at Palu and at Gimpu (see Figure 6.6). Shading of the lower right panel depicts the topography in m a.s.l, as is shown in the legend.

It is obvious that at daytime the TTI over the land is higher than at night, i.e. the vertical stability of the atmospheric boundary layer is more unstable during day than at night. Over the ocean, however, the vertical structure varies only a little and is relatively stable during all the time.

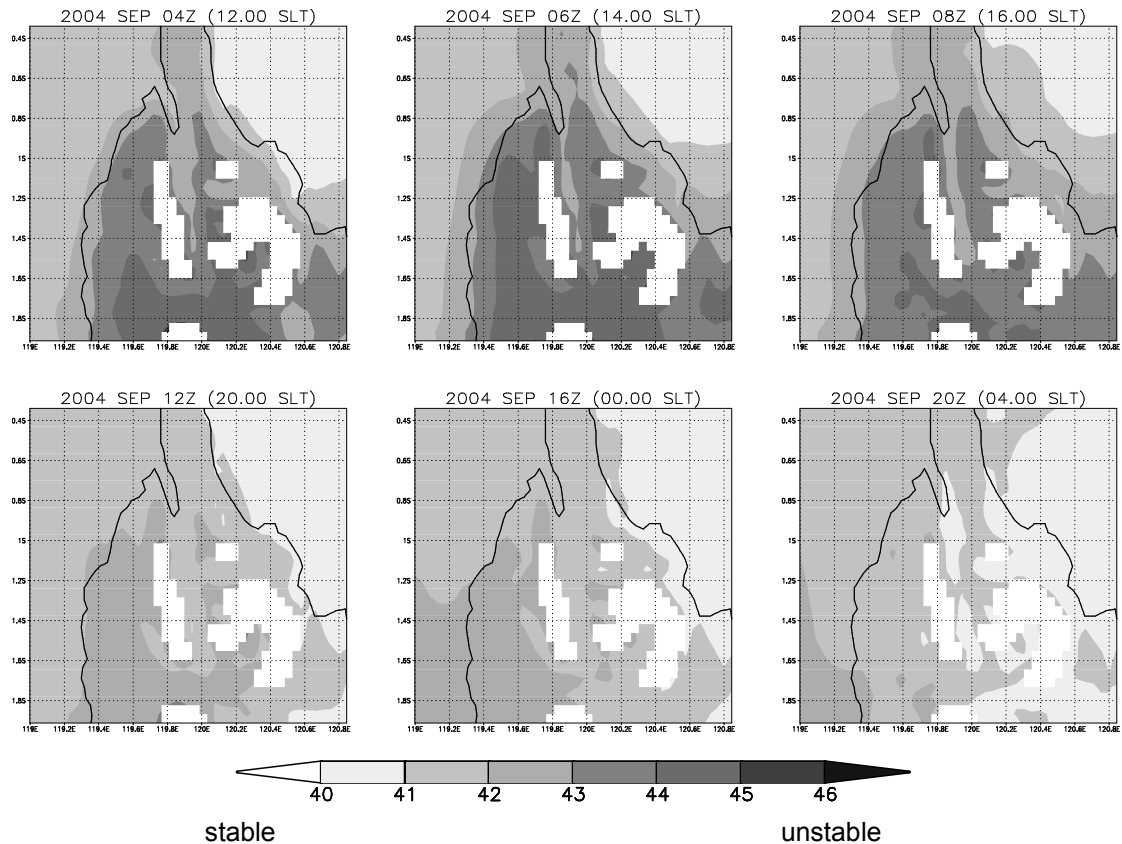


Figure 6.8: The Total Totals Index (TTI) values show the atmospheric stability at day time (upper panel) and night time (lower panel) averaged for September 2004. See text for definition of the TTI.

Different physical characteristics of the ocean and the land surfaces are the main factors causing locally different heating and energy exchange rates with the atmosphere, which drive the land sea-breeze circulation. The surface energy exchange processes are represented by latent and sensible heat fluxes. Figure 6.9 shows the distribution of latent heat fluxes on land and on sea during the day and night. At daytime the land surface receives the energy for evaporation and sensible heat production (see Figure 6.10) more rapidly compared to the sea. The surface heats up more rapidly and the air temperature increases accordingly (see the 2 metres air temperature Figure 6.11).

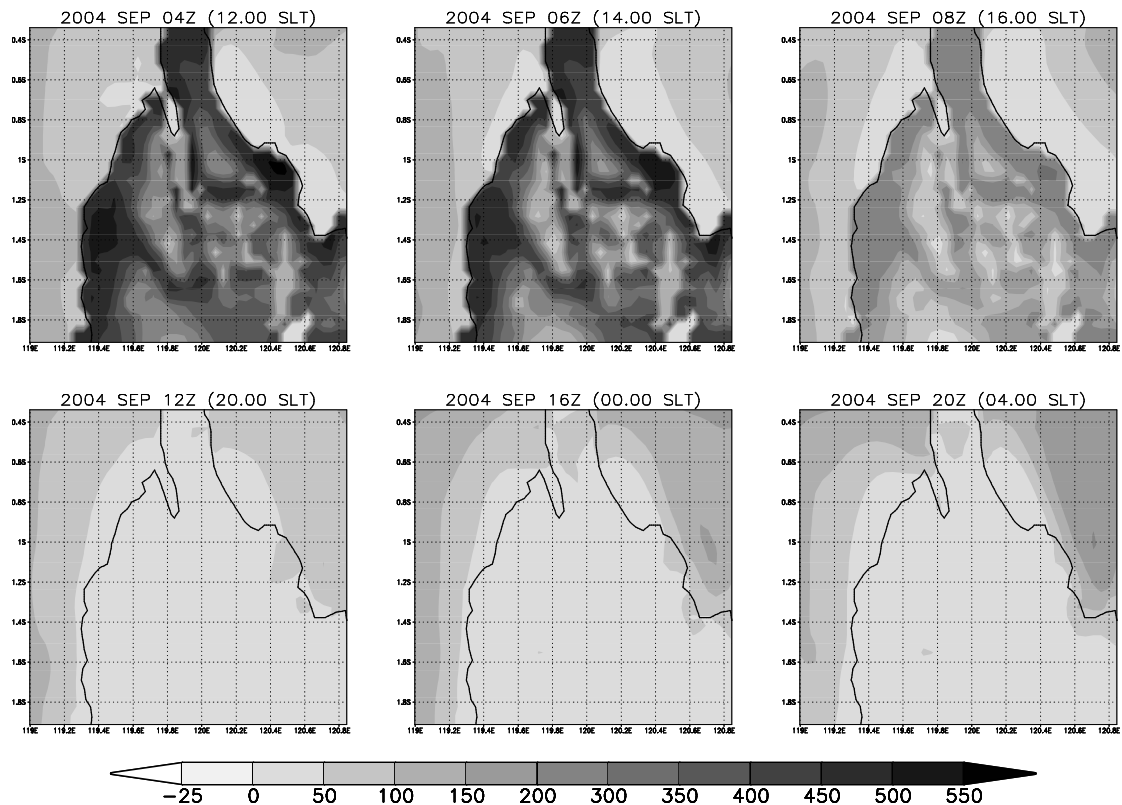


Figure 6.9: Distribution of latent heat fluxes ( $\text{W m}^{-2}$ ) on land and on sea during the day and night.

At night time, the land is cooling and the latent heat fluxes are smaller compared to the sea. The air temperature average during the day and night are shown in Figures 6.12a and 6.12b respectively. The land day minus night air temperature differences may reach up to 14 degrees, whereas on the sea the difference is only 2 degrees (Figure 6.12). On the sea, at one location the air temperature differences at daytimes and at nighttimes are not more than 1 degree, whereas over the land at one location the differences reaches up to 4 degrees.

The land-sea breeze circulation takes place within the planetary boundary layer. To know up to which level above the ground the land-sea breeze circulation occurs, Figure 6.13.a and Figure 6.13.b show the hourly wind speed and direction at several levels averaged during September 2004 at Palu and at Gimpu.



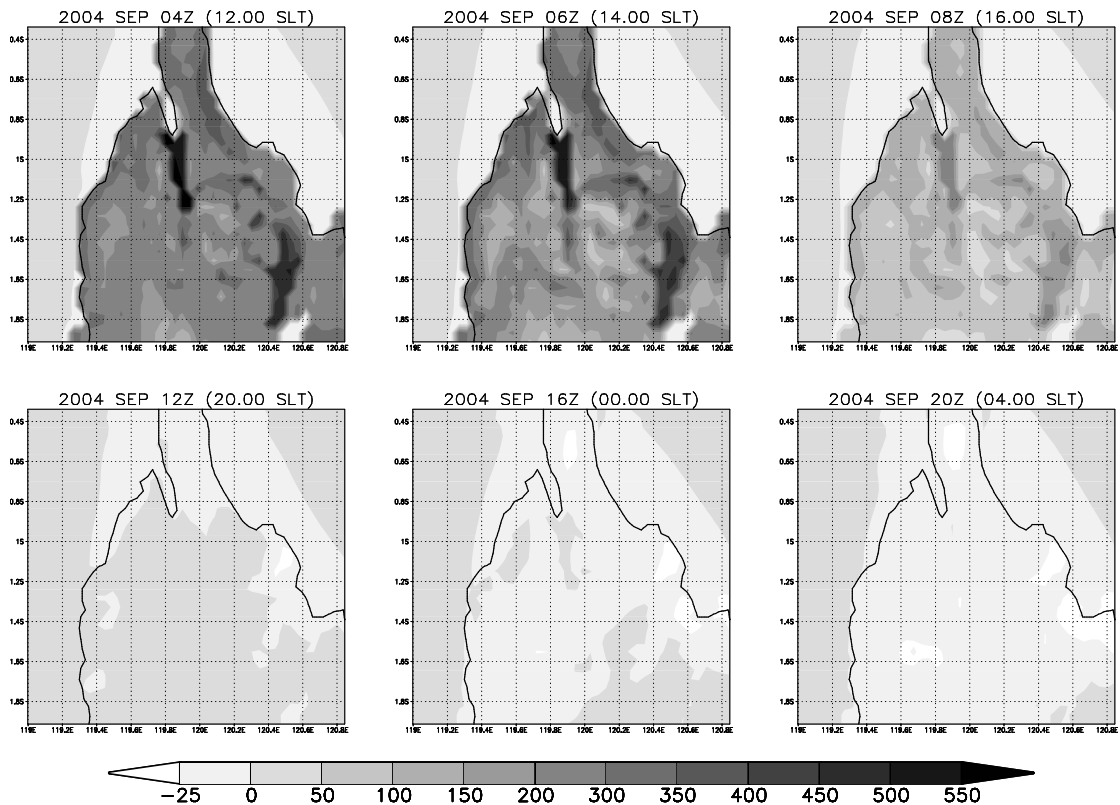


Figure 6.10: Same as Fig.6.9 but for sensible heat fluxes ( $\text{W m}^{-2}$ ).

As a result of the pressure gradient difference between land and sea looping of air masses takes place above the Palu region at day time (Figure 6.13 a). The upper level is located between 800 hPa and 850 hPa (~1.5 km - 1.1 km above ground). The wind minimum is found at the 950 hPa level or 350 meters above the ground. This upper level of looping characterises the top height of the atmospheric boundary layer. At night time the upper level looping takes place at 700 hPa.

At Gimpu (Figure 6.13.b) the upper level looping at daytime takes place at 650 hPa and the lower looping takes place at 950 hPa. At nighttimes the wind speeds are low on the land and the land breeze does not develop as pronounced as it has been discussed previously in this section (see Figure 6.4). The atmosphere on the land at night time is more stable and thus looping does not develop or stay weak. Figure 6.13 also show the wind speed at each level as contour lines. As indicated by the arrow length, the wind speed is high in the upper level and mostly westerly with a speed value of more than 7 m/sec.

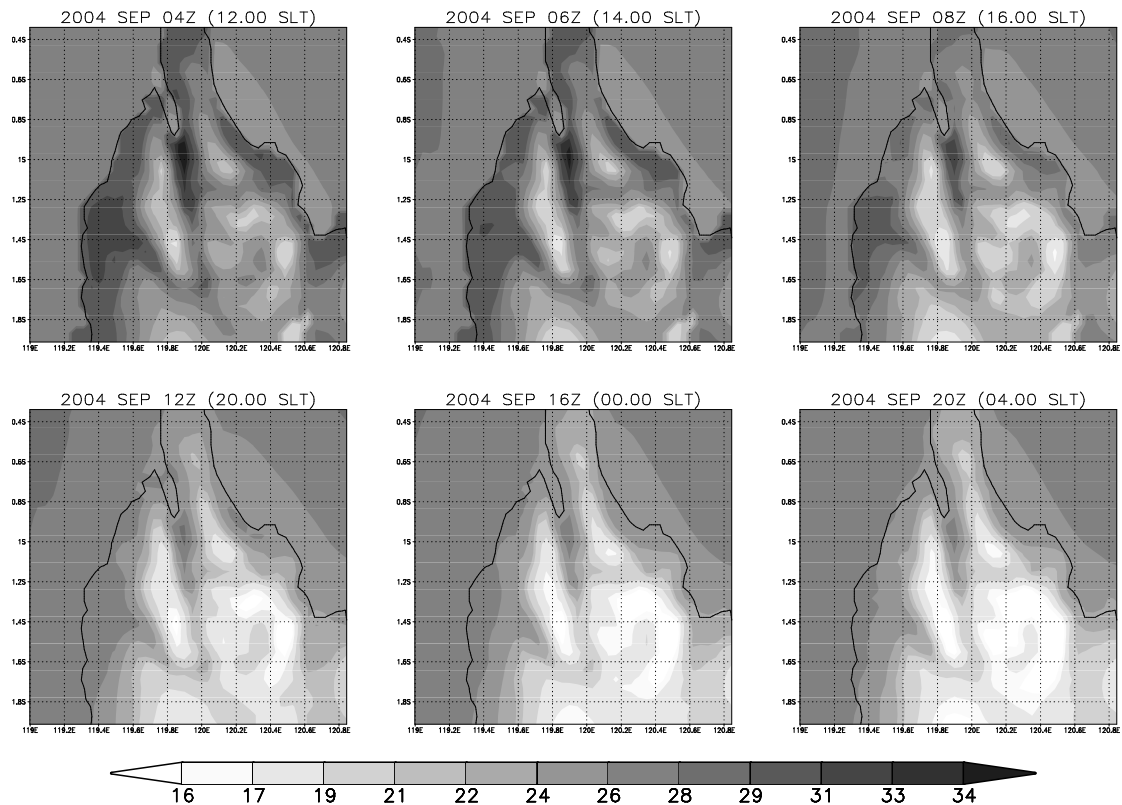


Figure 6.11: Daily average of air temperature ( $^{\circ}\text{C}$ ) at 2 m above the surface for September 2004.

#### 6.4. Discussion

Several atmospheric parameters from MM5 model simulation show reasonable values in terms of space and time distribution. Monthly rainfall rate in December 2003, for example, is high compared to the rate of June 2003 (Figure 6.4) and the wind circulation shows the Asian monsoon in December and the Australian monsoon in June. It is shown in the Chapter 2 that in Central Sulawesi the monsoon rainfall pattern is not dominant. The results of MM5 simulation is consistent with the Chapter 2 results where the monsoon rainfall pattern is within the MM5 model domain, whereas the anti-monsoon rainfall patterns which has a high rainfall in June and less rainfall in December are located beyond the second domain of the MM5 model.

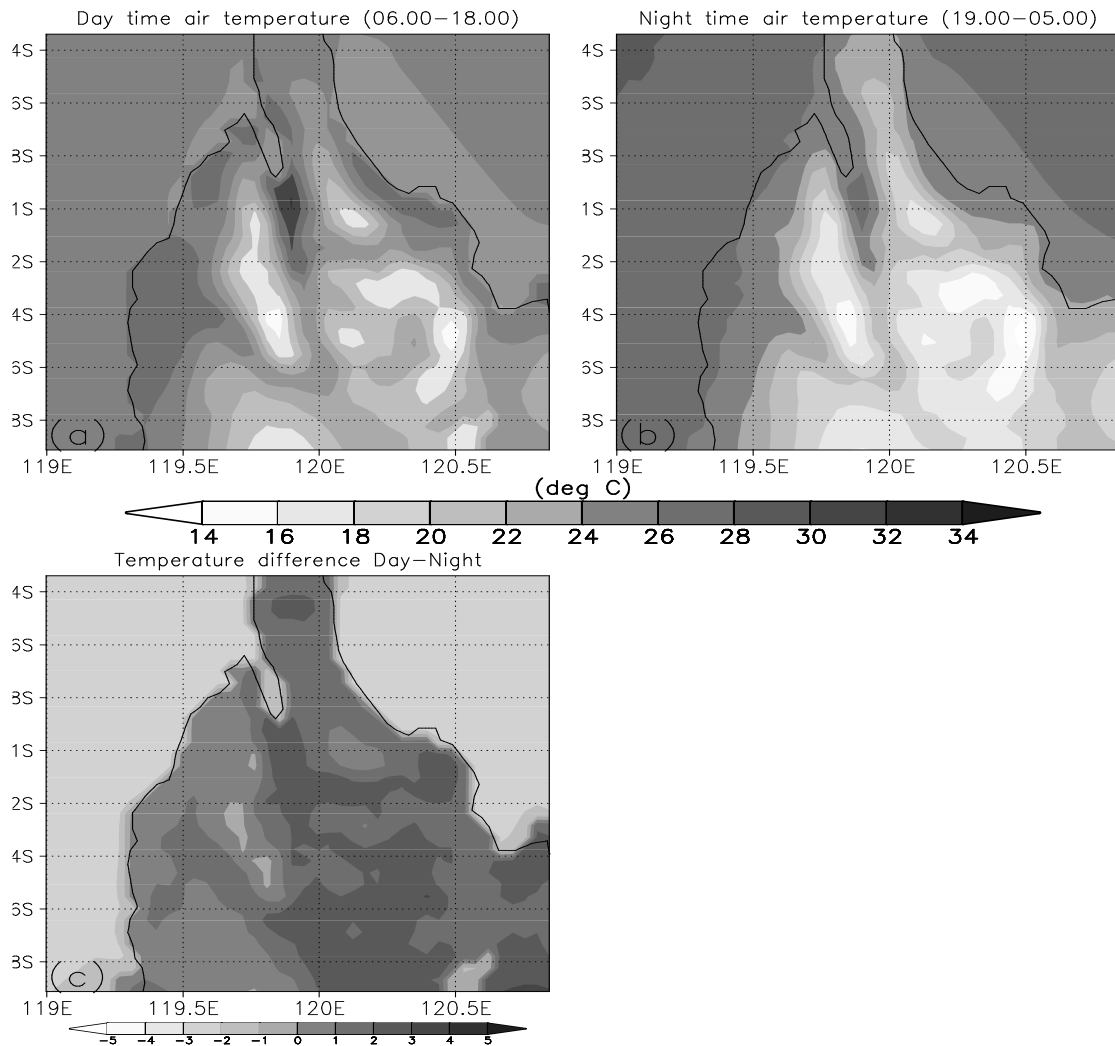


Figure 6.12: Mean air temperatures ( $^{\circ}\text{C}$ ) at day (a) and night time (b); the temperature difference between day time air temperatures and night time air temperatures (c).

The geographical position of Palu Bay and the existence of the Palu Valley on land generate a land-sea breeze circulation. The circulation penetrates along the valley to a distance of 75 km inland as is observed by wind direction in the Gimpu station.

The other parameters such as air temperature (Figure 6.11) also show a reasonable value in space and time distribution where the temperature in the mountainous region is lower compared to the lowland region, more specifically at the Palu Valley which is the hottest region compared to its surrounding area.

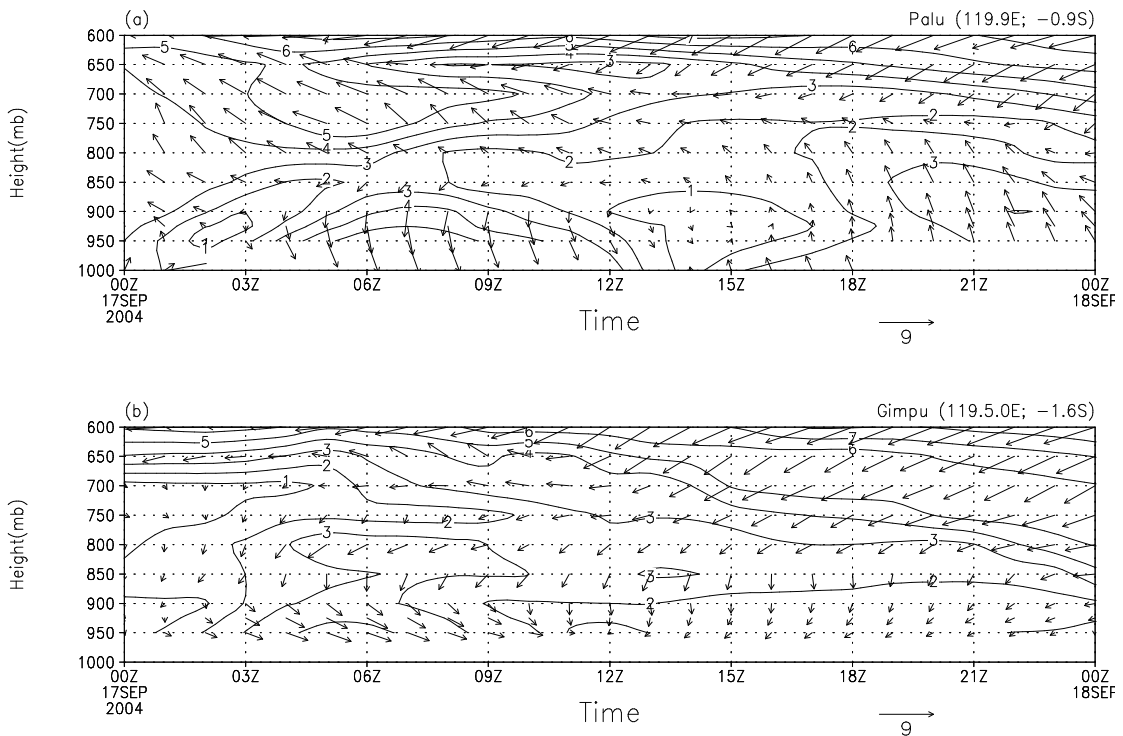


Figure 6.13: Daily cycle of wind speed and direction at several pressure levels at Palu (a) and Gimpu (b). The contour lines represent location of wind speed (1.0 m/sec interval).

Comparison of several atmospheric parameters can be represented by evapotranspiration which is the derived parameter calculated from air temperature, radiation, wind speed, water vapor pressure and air pressure. The calculation of evapotranspiration from regionalization of atmospheric parameters of the automatic weather station network of STORMA project has been performed using SVAT-regio model (Oltchev et al., 2005). A comparison of these values with the one calculated by atmospheric parameters from MM5 for September 2004 showed that the evapotranspiration values are in the range of  $55 - 152 \text{ mm month}^{-1}$ , whereas the results from MM5 are in the range of  $60 - 150 \text{ mm month}^{-1}$ . The evapotranspiration also reflects the surface characteristics, thus the surface parameters such as the land use, land cover, vegetation and soil physical parameters are well represented by the input of surface data and well interpolated by the sub model TERRAIN in the MM5 model.

## 6.5. Conclusions

The Mesoscale atmospheric Model MM5 with a 5 km horizontal resolution was able to simulate the local phenomenon of orographic rainfall in June 2003 and December 2003. These periods represent the two different seasons, namely the Australian and the Asian monsoon. The zonally average rainfall distribution along latitude 1.0° South corresponds very closely with the topography. The rainfall formation in this area is very strongly influenced by the mechanism of orographic lifting.

The Land-sea breeze around Palu Bay and in Palu Valley was investigated as a case study for September 2004. Wind observations along the valley from the coastal region (Mutiara Palu) to the end of the valley in Gimpu show the propagation of sea breeze until 75 km inland. This result is similar to the results of Hadi et al. (2002). They concluded that in Jakarta Bay the sea breeze circulation phenomenon occurs most pronouncedly during the period of July to October and it propagates up to distances of 60 to 80 km inland.

The analysis showed remarkable differences of surface heating between land and sea resulting large differences of the latent and sensible heat flux as well as the surface air temperature distributions between land and sea. These differences act as the driving force for the land sea breeze phenomenon. There, the pressure gradient between the land and the sea in the upper and lower level during the day and night causes the looping of air flow. At Palu the looping is clearly simulated by the model, i.e. at the lower level the wind blows onto the land and at the upper level the wind blows onto the sea during daytimes. The opposite happens at nighttimes. In Gimpu the looping can only be observed during day, whereas at night as the wind is calmer and the looping is not so clearly established.

With the fast growing computer technology, it is promising to apply the MM5 model for the operational purposes of numerical weather prediction in the Indonesian regions, together with research studies one of which has been discussed here.

## **CHAPTER 7**

### **MAIN CONCLUSIONS AND FUTURE RESEARCH**

#### 7.1. Main Conclusions

The dissertation concludes that three factors govern the climate and its variability in Sulawesi and especially in Central Sulawesi, Indonesia. They are the global impact's phenomenon ENSO (El Nino Southern Oscillation), the regional circulation of Asian-Australian Monsoon and the locally specific regional factors.

The research area IMPENSO in Central Sulawesi has the local climate characters. Some factors such as the geographical position, the existing of local circulation like the land-sea breeze circulation, the windward and leeward affect the climate condition. The climate variability in this region is influenced by the global scale phenomenon of ENSO events. Rainfall pattern classification using the cluster analysis method has divided the Central Sulawesi into 10 rainfall patterns. The two (monsoonal and anti-monsoonal patterns) of three rainfall patterns commonly found in the Indonesian regions exist in Central Sulawesi. The other pattern is a more local pattern characterized by low annual cycle of rainfall amount.

The simulated rainfall using the regional atmospheric model REMO applied here with an 18 km horizontal resolution has a good agreement with observed data in a flat region at South Sulawesi and less agreement in the mountainous region of Central Sulawesi. The model is used to investigate the rainfall variability related to the ENSO events. The satellite-based rainfall data can be used to complete the ground-based rainfall data for climate analyses and monitoring purposes.

Spectral analysis is used to study the time series of model and observed data in the frequency domain. Using three spectral analysis methods (MEM, MTM and wavelets) the mode of variability of the time series is detected. The wavelet analysis more obviously showed the periodicities and the time of occurrence of any period. The dominant mode of variability in Central Sulawesi is the ENSO events whereas in South Sulawesi the dominant mode is the annual cycle of monsoon circulation.

The mesoscale atmospheric model MM5 has completed the study of climate variability and the driven factors form the climate in Central Sulawesi. The MM5 can simulate the local factor like the land-sea breeze circulation and orographic rainfall as well as the Asian – Australian Monsoon circulation.

## 7.2. Implications for future research

The Indonesian Maritime Continent with a thousand islands scattered over the tropical ocean in the vicinity of the equator is a unique region for atmospheric processes. The convection is one of the important processes and still remains a big challenge to be studied using the atmospheric models since it is one of the major factors influencing local rainfall. The MM5 model with its non-hydrostatic parameterization is a useful basic tool to investigate and to quantitatively describe such processes.

It is proposed here that the atmospheric model MM5 can be applied as a Numerical Weather Prediction (NWP) tool for a daily weather forecast by the Indonesian national weather service (Meteorological and Geophysical Agency, BMG) together with research studies, one of which has been discussed here. The computer resources nowadays available are not a limiting factor anymore to run such models. Even so the global model as a boundary and initial condition for running a regional model is not restricted. Several tests using a PC Linux to make a 36-hour forecast over two nested domains of Sulawesi and Central Sulawesi are reasonable with respect to the forecast lead time.

## ACKNOWLEDGEMENTS

First of all I have to express my sincere praise to God (Allah) for giving me life, until I exceed a big step in my small life; finishing this dissertation.

I would like to thank very deeply to Prof. Dr. Gode Gravenhorst for his supervision and giving me the motivation since I was in Jakarta to study and to do research in the Institute of Bioclimatology, University of Göttingen, Germany. I express a high appreciation to the co-referee in my dissertation examination, Prof. Dr. Dick Hölscher.

The names mentioned below are persons, a team and institutions who contribute to the success of my study; therefore I would like to show my appreciation to them.

Dr. Gunawan Ibrahim, the Director of Meteorological and Geophysical Agency (1999-2005) in Jakarta where I worked has given me the permission to continue my study. I thank Dr. Daniela Jacob at the Max Planck Institute for Meteorology, Hamburg, from whom I got permission to study and use the REMO model. Mr. Podzun and Dr. Edvin Aldrian for their assistance during the setup of the REMO model and also to Dr. Edvin Aldrian for providing me the REMO 1/2° output as the boundary condition for REMO 1/6° which I worked with. I would like to thank Prof. Dr. Oswald Haan for guiding me in the setting up of the MM5 model on the parallels version of IBM machine at GWDG.

I am working in an inter-disciplinary research project, the IMPENSO (Impact of ENSO). As a group, I would like to thank all the members and the coordinator for realising one of applicable research within the German Climate Research Program, DEKLIM. They are Prof. Dr. Manfred Zeller, Prof. Dr. Gerhard Gerold, Dr. Regina Birner, Dr. Alwin Keil and Dr. Constanze Leemhuis. My research was supported by the German Federal Ministry of Research and Education (BMBF) and I would like to thank this institution for the scholarship. I express special thanks to Dr. A. Münzenberg at the BMBF as the project research manager. During collecting field data I was supported by a team from STORMA office in Tadulako University Palu



and a team from Meteorological Office Mutiara Palu. I would like to thank all members of these teams for all kinds of help and collaboration.

Working in the harmonic atmosphere at the Institute of Bioclimatology has given me much more experience on how to solve technical problems. I am very thankful to all of the institute's members, especially to Prof. Dr. Andreas Ibrom, Dipl.Phys. Heiner Kreilein and Mrs. Marie-Luise Baumann.

My family supported me with spirit and morale. I would like to thank my mother, my sister and brother. Their contribution to my success is invaluable and will be forever in my memory.

Finally, great appreciation is given to my wife Ai Pridasari, my children Safira Maulidina and Fajar Naufal Luthfi for their patience and deep understanding. Some nice family times were lost during my work. I dedicated this dissertation to them.

## ABREVIATIONS

AAM	Asia Australia Monsoon
AWS	Automatic Weather Station
AVHRR	Advanced Very High Resolution Radiometer
AR	Auto Regressive
BALTEX	Baltic Sea Experiment
BMBF	Bundes Ministerium fuer Bildung und Forschung Federal Ministry of Education and Research, Germany
BMG	Badan Meteorology dan Geofisika, Indonesian Meteorology and Geophysics Agency
CPC	Climate Prediction Centre
CMAP	CPC Merged Analysis of Rainfall
DEKLIM	Deutsches Klima/German Climate Research Program
DJF	December/January/February
DKRZ	Deutsches Klimarechenzentrum/German Climate Computing Centre
DMSP	Defence Meteorological Satellites Program
DWD	Deutscher Wetterdienst/German Weather Service
ECHAM4	ECMWF/Hamburg Atmospheric Model version 4
ECMWF	European Centre for Medium Range Weather Forecast
EM/DM	European Model/Deutche Model
ENSO	El Nino Southern Oscillation
EOF	Empirical Orthogonal Function
ERA 15	ECMWF Re-Analysis 15 years
FAO	Food and Agriculture Organisation
HCA	Hierarchical Cluster Analysis
GCM	Global Circulation Model
GFS	Global Forecast System
GOES	Geostationary Satellite Server
GPCC	Global Rainfall Climatology Centre
GPCP	Global Rainfall Climatology Project
GPI	GOES Rainfall Index
GTS	Global Telecommunication System
IMPENSO	Impact of ENSO project

---

JJA	June/July/August
ISO	Intra Seasonal Oscillation
ITCZ	Inter Continent Convergence Zone
ISLSCP	International Satellite Land-Surface Climatology Project
MEM	Maximum Entropy Method
MEI	Multivariate ENSO Index
MJO	Madden Julian Oscillation
MM5	Mesoscale Model 5 <sup>th</sup> generation
MPI-M	Max Planck Institute for Meteorology
MTM	Multi Taper Method
NCEP	National Centre for Environment Prediction
NESDIS	National Environmental Satellite, Data and Information Service
NOAA	National Oceanic and Atmospheric Administration
NWP	Numerical Weather Prediction
OLR	Out going Long wave Radiation
PBL	Planetary Boundary Layer
REMO	Regional Model, the MPI-M Regional Atmospheric model
SOI	Southern Oscillation Index
SON	September/October/November
SRTM	Shuttle Radar Topography Mission
SSM/I	Special Sensor Microwave Imager
SSTA	Sea Surface Temperature Anomaly
SVAT	Soil Vegetation Atmosphere Transfer model
TTI	Total Totals Index
USGS	United State Geographical Survey
WMO	World Meteorological Organisation

## REFERENCES

- Aldrian, E., 2002: Spatial Patterns of ENSO impact on Indonesian Rainfall. *J. Sains & Tek. Mod. Cuaca, BPP Teknologi*, 3, 5-15.
- Aldrian, E., 2003: Simulations of Indonesian rainfall with a Hierarchy of Climate Models. Examensarbeit Nr. 92, [Available from Max-Planck - Institut für Meteorologie, Bundesstrasse 55, D-20146, Hamburg, Germany.], 159 pp.
- Aldrian, E., and R.D. Susanto, 2003: Identification of three dominant rainfall regions within Indonesia and their relationship to sea surface temperature. *Int J Climatol* 23:1435–1452.
- Aldrian, E., L.Dümenis-Gates, D.Jacob, R.Podzum and D.Gunawan, 2004: Long-term simulation of Indonesian rainfall with the MPI-M regional model. *Climate Dynamic*. 22: 975-814.
- Alhamed,A., S. Lakshmivarahan, and D. Stensrud, 2001: Cluster Analysis of Multi model Ensemble Data from SAMEX. *Mon. Wea. Rev.*, 130, 226–256.
- Arkin, P.A., and B.N. Meisner, 1987: The relationship between large-scale convective rainfall and cold cloud over the Western Hemisphere during 1982-1984. *Mon. Wea. Rev.*, 115, 51-74.
- Badan Meteorologi dan Geofisika (BMG), 2002: Prakiraan Musim Kemarau 2002 di Indonesia. Jakarta. (In Indonesian language).
- Badan Meteorologi dan Geofisika Palu (BMG), 2001: Iklim di Sulawesi Tengah (In Indonesian language).
- Beck,C.,J.Grieser, and R.Bruno,2005: A new monthly rainfall climatology for the global land areas for period 1951 to 2000. GPCC, DWD. Germany.
- Berger, A. L., J. L. Melice, and L. Hinnov, 199: A strategy for frequency spectra of Quaternary climate records, *Clim. Dyn.*, 5, 227–240.
- Braak, C.,1929: The Climate of the Netherlands Indies. Vols. I and II. Verhandelingen No. 8, *Koninklijk Magnetisch en Meteorologisch Observatorium te Batavia*, 1602 pp.
- Chang, C-P.2004: Maritime Continent Monsoon, in Review Topic A3: Asian Winter Monsoon. Available at <http://www.weather.nps.navy.mil/~cpchang/IWM-III/R18-A3-AsianwinterMonsoon.pdf>.

- Chang,C-P., Z.Wang, J.Ju, and T.Li: 2004. On the Relationship between Western Maritime Continent Monsoon Rainfall and ENSO during Northern Winter. *J.Climate*, 17, 665-672.
- Chappellaz, J., J. M. Barnola, D. Raynaud, Y. S. Korotkevitch, and C. Lorius, 1990: Ice-core record of atmospheric methane over the past 160,000 years, *Nature*, 345, 127–131.
- Chung,Y.S.,MA.B Yoon and H.K.Kim,2004: On Climate variation and change observed in South Korea. *Climatic Change* 66: 151–161.
- DWD., 1995: Documentation des EM/DM-System. Edited by R. Schrödin. [Available from German Weather Service, Zentralamt, D-63004 Offenbach am Main].
- Davies, H.C., 1976: A lateral boundary formulation for multilevel prediction models. *Quart.J.Roy.Meteor. Soc.*, 102, 405 - 418.
- DeGaetano, A.T., 2001: Spatial grouping of United States climate stations using a hybrid clustering approach. *Int.J.Climatol.*, 21:791 – 808.
- Done,J.M.,L.R.Leung,C.A.Davis, and B.Kuo. 2004: Regional Climate Model using the WRF. Available at <http://www.mmm.ucar.edu/mm5/workshop/ws04/PosterSession/Done.James.pdf>
- Dudhia, J., 1989: Numerical Study of Convection Observed during the Winter Monsoon Experiment Using a Mesoscale Two-dimensional Model. *J.Atmos.Sci*, 46, 3077-3107.
- Dudhia, J., 1993: A Nonhydrostatic Version of the Penn State-NCAR Mesoscale Model: Validation Tests and Simulations of an Atlantic Cyclone and Cold Front, *Mon. Wea. Rev.*, 121, 1493–1513.
- Dudhia, J., 2005: MM5 Version 3.7 (The Final Version). <http://www.mmm.ucar.edu/rf/users/workshops/WS2005/abstracts/Session1/1-Dudhia.pdf>.
- Dudhia,J., D.Gill, K.Manning, W.Wang, C.Bruyere,S.Kelly, and K.Lackey, 2005: PSU/NCAR Mesoscale Modeling System.Tutorial Class Notes and User’s Guide: *MM5 Modeling System Version 3*. Mesoscale and Microscale Meteorology Division National Center for Atmospheric Research. Boulder,Colorado.
- EL-Askary. H, S. Sarkar, L. Chiu, M. Kafatos, and T. El-Ghazawi. 2004: Rain gauge derived rainfall variability over Virginia and its relation with the El Niño southern oscillation. *Advances in Space Research*, 33, 338–342.

- Ferraro, R., F. Weng, N. C. Grody, and A. Basist, 1996: An eight-year (1987-1994) time series of rainfall, clouds, water vapour, snow cover and sea ice derived from SSM/I measurements. *Bull. Amer. Meteor. Soc.*, 77, 891-905.
- Ferraro, R., 1997: Special sensor microwave imager derived global rainfall estimates for climatological applications. *J. Geophys. Res.*, 102(D14), 16,715-16735.
- Fovell B, and M. Fovell, 1993: Climate zones of the conterminous United States defined using cluster analysis. *Journal of Climate* 6: 2103–2135.
- Ghil, M., and Mo, K., 1991b: Intraseasonal oscillations in the global atmosphere-Part I: Southern Hemisphere, *J. Atm. Sciences*, 48, 780-790.
- Ghil, M., R. Allen, M. D. Dettinger, K. Ide, D. Kondrashov, M. E. Mann, A. W. Robertson, A. Saunders, Y. Tian, F. Varadi, and P. Yiou, 2002: Advanced spectral methods for climatic time series. *Rev. Geoph.*, 40:1-41.
- Gibson, J. K., P. Kallberg, S. Uppala, A. Hernandez, A. Nomura, and E. Serrano, 1997: The ECMWF Re-Analysis (ERA) 1. ERA Description., *ECMWF Reanalysis Project Report Series 1*, ECMWF, [Available from the European Centre for Medium-range Weather Forecasts, Reading, UK.], 71 pp.
- Gillian, M.M., S.J. Mason, and J.S. Galpin. 2001: Choice of Distance Matrices in Cluster Analysis: Defining Regions *J. Climate*, 7, 2790–2797.
- Gordon, A. L., and R. Fine, 1996: Pathways of water between the Pacific and Indian Oceans in the Indonesian seas. *Nature*, 379, 146–149.
- Gordon, A. L., R. D. Susanto, and A. Ffield, 1999: Throughflow within Makassar Strait. *Geophysical Research Letters*, 26, 3325–3328.
- Grell, G. A., J. Dudhia, and R. D. Stauffer, 1995: A Description of the Fifth-generation Penn State/NCAR Mesoscale Model (MM5), NCAR Tech. Note TN-98+STR, 122 pp. [Available from UCAR Communications, P. O. Box 3000, Boulder, CO 80307.].
- Gu, G., and C. Zhang, 2001: A spectrum analysis of synoptic-scale disturbances in the ITCZ. *J. Clim.* 14:2725-2739.
- Gunawan, D., and G. Gravenhorst, 2005a: Die Auswirkung von ENSO auf Niederschläge in Zentral-Sulawesi, Indonesien. German Climate Research Program, Final Symposium.

- Gunawan, D., and G.Gravenhorst, 2005b: Correlation between ENSO indices and Indonesian rainfall, *Journal Meteorologi dan Geofisika*, Accepted.
- Hadi, Tri W., T.Horinouchi, T.Tsuda, H.Hashiguchi and S.Fukao, 2002: Sea-Breeze Circulation over Jakarta, Indonesia: A Climatology Based on Boundary Layer Radar Observations, *Mon.Wea.Rev.*,130 (9), 2153-2166.
- Haylock,M., and J.McBride, 2001: Spatial coherence and predictability of Indonesian wet season rainfall, *J. Clim.*,14,3882–3887.
- Hendon, H.H., 2003: Indonesian rainfall variability: impacts of ENSO and local air–sea interaction. *J.Clim.*, 16 (11), 1775-1790.
- Hendon, H.H. and M. L. Salby, 1994: The life cycle of the Madden–Julian oscillation. *J. Atmos. Sci.*, **51**, 2225–2237.
- Hong, S.-Y., and H.-L. Pan, 1996: Nonlocal boundary layer vertical diffusion in a medium-range forecast model, *Mon. Wea. Rev.*, 124, 2322-2339.
- Huffman, G.J., 1997. Estimation of Root-Mean-Square Random Error for Finite Samples of Estimated Rainfall. *J. Appl. Meteor.*, 36 (9), 1191-1201.
- Huffman, G. J., R. F. Adler, M. Morrissey, D. T. Bolvin, S. Curtis, R. Joyce, B McGavock, and J. Susskind, 2001: Global rainfall at one-degree daily resolution from multi-satellite observations. *J. Hydromet.*, **2**, 36-50.
- IPCC, 2001: Climate Change 2001: The Scientific Basis. Contribution of Working Group I to the Third Assessment Report of the Intergovernmental Panel on Climate Change [Houghton, J.T.,Y. Ding, D.J. Griggs, M. Noguer, P.J. van der Linden, X. Dai, K. Maskell, and C.A. Johnson (eds.)]. Cambridge University Press, Cambridge, United Kingdom and New York, NY, USA, 881pp.
- Jacob, D. and M.Claussen, 1995: REMO - A Model for Climate Research and Weather Forecast. In: *First Study Conference on BALTEX* (ed. A. Omstedt). International BALTEX Publication No.3, International BALTEX Secretariat, GKSS-Research Center. P.O. Box 1160, D-21494 Geesthacht, Germany.
- Jacob, D., 2001: A note to the simulation of the annual and inter-annual variability of the water budget over the Baltic Sea drainage basin. *Meteorol.Atmos. Phys.*, **77**, 61–73.
- Jacob, D., B. J. J. M. V. den Hurk, U. Andræ, G. Elgered, C. Fortelius, L. P. Graham, S. D. Jackson, U. Karstens, C. Köpken, R. Lindau, R. Podzun, B. Roeckel, F. Rubel, B. H. Sass, R. N. B. Smith, and X. Yang, 2001: A comprehensive model

- inter-comparison study investigation the water budget during the BALTEX-PIDCAP period. *Meteorol. Atmos. Phys.*, **77**, 19–43.
- Jacob, D., and R. Podzun, 1997: Sensitivity Studies with the Regional Climate Model REMO. *Meteorology and Atmospheric Physics*, **63**, 119 - 129.
- Jevrejeva, S., J. C. Moore, and A. Grinsted, 2003: Influence of the Arctic Oscillation and El Nino-Southern Oscillation (ENSO) on ice conditions in the Baltic Sea: The wavelet approach, *J. Geophys. Res.*, **108** (D21), 4677.
- Jones, C. D. E. Waliser, J.-K. E. Schemm, W. K. M. Lau, 2000: Prediction skill of the Madden and Julian Oscillation in dynamical extended range forecasts. *Climate Dynamic*, **16**: 273 – 289.
- Ju, J., and J. M. Slingo, 1995: The Asian Summer Monsoon and ENSO, *Q. J. R. Meteorol. Soc.*, **121**, 1133-1168.
- Juneng, L., and F. T. Tangang, 2005: Evolution of ENSO-related rainfall anomalies in Southeast Asia region and its relationship with atmosphere–ocean variations in Indo-Pacific sector, *Climate Dynamics*, **25**: 337–350.
- Kalkstein, L. S., G. Tan, and J. A. Skindlov, 1987: An evaluation of three clustering procedures for use in synoptic climatological classification. *J. Clim. Appl. Met.*, **26**, 717-730.
- Kartens, U., R. Nolte-Holube and B. Rockel, 1996: Calculation of the Water Budget over Baltic Sea Cathment Area using Forecast Model REMO for June 1993, *Tellus 48A*, 684 - 692.
- Kay S. M., 1988: Modern spectral estimation. *Prentice Hall*, New Jersey, 544 pp.
- Keil, A., D. Gunawan, G. Gravenhorst, C. Leemhuis, G. Gerold, R. Birner and M. Zeller, 2005: IMPENSO; The Impact of ENSO (El Nino Southern Oscillation) on sustainable water management and the decision making community at a rainforest margin in Indonesia. German Aerospace Center, Bonn, 150-155.
- Kessler, E., 1969: On the distribution and continuity of water substance in atmospheric circulation, *Meteor. Monogr.*, **10**, No. 32, 84pp.
- Kim, K.-Y., and C. Chung, 2001: On the evolution of the annual cycle in the tropical Pacific, *J. Clim.* **14**, 991-994.
- Kim, K.-Y., 2002: Investigation of ENSO variability using cyclostationary EOFs of observational data, *Meteorol. Atmos. Phys.* **81**, 149-168.



- Kim, J., and S.-T. Soong. 2005: Simulation of a rainfall Event in the western United States. Available at <http://www.llnl.gov/str/pdfs/UCRL-JC-114412.pdf>
- Kim, K.-Y., and Y. Y. Kim, 2002: Mechanism of Kelvin and Rossby waves during ENSO events, *Meteorol. Atmos. Phys.* 81: 169-189.
- Kirono, D. G. C., and N. J. Tapper, 1999: ENSO rainfall variability and impacts on crop production in Indonesia, *Physical Geography*, 20(6): 508-519.
- Klausmann, A. M., M. Phadnis, and J. Scire, 2003: The application of MM5/WRF models to air quality assessments. Thirteenth PSU/NCAR Mesoscale Model Users' Workshop, NCAR, Boulder Colorado.
- Kottek, M., J. Grieser, C. Beck, B. Rudolf, and F. Rubel, 2006: World map of the Köppen-Geiger climate classification updated. *Meteorol. Z.*, 15, 259-263.
- Kuo, C., C. Lindberg, and D. J. Thomson, 1990: Coherence established between atmospheric carbon dioxide and global temperature, *Nature*, **343**, 709-713.
- Lall, U., and M. Mann, 1995: The Great Salt Lake: A barometer of low-frequency climatic variability, *Water Resources Research*, **31**, 2503-2515.
- Langmann, B., and A. Heil, 2004: Release and dispersion of vegetation and peat fire emissions in the atmosphere over Indonesia 1997/1998, *Atmos. Chem. Phys. Discuss.*, 4, 2117-2159.
- Leung, L. and Y. Qian, 2003: The sensitivity of rainfall and snowpack simulation to model resolution via nesting in regions of complex terrain. *J. Hydrometeorol.*, 4, 1025-1043.
- Lim, Y.-K., K.-Y. Kim and H.-S. Lee, 2002: Temporal and spatial evolution of the Asian Summer Monsoon in the seasonal cycle of synoptic fields. *J. Clim.*, 15, 3630-3644.
- Lim, Y.-K., 2004: Diagnosis of the Asian Summer Monsoon variability and the climate prediction of monsoon rainfall via physical decomposition. Dissertation of Dept. of Meteorology, the Florida State University.
- Lohmann, U and E. Roeckner, 1996: Design and performance of a new cloud microphysics scheme developed for the ECHAM general circulation model. *Climate Dynamics*, 12:557-572.
- Madden R. A., and P. R. Julian, 1971: Detection of a 40-50 day oscillation in the zonal wind in the tropical Pacific. *J. Atmos. Sci.*, **28**, 702-708.

- Majewski, D., 1991: The Europamodell of the Deutscher Wetterdienst. In : *ECMWF* course "Numerical methods in atmospheric models", Vol. 2, 147 - 191.
- Mann, M.E., U.Lall, and B.Saltzman, 1995: Decadal-to-century scale climate variability: insights into the rise and fall of the Great Salt Lake, *J. Geophys. Res.*, **22**, 937-940.
- Mann, M.E. and J.Park, 1996: Greenhouse warming and changes in the seasonal cycle of temperature: model versus observations, *Geophys. Res. Lett.*, **23**, 1111-1114.
- Mann, M.E. and J. Park, 1996: Joint spatiotemporal modes of surface temperature and sea level pressure variability in the northern hemisphere during the last century, *J. Clim.*, **9**, 2137-2162.
- Mann, M.E. and Lees, J.M., 1996: Robust estimation of background noise and signal detection in climatic time series, *Clim. Change*, **33**, 409-445.
- McBride, J., W. Drosowsky, D.G.C.Kirono, D.Gunawan, Soetanto, and P.A.Winarso, 1998. Interannual Variability of the Indonesia Monsoon. Extended Abstracts of the International Conference on Monsoon and Hydrologic Cycle. Kyongju, Korea: *Korean Meteorological Society*.
- McBride, J. 1999. Indonesia, Papua New Guinea and tropical Australia : the Southern Hemisphere Monsoon. In: D.Vincent and D.Karoly, D.(Eds.) *Meteorology of the Southern Hemisphere. American Meteorological Society*, Boston: 88-99.
- McCollum, J.R., A. Gruber, and M.B. Ba, 2000: Discrepancy between Gauges and Satellite Estimates of Rainfall in Equatorial Africa, *J.Appl. Meteor.*, **39**, 666-679.
- Miao, J.-F., L.J.M.Kroon, J.Vila-Guerau de Arellano, and A.A.M.Holtslag, 2003: Impact of topography and land degradation on the sea breeze over eastern Spain. *Meteorol.Atmos.Phy.*, **84**, 157-170.
- Mimmack, G.M., S.J.Mason and J.S.Galpin, 2000: Choice of distance matrice in Cluster Analysis: defining region. *J.Clim.*, **14**:2790 -2797.
- Mommersteeg, H., M. F. Loutre, R. Young, T. A. Wijmstra, and H. Hooghiemstra, 1995: Orbital forced frequencies in the 975,000 year pollen record from Tenagi Philippon (Greece), *Clim. Dyn.*, **11**, 4-24.
- Neale, R., and J. Slingo, 2001. The Diurnal Cycle of Convection in a Mesoscale Model. Available at: [http://www.met.rdg.ac.uk/~swrneale/mm5/mm5\\_results.html](http://www.met.rdg.ac.uk/~swrneale/mm5/mm5_results.html).

- Nordeng T.E., 1994: Extended versions of the convective parameterization scheme at ECMWF and their impact on the mean and transient activity of the model in the tropics; ECMWF Tech. Memo 206. Available from ECMWF, Reading, UK.
- Oltchev, A., A. Ibrom, J. Pries, S. Erasmi, C. Leemhuis, T. June, A. Rauf, H. Krelein, O. Panfyorov and G. Gravenhorst, 2005: Effect of land-use change on evapotranspiration and net ecosystem production of CO<sub>2</sub> in the tropical rain forest margin area in Indonesia: a regional modeling study. *The Stability of Rainforest Margins: Linking Ecological, Economic and Social Constraints of Land Use and Conservation Symposium*, Goettingen, Germany.
- Palmer, T.N., G.J. Shutts, R. Swinbank, 1996: Alleviation of a systematic westerly bias in general circulation and numerical weather prediction models through an orographic gravity wave drag parameterization. *Q. J. R. Meteorol. Soc.* **112**, 1001-1039.
- Park, J. and Maasch, K.A., 1993: Plio-pleistocene time evolution of the 100-kyr cycle in marine paleoclimate records, *J. Geophys. Res.*, **98**, 447-461.
- Penland, C., M. Ghil, and K. Weickmann, 1991: Adaptive filtering and maximum entropy spectra with application to changes in atmospheric angular momentum, *J. Geophys. Res.*, **96**, 22659-22671.
- Ramage, C.S. 1968: Role of a tropical "maritime continent" in the atmospheric circulation. *Mon. Wea. Rev.*, **96**, 365-370.
- Ramage, C.S., 1971: *Monsoon Meteorology*. Academic Press, New York, 196 pp.
- Rife, D.L. 1996. The effects of mountains and complex terrain on airflow and development of clouds and rainfall. Western Region Technical Attachment. 96-16. Available at <http://www.wrh.noaa.gov/wrh/96TAs/TA9616/ta96-16.html>
- Riley, J., H.S. Cooley, Y. He, and M.S. Torn, 2003: Coupling MM5 with ISOLSM: Development, Testing, and Applications. Thirteenth PSU/NCAR Mesoscale Model Users' Workshop, NCAR, Boulder Colorado.
- Roe, G.H., 2005. Orographic Rainfall. *Annu. Rev. Earth Planet. Sci.* **33**:645-71.
- Ropelewski, C.F., and M.S. Halpert, 1987: Global and Regional Scale Rainfall Pattern Associated with the El Niño Southern Oscillation (ENSO), *Mon. Wea. Rev.*, **115**, 1606 - 1626.

- Roswintiarti, O., and S. Raman, 2003: Three-dimensional Simulation of Mean Air Transport During the 1997 Forest Fire in Kalimantan, Indonesia using a Mesoscale Numerical Model, *Pure Appl. Geophys.*, 160, 429-438.
- Rudolf, B., F. Tobias, and U. Schneider, 2001: The Global Rainfall Climatology Center (GPCP): Operational Analysis of Rainfall Based on Surface Observation. Deutscher Wetterdienst, Offenbach, Germany.
- Rudolf, B., 2000: Satellite-Based Global Rainfall Estimates and Validation Results. SAF Training Workshop - Climate Monitoring. Dresden. Germany.
- Rudolf, B., H. Hauschild, W. Rueth, and U. Schneider, 1994: Terrestrial Rainfall Analysis: Operational Method and Required Density of Point Measurements. NATO ASI I/26, Global Rainfalls and Climate Change (Ed. M. Desbois and F. Desalmand), *Springer Verlag Berlin*, 173 - 186.
- Rudolf, B., 1993: Management and analysis of rainfall data on a routine basis. Proc. Internat. WMO/IAHS/ETH Symp. On Precip. And Evap., Slovak Hydromet. Inst., Bratislava, Sept. 1993, 69-76.
- Slingo, J., P. Innes, R. Neale, S. Woolnough, and G-Y. Yang., 2003: Scale interactions on diurnal to seasonal timescales and their relevance to model systematic errors, *Annals of Geophysics*, 46, 139 – 155.
- Smith, N.P., 1998. Observations of the Rainfall-Evaporation Balance in Northern Florida Bay. DeWitt Smith, National Park Service, Everglades National Park, Homestead, Florida. Available at [http://www.aoml.noaa.gov/flbay/98ab\\_smith.html](http://www.aoml.noaa.gov/flbay/98ab_smith.html).
- Smith, T.M., C.F. Ropelewski, and F. Chester, 1997: Quantifying Southern Oscillation–Rainfall Relationships from an Atmospheric GCM, *J. Clim.* 10 (9), 2277-2284.
- Soman, M. K., and J. M. Slingo, 1997: Sensitivity of the Asian Summer Monsoon to aspects of the sea surface temperature anomalies in the tropical Pacific Ocean, *Q. J. R. Meteorol. Soc.*, 123, 309-336.
- Stooksbury, D.E., and R.J. Michaels, 1991: Cluster Analysis of South-eastern US climate stations. *Theor. Appl. Climatol.*, 44:143-150.
- Sundqvist H., 1978: A parameterization scheme for non-convective condensation including prediction of cloud water content, *Q. J. R. Meteorol. Soc.*, **104**, 677-690.

- Sturman,A. and Tapper,N, 1996: The weather and climate of Australia and New Zeland. *Oxford University Press*, Melbourne, 476 pp.
- Struss,D and J. Plieske, 1998: The use of micro satellite markers for detection of genetic diversity in barley populations. *Theor. Appl. Genet.*, 97: 308 -315.
- Tadross, M. A., W. J. Gutowski Jr, B. C. Hewitson, C. Jack, and M. New, 2006: MM5 simulations of interannual change and the diurnal cycle of southern African regional climate. *Theor. Appl. Climatol.* 86, 63–80.
- Thomson, D.J., 1982: Spectrum estimation and harmonic analysis, *Proc. IEEE*, **70**, 1055-1096.
- Tiedke, M., 1989: A comprehensive mass flux scheme for cumulus parameterization in large scale models. *Mon. Wea. Rev.*, 117, 1779 - 1800.
- Tim LI, Y.-C. Tung and J.-W. Hwu, 2005: Remote and Local SST Forcing in Shaping Asian-Australian Monsoon Anomalies. *J.Met.Soc.Japan*, **83**, 153-167.
- Tiwari, R. K. and K. N. N. Rao, 2004: Signature of ENSO Signals in the Coral Growth Rate Record of Arabian Sea and Indian Monsoons. *Pure Appl. Geophys.* 161: 413–427.
- Tiwari, R. K. and S.Sri Laksmi, 2005: Signature of ENSO and NAO signals in Indian subcontinent system. Available at <http://www.cea-igp.ac.cn/English.files/AOGS%20proceedings.htm>
- Torrence, C., and G.P. Compo. 1998: A practical guide to wavelet analysis. *B. Am. Meteor. Soc.* 79, 61 – 78.
- Torrence, C., and P.J. Webster, 1999: Interdecadal Changes in the ENSO–Monsoon System. *J. Clim.*, 12 (8): 2679-2690.
- Tosic,I and M. Unkasevic, 2005: Analysis of rainfall series for Belgrade. *Theor. Appl. Climatol.*, 80, 67–77.
- Tomassetti, B., E. Coppola, M. Verdecchia, and G. Visconti, 2005: Coupling a distributed Grid based Hydrological Model and MM5 Meteorological Model for Flooding alert Mapping, *Advances in Geosciences*, 2, 59–63.
- Treffeisen, R., A. Herber, J. Strom, M. Shiobara, T. Yamanouchi, S. Yamagata, K. Holmen, M. Kriews and O. Schrems.2004: Interpretation of Arctic aerosol properties using cluster analysis applied to observations in the Svalbard area, *Tellus B*, 56:5 457.

- Unal, Y., T. Kindap and M. Karaca, 2003: Redefining the climate zones of Turkey using Cluster Analysis. *Int. J. Climatol.*, 23:1045-1055.
- Untch, A. and M. Hortal, 2002: A finite-element scheme for the vertical discretization of the semi-Lagrangian version of the ECMWF model. ECMWF Technical Memorandum 382.
- Vautard, R., and M. Ghil, 1989: Singular spectrum analysis in nonlinear dynamics, with applications to paleoclimatic time series, *Physica D*, **35**, 395-424.
- Vautard, R., M. Beekmann, B. Bessagnet, N. Blond, A. Hodzic, C. Honore, L. Malherbe, L. Menut, L. Rouil, and J. Roux, 2004: The Use of MM5 for Operational Ozone/NOx/ Aerosol Prediction in Europe: Strengths and Weakness of MM5. The 5<sup>th</sup> WRF/14<sup>th</sup> MM5 Users' Workshop NCAR, Boulder, Colorado.
- Waliser, D. E., R. Murtugudde, and L. E. Lucas, 2003: Indo-Pacific Ocean response to atmospheric intraseasonal variability: 1. Austral summer and the Madden-Julian Oscillation, *J. Geophys. Res.*, 108(C5), 3160, doi: 10.1029/2002JC001620.
- Wang, B., R. Wu, and L. Tim, 2003: Atmosphere–Warm Ocean Interaction and Its Impacts on Asian–Australian Monsoon Variation, *J. Clim.* 16:1195-1211.
- Wang, B. and Y. Wang, 1996: Temporal structure of the Southern Oscillation as revealed by waveform and wavelet analysis, *J. Clim.*, 9, 1586–1598.
- Weng, H., and K-M. Lau, 1994: Wavelets, period doubling, and time-frequency localization with application to organization of convection over the tropical western Pacific. *J. Atmos. Sci.*, 51, 2523–2541.
- Whitten, A. J., M. Muslimin and G.S. Henderson. 1988: The ecology of Sulawesi. Gadjah Mada Univ. Pr. Bulaksumur, Yogyakarta, Indonesia.
- Wikipedia, 2006: East Asian rainy season. <http://en.wikipedia.org/wiki/Meiyu>.
- Wilheit, T., A. Chang and L. Chiu, 1991: Retrieval of monthly rainfall indices from microwave radiometric measurements using probability distribution function. *J. Atmos. Ocean. Tech.*, 8, 118-136.
- Wilks, D.S., 1995: Statistical methods in the atmospheric sciences. *Academic Press*, San Diego, 467 pp.
- Wyser, K., 2001: The mesoscale model MM5 as a regional climate model. Regional Climate Group, Earth Science Centre, Göteborg University. 5 pp.

- Xue, Y., P. J. Sellers, J. L. Kinter III, and J. Shukla, 1991: A Simplified biosphere model for global climate studies. *J. Clim.*, 4, 345 – 362.
- Yiou, P., M. Ghil, J. Jouzel, D. Paillard, and R. Vautard, 1994: Nonlinear variability of the climatic system, from singular and power spectra of Late Quaternary records, *Clim. Dyn.*, 9, 371–389.

Name : Dodo Gunawan  
Gender : Male  
Date of birth : 3<sup>rd</sup> May 1963  
Place of birth : Subang, West Java, Indonesia  
Civil status : Married, 2 children  
Private address : Griya Asri I No.D20/9, Tambun, Bekasi, Indonesia  
Office Address : Jl.Angkasa I No.2, 10720 Kemayoran, Jakarta, Indonesia.

**Education**

1971 – 1976 : Elementary School, SDN Wangunreja, Subang, Indonesia  
1977 – 1980 : Junior High School, SMPN Babakan, Cirebon, Indonesia  
1980 – 1983 : Senior High School, SMAN Sindanglaut, Cirebon, Indonesia  
1983 – 1988 : Bachelor degree, Agrometeorology, Bogor Agricultural University (IPB) Bogor, Indonesia  
1994 – 1995 : Master degree, Meteorology, Universite Blaise Pascal, Clermont Ferrand, France  
Oct.2001 – Dec.2006 : PhD work, Institute of Bioclimatology, Georg-August Universität, Göttingen, Germany

**Occupation**

1992 – 2002 : Prediction and Services Division,  
Meteorological and Geophysical Agency (BMG),  
Jakarta, Indonesia.  
Since 2004 : Research and Development Centre, BMG  
Jakarta, Indonesia.